Pergamon

J. Mech. Phys. Solids, Vol. 46, No. 6, pp. 955–1007, 1998

Printed in Great Britain
0022–5096/98 $19.00+0.00

PII: S0022–5096(98)00009–X

ASYMPTOTIC ANALYSIS OF STABILITY FOR PRISMATIC SOLIDS UNDER AXIAL LOADS

W. SCHERZINGER and N. TRIANTAFYLLIDIS*

Department of Aerospace Engineering, The University of Michigan, Ann Arbor, Michigan 48109-2140, U.S.A.

(*Received* 1 *September* 1997)

ABSTRACT

This work addresses the stability of axially loaded prismatic beams with any simply connected cross-section. The solids obey a general class of rate-independent constitutive laws, and can sustain finite strains in either compression or tension. The proposed method is based on multiple scale asymptotic analysis, and starts with the full Lagrangian formulation for the three-dimensional stability problem, where the boundary conditions are chosen to avoid the formation of boundary layers. The calculations proceed by taking the limit of the beam's slenderness parameter, ε ($\varepsilon^2 \equiv$ area/length^2), going to zero, thus resulting in asymptotic expressions for the critical loads and modes. The analysis presents a consistent and unified treatment for both compressive (buckling) and tensile (necking) instabilities, and is carried out explicitly up to $O(\varepsilon^4)$ in each case.

The present method circumvents the standard structural mechanics approach for the stability problem of beams which requires the choice of displacement and stress field approximations in order to construct a nonlinear beam theory. Moreover, this work provides a consistent way to calculate the effect of the beam's slenderness on the critical load and mode to any order of accuracy required. In contrast, engineering theories give accurately the lowest order terms ($O(\varepsilon^2)$—Euler load—in compression or $O(1)$—maximum load—in tension) but give only approximately the next higher order terms, with the exception of simple section geometries where exact stability results are available.

The proposed method is used to calculate the critical loads and eigenmodes for bars of several different cross-sections (circular, square, cruciform and L-shaped). Elastic beams are considered in compression and elastoplastic beams are considered in tension. The $O(\varepsilon^2)$ and $O(\varepsilon^4)$ asymptotic results are compared to the exact finite element calculations for the corresponding three-dimensional prismatic solids. The $O(\varepsilon^4)$ results give significant improvement over the $O(\varepsilon^2)$ results, even for extremely stubby beams, and in particular for the case of cross-sections with commensurate dimensions. © 1998 Elsevier Science Ltd. All rights reserved.

Keywords: A. buckling, B. beams and columns, B. elastic–plastic material, B. finite strain, C. asymptotic analysis.

1. INTRODUCTION AND MOTIVATION

The stability of prismatic solids under axial load is one of the oldest and most classical problems in structural mechanics. More specifically, the first investigations of the buckling of columns under axial compression go back about two centuries to Euler and his study of the elastica, while the initial investigations of necking in bars, by Considère, are already more than a century old.

* To whom correspondence should be addressed.

Although for a long time the stability problems in compression and tension were treated independently, the approach followed in each case was the standard one of structural mechanics: from the general equations of the three-dimensional solid an approximate one-dimensional (nonlinear) beam theory is derived for the prismatic structure in question; the stability analysis follows by examining the resulting one-dimensional beam model under uniaxial loading.

For axially compressed elastic beams, their critical load and mode depend essentially on the geometry of the cross-section. There is a voluminous engineering literature on this subject. Over the years the structural theories for the compressive stability of beams have been refined for the case of more complicated geometries and, in particular, for thin walled sections where there is an interaction between bending and torsional modes (as opposed to simply connected sections with commensurate dimensions where the critical mode is a bending one). The interested reader is referred to the standard monographs of Timoshenko (1936) or Brush and Almroth (1975) for a classical treatment of this topic.

For the case of bars in tension, their stability depends essentially on the constitutive equation. For the case of typical structural metals, their critical displacement occurs past the displacement corresponding to a maximum load for a uniformly strained bar. For certain elastomers which exhibit no maximum load in their uniaxial response, no necking instabilities are detected. Due to the essential dependence of necking on the constitutive law, the bulk of the engineering literature devoted to this subject pertains to the necking of circular or rectangular sections (e.g. see Bridgman, 1952).

It should be mentioned that in the early structural mechanics literature, compression and tension problems were analyzed independently without recognizing that they were both treatable within the same framework, i.e. as bifurcation induced stability problems of the same prismatic structure under uniaxial loads of different signs. This latter approach started appearing in the 1950's with the advent of nonlinear continuum mechanics for finite deformations, and the corresponding general methodology for hyperelastic solids was given by Green *et al.* (1952).

It should also be pointed out that the above mentioned engineering approach, of first deriving a nonlinear structural theory and then investigating its stability under axial loads, gives an approximation of the critical load and eigenmode which depends on the nonlinear beam theory employed. It also makes difficult the correction of results to account for stubby beams. Knowledge of the exact results and of the validity of the engineering approximations is therefore highly desirable.

The most straightforward way to assess the validity of the stability results obtained using the above mentioned structural approach is by comparing them to the critical loads and modes based on exact calculations involving the full three-dimensional formulation of the stability problem in question. For the case of relatively simple geometries, i.e. rectangular blocks in two-dimensions (under plane strain conditions) or cylinders in three-dimensions, one can obtain the stability results analytically. The first such calculations were applied to specific hyperelastic materials (e.g. Levinson, 1968 for the compression of a rectangular block under plane strain, Wilkes, 1955 for a cylinder under end thrust or Green and Spencer, 1959 for combined extension and torsion). Subsequent investigations considered more general classes of constitutive equations. More specifically, Hill and Hutchinson (1975) and Young (1976) examined

the bifurcation instability of a rectangular block under plane strain in uniaxial tension and compression, respectively, for any incrementally linear hypoelastic material, thus covering both rubber-elasticity and rate-independent metal plasticity. In addition, by taking the limit of the block's slenderness ratio going to zero, they provided asymptotic expansions for the critical load and modes. The leading order terms in these expansions correspond to the known structural theory results (the Euler buckling load in compression and the maximum load in tension). Similar asymptotic results were also obtained by Hutchinson and Miles (1974) for the bifurcation of an elastoplastic cylinder in tension. However, for the more general and, practically speaking, more interesting case of an arbitrary section where analytical expressions for the critical load and mode are not available, the only option thus far, besides the engineering theory, has been a full numerical solution to each problem.

The motivation for our work is the following: is there any consistent and general way to find the critical load and mode of an axially loaded beam with any simply connected cross-section, as a function of its cross-sectional geometry and material properties to any degree of desired accuracy while still using a one-dimensional beam type analysis? Our answer is yes, and hinges on reversing the order of taking the structural approximation (to construct a beam theory) and performing the stability analysis (to find the critical load and mode). In the present work we follow the approach introduced by Triantafyllidis and Kwon (1987) for the stability of thin walled structures. First we formulate the exact stability problem for the three-dimensional prismatic solid and only afterwards do we take the limit of the beam's slenderness, ε ($\varepsilon^2 \equiv$ area/length^2), going to zero, in order to find the critical load and mode in terms of the slenderness.

To achieve our task of taking the limit of the critical load and mode for the three-dimensional stability problem of a prismatic beam with a simply connected section, we make use of some recent developments in applied mathematics which use multiple scale asymptotic techniques to derive a consistent one-dimensional (beam) theory for prismatic, linearly elastic solids based on the general three-dimensional equations of linear elasticity. The rich history of the mathematical derivations of the engineering beam equations from the three-dimensional equations of elasticity—which is a classical problem in mechanics and applied mathematics—is beyond the scope of this work. It suffices to say that the multiple scale asymptotic technique employed here has its origins in the work of Rigolot (1972) on the derivation of an asymptotic theory for linear elastic beams. Of the number of subsequent works that followed on the same subject and used the same technique, we mention the work of Trabucho and Viaño (1989) which has been of particular help to our analysis. In this work, the governing one-dimensional equations for a prismatic linear elastic solid up to $O(\varepsilon^6)$ are derived from the three-dimensional equations of isotropic linear elasticity. Their methodology has been appropriately modified to account for an eigenvalue problem with stress-dependent incremental moduli.

The outline of the present work is as follows: the general formulation for the stability problem of a finite strained, rate-independent three-dimensional prismatic solid, the rescaling of the problem according to the beam's slenderness parameter, and the corresponding asymptotic expansions for the critical load and mode are stated at the beginning of Section 2. The results for the asymptotic expansions of the critical

load up to $O(\varepsilon^4)$ and mode up to $O(\varepsilon^2)$ in both tension and compression are given, without a derivation, in the remainder of Section 2. The choice of constitutive laws is recorded in Section 3, while Section 4 contains a brief description of the numerical calculations for the exact three-dimensional problem and of the cross-section dependent constants involved in the asymptotic solutions. The results are presented in Section 5 and include the comparison of the exact and asymptotic critical loads up to $O(\varepsilon^4)$ and eigenmodes up to $O(\varepsilon^2)$ for both tension and compression of prismatic beams with several different cross-sections. In the interest of completeness of the presentation, all the derivations of the general asymptotic results of Section 2 are given in detail in the Appendix for the benefit of the interested reader.

2. ASYMPTOTIC FORMULATION

In this section, the stability theory for beams with simply connected cross-sections under axial loading is developed using an asymptotic approach. In the first part, the general stability problem for a rate-independent prismatic solid is formulated, followed by the description of the asymptotic method. In the second and third parts, respectively, the asymptotic expressions for the critical load and eigenmode for the cases of compression and tension are presented without proof. A detailed derivation of the asymptotic results for compression and tension is given in the Appendix.

2.1. *General formulation*

The geometry and boundary conditions for the stability problem are shown in Fig. 1. The prismatic solid has a length L and a simply connected cross-section with

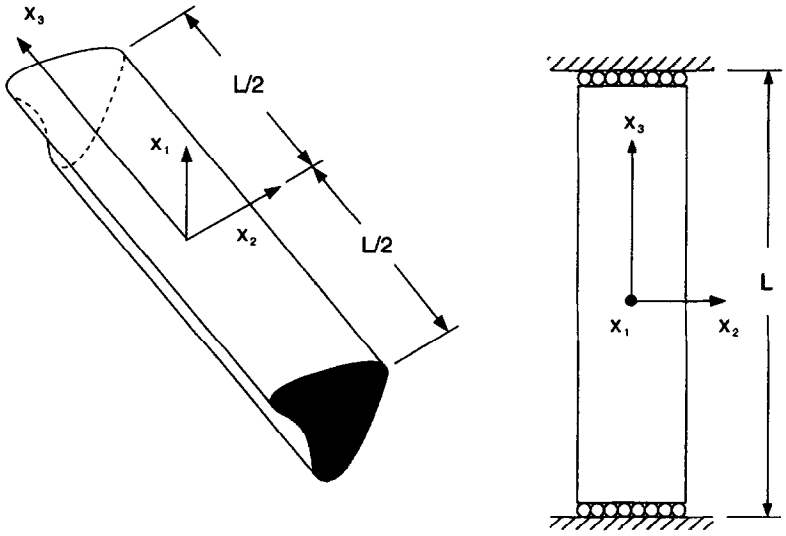

Fig. 1. Schematic representation of the geometry and boundary conditions of an axially loaded prismatic beam.

area A in its undeformed stress-free configuration, which is used as the reference configuration (full Lagrangian description). To avoid the presence of boundary layer effects near both ends, it is assumed that the two ends, $x_3 = \pm L/2$, remain flat and are free of shear tractions. Rate-independent, incrementally linear solids, which cover finite elasticity and elastoplasticity, are considered. It is additionally assumed that the material is initially isotropic, and due to the imposed axial loading, it remains isotropic in the x_1x_2 plane. The x_3 axis, the axis of loading, is an axis of orthotropy for the material.

The load parameter for the problem is the axial stretch ratio, λ. In compression $\lambda < 1$, and in tension $\lambda > 1$. For the stability problem we seek the critical stretch ratio, λ_c, which is the value of λ corresponding to the first bifurcation encountered during a monotonic loading process.

For the rate-independent solids considered here, the stability problem is governed by Hill's (1957) stability functional†

$$\mathscr{F}(\mathbf{u}, \lambda) = \frac{1}{2}\int_V L_{ijkl}(\lambda)u_{k,l}u_{i,j}\,\mathrm{d}V, \tag{1}$$

where u_i is the velocity field‡ and L_{ijkl} are the incremental moduli relating the rate of the transpose of the first Piola–Kirchhoff stress, Π_{ji}, to the rate of the deformation gradient, $u_{k,l}$, as follows

$$\Pi_{ji} = L_{ijkl}u_{k,l}. \tag{2}$$

The incremental moduli are evaluated on the principal path whose stability is under investigation. Positive definiteness of $\mathscr{F}$ along the principal path ensures a unique solution to the incremental equilibrium equations and stability for the structure. For a well posed problem§ $\mathscr{F}$ is positive definite in the unstressed state, i.e. when $\lambda = 1$. Assuming $\mathscr{F}$ to be a continuous function of λ, $\mathscr{F}$ will be positive definite for all values of λ such that $|\lambda - 1| < |\lambda_c - 1|$. Loss of positive definiteness of $\mathscr{F}$ corresponds to a nontrivial solution to the eigenvalue equation $\delta\mathscr{F} = 0$. The associated eigenvalue problem can be more conveniently written as

$$\int_V (\Pi_{ji} - L_{ijkl}u_{k,l})\delta\Pi_{ji}\,\mathrm{d}V = 0, \tag{3}$$

$$\int_V \Pi_{ji}\delta u_{i,j}\,\mathrm{d}V = 0. \tag{4}$$

Note that (3) are the linearized incremental constitutive relations for the material and (4) are the incremental equilibrium relations for the solid.

In the problem considered here the mode, $\mathbf{u}(x_i)$, satisfies the following essential (kinematic) conditions

$$u_3(x_1, x_2, \pm L/2) = 0, \tag{5}$$

† Here and subsequently Greek indices range from 1–2 and Latin indices range from 1–3.

‡ To avoid notational confusion the velocity and stress-rate will not be shown with a superimposed dot.

§ It is additionally assumed that $L_{ijkl} = L_{klij}$ (major symmetry for incremental moduli) which ensures a self adjoint system and hence real eigenvalues.

$$\int_A u_\alpha \, dA = \int_A \varepsilon_{\alpha\beta} x_\alpha u_\beta \, dA = 0 \quad \text{at } x_3 = 0, \tag{6}$$

with $\varepsilon_{\alpha\beta}$ defined as the alternating symbol in two dimensions ($\varepsilon_{11} = \varepsilon_{22} = 0, \varepsilon_{12} = -\varepsilon_{21} = 1$), and where (5) is the flat surface boundary condition for the two ends while (6) exclude rigid body modes. In addition to the above conditions, the mode normalization is enforced by

$$\int_V u_i v_i \, dV = C, \tag{7}$$

with appropriately chosen vector field v_i and constant C. The eigenmode at λ_c does not have to be unique within the context of this analysis.

To begin the analysis the domain of the problem is normalized by dividing the dimensions of the beam by its length L. The new domain has a length of one and an area of $\varepsilon^2 = A/L^2$. It can be seen that the domain depends on the parameter ε. The goal of the analysis presented here is to solve the stability problem on a normalized domain that is independent of ε. It is assumed that the cross-section has commensurate x_1 and x_2 dimensions. Consequently, the domain is rescaled with the parameter ε as follows

$$x_\alpha \to \varepsilon x_\alpha, \quad x_3 \to x_3. \tag{8}$$

To obtain the incremental equilibrium eqn (4) in the normalized domain with all terms of the same order, the mode and stress-rate are rescaled in the following manner, leading to the redefinition of the problem on the normalized domain, $\omega \times [-1/2, 1/2]$, which has unit area, $\int_\omega d\omega = 1$, and unit length,

$$u_\alpha \to \varepsilon^{-1} u_\alpha, \quad u_3 \to u_3 \tag{9}$$

$$\Pi_{\alpha\beta} \to \varepsilon^2 \Pi_{\alpha\beta}, \quad \Pi_{\alpha 3} \to \varepsilon \Pi_{\alpha 3}, \quad \Pi_{3\beta} \to \varepsilon \Pi_{3\beta}, \quad \Pi_{33} \to \Pi_{33}. \tag{10}$$

By introducing the rescaled variables (8)–(10) into the governing eqns (3), (4) we obtain the following variational equations for the field quantities, $\mathbf{u}(\varepsilon)$ and $\boldsymbol{\Pi}(\varepsilon)$, defined on the normalized domain

$$\varepsilon^{-2}[-b_{-2}(\mathbf{L}(\lambda(\varepsilon)), \mathbf{u}(\varepsilon), \delta\boldsymbol{\Pi})] + [a_0(\boldsymbol{\Pi}(\varepsilon), \delta\boldsymbol{\Pi}) - b_0(\mathbf{L}(\lambda(\varepsilon)), \mathbf{u}(\varepsilon), \delta\boldsymbol{\Pi})]$$
$$+ \varepsilon^2[a_2(\boldsymbol{\Pi}(\varepsilon), \delta\boldsymbol{\Pi}) - b_2(\mathbf{L}(\lambda(\varepsilon)), \mathbf{u}(\varepsilon), \delta\boldsymbol{\Pi})] + \varepsilon^4[a_4(\boldsymbol{\Pi}(\varepsilon), \delta\boldsymbol{\Pi})] = 0 \tag{11}$$

$$c_0(\boldsymbol{\Pi}(\varepsilon), \delta\mathbf{u}) = 0. \tag{12}$$

which are expressed in terms of the bilinear forms defined below

$$b_{-2}(\mathbf{L}(\lambda(\varepsilon)), \mathbf{u}(\varepsilon), \delta\boldsymbol{\Pi}) = \int_{1/2}^{1/2} \int_\omega [L_{33\gamma\delta} u_{\gamma,\delta} \delta\Pi_{33}] \, d\omega \, dx_3, \tag{13}$$

$$b_0(\mathbf{L}(\lambda(\varepsilon)), \mathbf{u}(\varepsilon), \delta\boldsymbol{\Pi}) = \int_{-1/2}^{1/2} \int_\omega [L_{\alpha\beta\gamma\delta} u_{\gamma,\delta} \delta\Pi_{\beta\alpha} + (L_{\alpha 3\gamma 3} u_{\gamma,3} + L_{\alpha 33\delta} u_{3,\delta}) \delta\Pi_{3\alpha}$$
$$+ (L_{3\beta\gamma 3} u_{\gamma,3} + L_{3\beta 3\delta} u_{3,\delta}) \delta\Pi_{\beta 3} + L_{3333} u_{3,3} \delta\Pi_{33}] \, d\omega \, dx_3, \tag{14}$$

$$b_2(\mathbf{L}(\lambda(\varepsilon)), \mathbf{u}(\varepsilon), \delta\mathbf{\Pi}) = \int_{-1/2}^{1/2} \int_{\omega} [L_{\alpha\beta 33} u_{3,3} \delta\Pi_{\beta\alpha}] \, \mathrm{d}\omega \, \mathrm{d}x_3, \tag{15}$$

$$a_0(\mathbf{\Pi}(\varepsilon), \delta\mathbf{\Pi}) = \int_{-1/2}^{1/2} \int_{\omega} [\Pi_{33} \delta\Pi_{33}] \, \mathrm{d}\omega \, \mathrm{d}x_3, \tag{16}$$

$$a_2(\mathbf{\Pi}(\varepsilon), \delta\mathbf{\Pi}) = \int_{-1/2}^{1/2} \int_{\omega} [\Pi_{3\alpha} \delta\Pi_{3\alpha} + \Pi_{\beta 3} \delta\Pi_{\beta 3}] \, \mathrm{d}\omega \, \mathrm{d}x_3, \tag{17}$$

$$a_4(\mathbf{\Pi}(\varepsilon), \delta\mathbf{\Pi}) = \int_{-1/2}^{1/2} \int_{\omega} [\Pi_{\beta\alpha} \delta\Pi_{\beta\alpha}] \, \mathrm{d}\omega \, \mathrm{d}x_3, \tag{18}$$

$$c_0(\mathbf{\Pi}(\varepsilon), \delta\mathbf{u}) = \int_{-1/2}^{1/2} \int_{\omega} [\Pi_{\beta\alpha} \delta u_{\alpha,\beta} + \Pi_{3\alpha} \delta u_{\alpha,3} + \Pi_{\beta 3} \delta u_{3,\beta} + \Pi_{33} \delta u_{3,3}] \, \mathrm{d}\omega \, \mathrm{d}x_3. \tag{19}$$

Notice that the governing equations, (11) and (12), depend solely on ε^2. Consequently, for slender prismatic bars, those with $\varepsilon \ll 1$, we adopt the following regular asymptotic expansions for the critical stretch ratio $\lambda_c(\varepsilon)$, eigenmode $\mathbf{u}(\varepsilon)$, stress-rate $\mathbf{\Pi}(\varepsilon)$, and incremental moduli $\mathbf{L}(\varepsilon)$ in terms of ε^2

$$\lambda_c = \lambda_0 + \varepsilon^2 \lambda_2 + \varepsilon^4 \lambda_4 + \cdots \tag{20}$$

$$\mathbf{u} = \overset{0}{\mathbf{u}} + \varepsilon^2 \overset{2}{\mathbf{u}} + \varepsilon^4 \overset{4}{\mathbf{u}} + \cdots \tag{21}$$

$$\mathbf{\Pi} = \overset{0}{\mathbf{\Pi}} + \varepsilon^2 \overset{2}{\mathbf{\Pi}} + \varepsilon^4 \overset{4}{\mathbf{\Pi}} + \cdots \tag{22}$$

$$\mathbf{L} = \overset{0}{\mathbf{L}} + \varepsilon^2 \overset{2}{\mathbf{L}} + \varepsilon^4 \overset{4}{\mathbf{L}} + \cdots. \tag{23}$$

From the governing eqns (11), (12), boundary conditions (5), (6), and mode normalization condition (7) for the stability problem, rescaled in terms of the slenderness parameter ε^2, asymptotic solutions to the actual stability problem are constructed with the help of the expansions (20)–(23) for compressive and tensile loadings. Results for compression and tension are presented without proof in the following two sections. Appropriate references to certain key equations from the detailed derivations in the appendix are given along the way to help the more devoted reader.

2.2. *Compression*

To begin the analysis for the case of compression, it is noted that the buckling load for a beam with a finite length but a vanishingly small area is zero. Since the critical load vanishes, the critical strain should tend to zero, i.e. $\varepsilon_c = \ln \lambda_c = 0$ as $\varepsilon \to 0$, which implies $\lambda_0 = 1$. The expression for λ_c can now be written as

$$\lambda_c = 1 + \varepsilon^2 \lambda_2 + \cdots. \tag{24}$$

Since $\lambda_c < 1$ in compression, we must have $\lambda_2 < 0$. Also note that the lowest order incremental moduli, $\overset{0}{\mathbf{L}} = \mathbf{L}(1)$, are isotropic, since the material is assumed to be initially isotropic.

2.2.1. *Derivation of* λ_2, $\overset{0}{\mathbf{u}}_1$. The next terms sought in the expansion of λ_c and $\mathbf{u}$ are λ_2

and $\overset{0}{\mathbf{u}}$. From the asymptotic procedure just outlined, it can be shown that the lowest order terms in the expansion of the mode are found in terms of $\overset{0}{z}_\alpha(x_3)$ [see (A41)], the transverse components of the mode along the x_3 axis

$$\overset{0}{u}_\alpha = \overset{0}{z}_\alpha(x_3), \quad \overset{0}{u}_3 = -x_\alpha \overset{0}{z}_{\alpha,3}(x_3). \tag{25}$$

Examining (25) it is seen that the lowest order term for the mode agrees with the Bernoulli–Euler–Navier beam bending assumption, i.e. plane sections remain plane and normal to the deformed middle line.

To completely determine $\overset{0}{u}_i$ in (25) it is necessary to find $\overset{0}{z}_\alpha(x_3)$. To this end we define the differential operator

$$\mathscr{L}^c_{\alpha\beta}[\cdot] \equiv -I_{\alpha\beta}\frac{d^4[\cdot]}{dx_3^4} + \lambda_2 \delta_{\alpha\beta}\frac{d^2[\cdot]}{dx_3^2} \tag{26}$$

where $I_{\alpha\beta}$ are the normalized moments of inertia, and $\delta_{\alpha\beta}$ is the Kronecker symbol in two dimensions ($\delta_{11} = \delta_{22} = 1, \delta_{12} = \delta_{21} = 0$). The governing ordinary differential equations and boundary conditions for $\overset{0}{z}_\alpha(x_3)$ are shown to satisfy [see (A47)]

$$\mathscr{L}^c_{\alpha\beta}[\overset{0}{z}_\beta] = 0, \tag{27}$$

$$\overset{0}{z}_{\alpha,3}(x_3) = 0 \quad \text{at } x_3 = \pm\tfrac{1}{2}. \tag{28}$$

The solution of the eigenvalue problem, (27) and (28), gives λ_2, taken to be the lowest eigenvalue in absolute value, and the corresponding mode, $\overset{0}{z}_\alpha(x_3)$

$$\lambda_2 = -\pi^2 I_{\alpha\beta}\hat{z}_\alpha \hat{z}_\beta, \tag{29}$$

$$\overset{0}{z}_\alpha(x_3) = \hat{z}_\alpha \sin(\pi x_3), \tag{30}$$

where, from (6), the kinematical constraint against rotation, and (7), the model normalization, $\hat{z}_\alpha$ are found as the solution to the following system of equations

$$\varepsilon_{\alpha\beta} I_{\beta\gamma}\hat{z}_\gamma \hat{z}_\alpha = 0; \quad \hat{z}_\alpha \hat{z}_\alpha = 1. \tag{31}$$

For the case where either $I_{11} - I_{22} \neq 0$ or $I_{12} \neq 0$ the above homogeneous system in $\hat{z}_\alpha$ admits the solutions $(\hat{z}_1, \hat{z}_2) = (\cos\beta, \sin\beta)$ or $(\sin\beta, \cos\beta)$ with $-\pi/4 \leqslant \beta \leqslant \pi/4$ (the negative solutions give the same mode). The wanted solution $\hat{z}_\alpha$ is the one of the two choices which minimizes $I_{\alpha\beta}\hat{z}_\alpha\hat{z}_\beta$, since according to (29) we are interested in the lowest buckling load. The case $I_{11} = I_{22}$ and $I_{12} = 0$ gives an infinity of possible solutions $(\hat{z}_1, \hat{z}_2) = (\cos\beta, \sin\beta)$ where β is any arbitrary angle $-\pi/2 \leqslant \beta \leqslant \pi/2$. For this latter case $\hat{z}_\alpha$ are indeterminate from λ_2, but this special case will be discussed again following the presentation of λ_4 in the next subsection.

2.2.2. *Derivation of* λ_4, $\overset{2}{\mathbf{u}}_i$. Attention is subsequently turned to the derivation of λ_4 and $\overset{2}{\mathbf{u}}$. We begin with the expressions found for $\overset{2}{u}_i$ [see (A49) and (A57)]

$$\begin{aligned}
\overset{2}{u}_\alpha &= \overset{2}{z}_\alpha(x_3) + \varepsilon_{\alpha\beta}x_\beta \overset{2}{z}(x_3) + \nu\phi_{\alpha\beta}(x_1, x_2)\overset{0}{z}_{\beta,33}(x_3), \\
\overset{2}{u}_3 &= \overset{2}{z}_3(x_3) - x_\alpha \overset{2}{z}_{\alpha,3}(x_3) - w(x_1, x_2)\overset{2}{z}_{,3}(x_3) + \lambda_2(1+\nu)x_\alpha \overset{0}{z}_{\alpha,3}(x_3) \\
&\quad + [\nu\theta_\alpha(x_1, x_2) + (1+\nu)\eta_\alpha(x_1, x_2)]\overset{0}{z}_{\alpha,333}(x_3),
\end{aligned} \tag{32}$$

where $\phi_{\alpha\beta}(x_1, x_2)$, $\theta_\alpha(x_1, x_2)$, $\eta_\alpha(x_1, x_2)$, and $w(x_1, x_2)$ are auxiliary functions defined on the normalized cross section, ω [see (A50) and (A54)–(A56)]. The function $w(x_1, x_2)$ is the well known warping function from the theory of torsion of prismatic beams. Another function arising from the theory of torsion of prismatic beams that also appears in the analysis is the Saint-Venant stress function, $\psi(x_1, x_2)$ [see (A60)]. The auxiliary constants, J, I^ψ_α, I^w_α, H_α, K, $K^\theta_{\alpha\beta}$, $K^\eta_{\alpha\beta}$, $L^\theta_{\alpha\beta}$, and $L^\eta_{\alpha\beta}$, appearing in the following results, are defined with the help of these functions and are found in the Appendix.

Using the functions presented above, simplified expressions for $\overset{2}{z}(x_3)$ and $\overset{2}{z}_3(x_3)$ can be determined. The governing differential equation and boundary conditions for $\overset{2}{z}(x_3)$ are found to be [see (A62)]

$$\overset{2}{z}_{,33}(x_3) = \left[\frac{\nu I^\psi_\alpha + (1+\nu) I^w_\alpha}{J}\right] \overset{0}{z}_{\alpha,3333}(x_3), \tag{33}$$

$$\overset{2}{z}(x_3) = 0 \quad \text{at } x_3 = 0,$$

$$\overset{2}{z}_{,3}(x_3) = 0 \quad \text{at } x_3 = \pm\tfrac{1}{2}. \tag{34}$$

Solving (33) subject to (34) gives

$$\overset{2}{z}(x_3) = -\hat{z}_\alpha \pi^2 \left[\frac{\nu I^\psi_\alpha + (1+\nu) I^w_\alpha}{J}\right] \sin(\pi x_3). \tag{35}$$

The governing differential equation and boundary conditions for $\overset{2}{z}_3(x_3)$ are [according to (A67)]

$$\overset{2}{z}_{3,33}(x_3) = \nu H_\alpha \overset{0}{z}_{\alpha,33333}(x_3), \tag{36}$$

$$\overset{2}{z}_3(x_3) = 0 \quad \text{at } x_3 = \pm\tfrac{1}{2}. \tag{37}$$

Solving (36) subject to (37), $\overset{2}{z}_3(x_3)$ is

$$\overset{2}{z}_3(x_3) = -\hat{z}_\alpha \pi^3 \nu H_\alpha \cos(\pi x_3). \tag{38}$$

From (32), to fully determine $\overset{2}{u}_i$ the function $\overset{2}{z}_\alpha(x_3)$ must also be found. The governing differential equations and boundary conditions for $\overset{2}{z}_\alpha(x_3)$ are found to be [see (A81)]

$$\mathscr{L}^c_{\alpha\beta}[\overset{2}{z}_\beta] = M_\alpha \sin(\pi x_3), \tag{39}$$

$$\begin{aligned} M_\alpha = {} & -\lambda_4 \pi^2 \hat{z}_\alpha + \pi^6 \left\{ (I_{\gamma\delta} \hat{z}_\gamma \hat{z}_\delta)^2 \left(\frac{1}{2E} \frac{\mathrm{d}E}{\mathrm{d}\lambda}\bigg|_{\lambda=1} - 1 - 3\nu \right) \hat{z}_\alpha + \nu (I_{\gamma\delta} \hat{z}_\gamma \hat{z}_\delta) \varepsilon_{\eta\alpha} \varepsilon_{\xi\beta} I_{\eta\xi} \hat{z}_\beta \right. \\ & - \frac{1}{2} \left(\frac{\nu}{1+\nu} \right) (\nu K \hat{z}_\alpha + \nu K^\theta_{\alpha\beta} \hat{z}_\beta + (1+\nu) K^\eta_{\alpha\beta} \hat{z}_\beta) - (\nu L^\theta_{\alpha\beta} \hat{z}_\beta + (1+\nu) L^\eta_{\alpha\beta} \hat{z}_\beta) \\ & \left. + \frac{1}{2J} [\nu I^\psi_\gamma \hat{z}_\gamma + (1+\nu) I^w_\gamma \hat{z}_\gamma] \left[\frac{\nu}{1+\nu} (\varepsilon_{\alpha\beta} H_\beta + K^w_\alpha) + I^w_\alpha \right] \right\}, \end{aligned}$$

$$\overset{2}{z}_{\alpha,3}(x_3) = 0 \quad \text{at } x_3 = \pm\frac{1}{2}. \tag{40}$$

From linear operator theory, and in view of the singularity of $\mathscr{L}^c_{\alpha\beta}$ for λ_2, a solution to (39) exists when $M_\alpha \hat{z}_\alpha = 0$. Hence, the solution of the above problem, (39) and (40), gives λ_4 and the corresponding mode, $\overset{2}{z}_\alpha(x_3)$

$$\lambda_4 = \pi^4 \left\{ (I_{\alpha\beta}\hat{z}_\alpha\hat{z}_\beta)^2 \left(\frac{1}{2E}\frac{\mathrm{d}E}{\mathrm{d}\lambda}\bigg|_{\lambda=1} - 1 - 3\nu \right) + \nu (I_{\alpha\beta}\hat{z}_\alpha\hat{z}_\beta)(\varepsilon_{\eta\delta}\varepsilon_{\xi\gamma} I_{\eta\xi}\hat{z}_\delta\hat{z}_\gamma) \right.$$

$$- \frac{1}{2}\left(\frac{\nu}{1+\nu}\right)(\nu K + \nu K^\theta_{\alpha\beta}\hat{z}_\alpha\hat{z}_\beta + (1+\nu)K^\eta_{\alpha\beta}\hat{z}_\alpha\hat{z}_\beta) - (\nu L^\theta_{\alpha\beta}\hat{z}_\alpha\hat{z}_\beta + (1+\nu)L^\eta_{\alpha\beta}\hat{z}_\alpha\hat{z}_\beta)$$

$$\left. + \frac{1}{2J}[\nu I^\psi_\alpha \hat{z}_\alpha + (1+\nu)I^w_\alpha \hat{z}_\alpha]\left[\frac{\nu}{1+\nu}(\varepsilon_{\beta\delta}H_\delta + K^w_\beta) + I^w_\beta\right]\hat{z}_\beta \right\}, \tag{41}$$

$$\overset{2}{z}_\alpha(x_3) = \{\pi^{-4}[I_{\beta\beta} - 2I_{\beta\gamma}\hat{z}_\beta\hat{z}_\gamma]^{-1} M_\alpha + \hat{C}\hat{z}_\alpha\} \sin(\pi x_3), \tag{42}$$

where the constant $\hat{C}$ in (42) is found from the mode normalization condition [see (7)]

$$\int_{-1/2}^{1/2}\int_\omega \overset{0}{u}_i \overset{2}{u}_i \,\mathrm{d}\omega\,\mathrm{d}x_3 = 0. \tag{43}$$

According to our discussion at the end of the previous subsection, special provision must be made for the case $I_{11} = I_{22}$ and $I_{12} = 0$. In this instance, from (39) and (40), $\overset{2}{z}_\alpha(x_3) = \hat{C}\overset{0}{z}_\alpha(x_3)$ and compatibility dictates $M_\alpha = 0$. Observe from (39) that the system $M_\alpha = 0$ is homogeneous and linear in $\hat{z}_\alpha$ with λ_4 as its eigenvalue and $\hat{z}_\alpha$ as the corresponding eigenvector, i.e. $\lambda_4\hat{z}_\alpha = C_{\alpha\beta}\hat{z}_\beta$ where $C_{\alpha\beta}$ are easily identifiable constants. Since the expression (41) is still valid for the special case at hand, the wanted $\hat{z}_\alpha$ is the vector that maximizes λ_4 [and hence provides the lowest critical strain according to (24)]. For the particular case that $C_{\alpha\beta} = C\delta_{\alpha\beta}$, $\lambda_4 = C$ but the eigenvector $\hat{z}_\alpha$ is no longer unique. This latter case is not just an academic curiosity but can easily occur in applications. For the case of D_4 symmetry of the cross-section ω, i.e. for the symmetry of the square, $K^\theta_{\alpha\beta} = K^\theta\delta_{\alpha\beta}$, $K^\eta_{\alpha\beta} = K^\eta\delta_{\alpha\beta}$, $L^\theta_{\alpha\beta} = L^\theta\delta_{\alpha\beta}$, $L^\eta_{\alpha\beta} = L^\eta\delta_{\alpha\beta}$, and $I^\psi_\alpha = I^w_\alpha = 0$, in which case $\hat{z}_\alpha$ is indeterminate from this step of the analysis. The circular, square and cruciform sections in the applications fall in that category of a double eigenvalue at λ_c for all values of the slenderness parameter ε. To determine $\hat{z}_\alpha$ in this case, one needs to perform a nonlinear post buckling analysis for interacting modes (see Triantafyllidis and Peek, 1992) and find the correct initial tangent $\hat{z}_\alpha$ of the eigenmode.

2.3. *Tension*

We begin the analysis for the case of tension by noting that a beam with a vanishingly small area and a finite length has an instability corresponding to its maximum load. Consequently, λ_0, the first term in the expansion for λ_c is found when the nominal stress rate in the uniaxial tension is zero, or equivalently when the uniaxial tangent modulus, $E(\lambda)$[$(E(\lambda) \equiv \Pi_{33}(\lambda)/\lambda$, see also (A91)], vanishes

$$\overset{0}{\Pi}_{33} = 0 \Rightarrow E(\lambda_0) = 0. \tag{44}$$

It is also noted, unlike the analysis in compression, that $\lambda_0 \neq 1$. Therefore the lowest order terms in the expansion of the incremental moduli, $\overset{0}{\mathbf{L}}$, will, in general, be orthotropic.

2.3.1. *Derivation of* λ_2, $\overset{0}{\mathbf{u}}_1$. The next terms sought in the expansion of λ_c and $\mathbf{u}$ are λ_2 and $\overset{0}{\mathbf{u}}$. From the asymptotic analysis introduced in Section 2.1, the lowest order terms in the expansion of the mode are found to have the form [see (A87)]

$$\overset{0}{u}_\alpha = 0, \quad \overset{0}{u}_3 = \overset{0}{z}_3(x_3). \tag{45}$$

In analogy to the analysis in compression, the governing differential equation and boundary conditions for $\overset{0}{z}_3(x_3)$ give an eigenvalue problem where λ_2 is the lowest eigenvalue and $\overset{0}{z}_3(x_3)$ is the corresponding mode. We introduce the differential operator,†

$$\mathscr{L}'[\cdot] = -(\nu^2 S)_0 I_{\alpha\alpha} \frac{d^4[\cdot]}{dx_3^4} + \lambda_2 \left(\frac{dE}{d\lambda}\right)_0 \frac{d^2[\cdot]}{dx_3^2}, \tag{46}$$

where $\nu(\lambda)$ is the instantaneous Poisson's ratio [see definition in (A90)], and $S(\lambda)$ is the axial component of the second Piola–Kirchhoff stress in uniaxial tension. The governing differential equation and boundary conditions for $\overset{0}{z}_3(x_3)$ are shown to be [see (A107)]

$$\mathscr{L}'[\overset{0}{z}_3] = 0, \tag{47}$$

$$\overset{0}{z}_3 = 0 \quad \text{at } x_3 = \pm\tfrac{1}{2}. \tag{48}$$

The solution to the eigenvalue problem, (47) and (48) is

$$\overset{0}{z}_3(x_3) = \hat{z}\cos(\pi x_3), \tag{49}$$

$$\lambda_2 = -\pi^2 I_{\alpha\alpha}\left(\frac{\nu^2 S}{dE/d\lambda}\right)_0. \tag{50}$$

Using once more the mode normalization condition (7) in conjunction with the asymptotic expansion in (21), and choosing $C = 1/2$, gives $\hat{z} = 1$.

2.3.2. *Derivation of* λ_4, $\overset{2}{\mathbf{u}}_1$. Attention is next focused on the derivation of λ_4 and $\overset{2}{\mathbf{u}}$. We start with the results obtained for $\overset{2}{u}_i$ [see (A95) and (A98)]. The following expressions for $\overset{2}{u}_i$ are found

$$\overset{2}{u}_\alpha = -\overset{0}{\nu} x_\alpha \overset{0}{z}_{3,3}(x_3),$$

$$\overset{2}{u}_3 = \overset{2}{z}_3(x_3) + \left(\nu \frac{L_{3113}}{L_{3131}}\right)_0 \rho(x_1, x_2) \overset{0}{z}_{3,33}(x_3), \tag{51}$$

where the auxiliary function $\rho(x_1, x_2)$ is defined on the normalized cross-section ω [see (A97)]. The only unknown function required to fully determine $\overset{2}{u}_i$ in (51) is $\overset{2}{z}_3(x_3)$. The governing differential equation for $\overset{2}{z}_3(x_3)$ will also give λ_4.

The finding of $\overset{2}{z}_3(x_3)$ requires introducing the auxiliary function $\overset{4}{g}_\alpha(x_1, x_2)$, also

†4 A zero subscript, $(\cdot)_0$, denotes the evaluation of the quantity $(\cdot)$ at λ_0.

defined on the normalized cross-section ω [see (A114)]. Upon closer inspection, since $\overset{0}{L}_{\alpha\beta\gamma\delta}$ are isotropic in the x_1x_2 plane, the equation for $\overset{4}{g}_\alpha$ is the variational statement of a plane elasticity problem which can be solved numerically for an arbitrary section ω.

The governing differential equation and boundary conditions for $\overset{2}{z}_3(x_3)$ are

$$\mathscr{L}^t[\overset{2}{z}_3] = M\cos(\pi x_3), \tag{52}$$

$$M = -\lambda_4\pi^2\hat{z} + \frac{\pi^6\hat{z}}{(\mathrm{d}E/\mathrm{d}\lambda)_0}\left\{\frac{I_{\alpha\alpha}^2}{2}\left[\frac{\mathrm{d}}{\mathrm{d}\lambda}\left(\frac{v^4S^2}{\mathrm{d}E/\mathrm{d}\lambda}\right)\right]_0 - (vS)_0A_g - \left(vL_{1133}\frac{L_{1331}}{L_{3131}}\right)_0 A_{\rho g} - \left[L_{3333}\left(v\frac{L_{1331}}{L_{3131}}\right)^2\right]_0 A_{\rho\rho}\right\},$$

$$\overset{2}{z}_3 = 0 \quad \text{at } x_3 = \pm\frac{1}{2}, \tag{53}$$

where the constants A_g, $A_{\rho g}$ and $A_{\rho\rho}$ are given in terms of the above introduced auxiliary functions ρ and $\overset{4}{g}_\alpha$ [see definitions (A126)]. From linear operator theory, and in view of the singularity of $\mathscr{L}^t$ for λ_2, a solution to (52) exists when $M\hat{z} = 0$. Since it is assumed that $\hat{z} \neq 0$, $M = 0$ and (52) reduces to the homogeneous equation which, in view of the mode normalization condition, gives $\overset{2}{z}_3 = 0$. Also, in view of the fact that $M = 0$, the following expression for λ_4 is found

$$\lambda_4 = \frac{\pi^4}{(\mathrm{d}E/\mathrm{d}\lambda)_0}\left\{\frac{I_{\alpha\alpha}^2}{2}\left[\frac{\mathrm{d}}{\mathrm{d}\lambda}\left(\frac{v^4S^2}{\mathrm{d}E/\mathrm{d}\lambda}\right)\right]_0 - (vS)_0A_g - \left(vL_{1133}\frac{L_{1331}}{L_{3131}}\right)_0 A_{\rho g} - \left[L_{3333}\left(v\frac{L_{1331}}{L_{3131}}\right)^2\right]_0 A_{\rho\rho}\right\}. \tag{54}$$

This concludes the analysis in tension up to fourth order for λ_c. Higher order terms can be found in a similar manner.

3. CONSTITUTIVE LAWS

In this section specific material models are proposed for the stability analysis of the axially loaded beam. For the compressive case, the lowest bifurcation strain of the beam goes to zero for a vanishingly small cross section, and the corresponding asymptotic analysis, presented in the previous section, requires all material properties evaluated at zero strain. Since the response of most common structural materials about their unstressed state is elastic, a hyperelastic model has been adopted for the corresponding stability calculations. This choice gives us a consistent way of considering finite strains within the same material formulation, a necessary feature in view of our calculations for very stubbly beams (up to $\varepsilon = 1$).

For the tensile case, the lowest bifurcation strain of the beam approaches the necking strain (i.e. strain at maximum load) of the material as the cross sectional area

goes to zero. Motivated by metal plasticity, a J_2 deformation theory, which is fitted to a power law type uniaxial response capable of exhibiting a maximum load at reasonable levels of strain, is adopted for the stability calculations. The choice of the deformation theory version of the most popular theory of plasticity is due to its advantages for predicting experimental results involving a proportional loading path. The interested reader is referred to the detailed discussion of this subject in the review article by Hutchinson (1974).

3.1. *Elastic material*

The hyperelastic material model used in compression is a compressible version of the Mooney–Rivlin material. Assuming some compressibility, with an initial Poisson's ratio ν ($0 < \nu < 1/2$), a generalization of the standard incompressible Mooney–Rivlin material can be constructed (see Ogden, 1984) with the following strain energy density

$$W = A\left(\frac{I_1}{I_3^{1/3}} - 3\right) + B\left(\frac{I_2}{I_3^{2/3}} - 3\right) + \frac{A+B}{24}\frac{1+\nu}{1-2\nu}\left(I_3^2 - \frac{1}{I_3^2}\right)^2, \tag{55}$$

where I_1, I_2 and I_3 are the three invariants of the right Cauchy–Green tensor, $C_{ij} = F_{ki}F_{kj}$ where F_{ij} is the deformation gradient, namely

$$I_1 = C_{ii}, \quad I_2 = \tfrac{1}{2}[(C_{ii})^2 - C_{ij}C_{ij}], \quad I_3 = \tfrac{1}{6}\varepsilon_{ikm}\varepsilon_{jln}C_{ij}C_{kl}C_{mn}, \tag{56}$$

where ε_{ijk} is the alternating symbol in three dimensions.

The incremental moduli for this hyperelastic material, required in the general stability analysis [see (2)], are given by

$$L_{ijkl} = \frac{\partial^2 W}{\partial F_{ij}\,\partial F_{kl}}. \tag{57}$$

The uniaxial tangent modulus, $E(\lambda)$, relating the rate of the first Piola–Kirchhoff stress to the rate of the axial stretch ratio, defined in Section 2.3, is calculated numerically in terms of the incremental moduli, $L_{ijkl}(\lambda)$, which are evaluated on the principal equilibrium path [see definition (A91)]. For the asymptotic analysis in compression, the material properties enter through $E(\lambda)$ and $\mathrm{d}E(\lambda)/\mathrm{d}\lambda$ evaluated at $\lambda = \lambda_0 = 1$. For the exact FEM calculations, the incremental moduli are derived from (55) and (57).

3.2. *Elastoplastic material*

The hypoelastic model used in tension is a rate-independent plasticity model introduced by Stören and Rice (1975). It is a finite strain version of J_2 deformation theory of plasticity and its merits as a constitutive choice for stability calculations involving finitely strained metallic structures under a proportional loading path are extensively discussed in that reference. The incremental moduli of that theory expressed in the full Lagrangian formulation required by our general analysis are given by

$$L_{ijkl} = \frac{E_s}{1+\nu_s}\left[\frac{1}{2}(C^{-1}_{ik}C^{-1}_{jl}+C^{-1}_{il}C^{-1}_{jk})+\frac{\nu_s}{1-2\nu_s}C^{-1}_{ij}C^{-1}_{kl} - \frac{3}{2}\frac{\left(\frac{E_s}{E_t}-1\right)}{\left(\frac{E_s}{E_t}-\frac{1-2\nu_s}{3}\right)}\frac{S'_{ij}S'_{kl}}{\tau_e^2}\right] - \frac{1}{2}(S_{ik}C^{-1}_{jl}+S_{il}C^{-1}_{jk}+S_{jk}C^{-1}_{il}-S_{jl}C^{-1}_{ik}), \quad (58)$$

where E_s is the secant modulus and E_t is the tangent modulus for the uniaxial stress–strain curve

$$E_s = \frac{\tau}{\varepsilon}, \quad E_t = \frac{d\tau}{d\varepsilon}, \quad (59)$$

with τ being the Kirchhoff stress and ε the natural (logarithmic) strain. Both functions are taken to depend on the equivalent stress, τ_e, by considering a specific uniaxial response as it will be specified in the sequel. The physical components of the right Cauchy–Green tensor are C_{ij}, and C^{-1}_{ij} are the components of its inverse. The deviatoric stress components of the second Piola–Kirchhoff stress, S'_{ij}, are given by

$$S'_{ij} = S_{ij} - \tfrac{1}{3}C^{-1}_{ij}S_{kl}C_{kl}, \quad (60)$$

and the equivalent stress, τ_e, is expressed in terms of the second Piola–Kirchhoff stress deviator by

$$\tau_e^2 = \tfrac{3}{2}S'_{ij}S'_{ij}. \quad (61)$$

Finally, the secant Poisson ratio, ν_s, which is also a function of τ_e, is defined as follows

$$\nu_s = \frac{1}{2} - \frac{E_s}{E}\left(\frac{1}{2}-\nu\right). \quad (62)$$

It can be seen that for a material in the elastic range, $E_s = E$ and $\nu_s = \nu$, and as the material deforms deep into the plastic range, $E_s \to 0$ and $\nu_s \to 1/2$.

Some additional relations for the case of uniaxial tension, involving the Young's modulus $E(\lambda)$, the Poisson's ratio $\nu(\lambda)$, and the second Piola–Kirchhoff stress $S(\lambda)$, which enter the asymptotic stability results for tension need to be recorded at this point. In uniaxial tension the only non-zero component of the stress is the axial component

$$S(\lambda) = \frac{\tau}{\lambda^2}. \quad (63)$$

The uniaxial tangent modulus, $E(\lambda)$, introduced at the beginning of Section 2.3, is related to the tangent modulus, E_t, by

$$E(\lambda) = \frac{E_t}{\lambda^2} - S(\lambda). \tag{64}$$

The secant Poisson's ratio can be found by considering the following relation between the axial logarithmic strain, $\varepsilon = \ln \lambda$, and the transverse logarithmic strains, $\varepsilon_\alpha = \ln \lambda_\alpha$,

$$\varepsilon_1 = \varepsilon_2 = -\nu_s \varepsilon \tag{65}$$

from which the following expression can be deduced for the instantaneous Poisson's ratio, $\nu(\lambda)$, [see definition (A90)]

$$\nu(\lambda) = -\frac{\mathrm{d}\lambda_1}{\mathrm{d}\lambda} = \lambda_1 \left(\frac{\mathrm{d}\nu_s}{\mathrm{d}\lambda} \varepsilon + \frac{\nu_s}{\lambda} \right). \tag{66}$$

All the above recorded results are valid for a J_2 deformation theory model with an arbitrary uniaxial response. The specific uniaxial stress–strain behavior used in our calculations is a piecewise power law. Given the Young's modulus, E, and the yield strain, ε_y (and hence the yield stress, $\tau_y = E\varepsilon_y$), the stress–strain behavior for this model is assumed to be

$$\tau = \begin{cases} E\varepsilon & \text{if } \tau \leqslant \tau_y \\ \tau_y \left(\dfrac{\varepsilon}{\varepsilon_y} \right)^{1/m} & \text{if } \tau > \tau_y \end{cases} \tag{67}$$

where $m > 1$ and ε is the natural (logarithmic) strain ($\varepsilon = \ln \lambda$). The secant modulus for the piecewise power law is then found to be

$$E_s = \begin{cases} E & \text{if } \tau \leqslant \tau_y \\ E \left(\dfrac{\tau}{\tau_y} \right)^{1-m} & \text{if } \tau > \tau_y \end{cases} \tag{68}$$

while the tangent modulus is given by

$$E_t = \begin{cases} E & \text{if } \tau \leqslant \tau_y \\ \dfrac{E_s}{m} & \text{if } \tau > \tau_y \end{cases}. \tag{69}$$

For the power law material model the evaluation of the material properties at λ_0 can be simplified by noting that $\varepsilon_0 = \ln \lambda_0 = 1/m$. Using this observation along with (67)–(69) in (63), (64) and (66) we can evaluate at λ_0, $S(\lambda)$, $E(\lambda)$ and $\nu(\lambda)$ and their derivatives with respect to λ.

4. NUMERICAL SOLUTIONS

Accurate numerical solutions are sought for the three-dimensional stability problem for beams with several simply connected cross-sections. Their results, which by abuse of language are subsequently referred to as "exact" solutions, are compared to the

approximate asymptotic solutions presented in Section 2. It should be pointed out that the auxiliary geometric functions defined on the cross-section (i.e. θ_α, η_α, w and ψ), which are required for the asymptotic solutions, are also calculated numerically.

4.1. *Three-dimensional solution*

The exact three-dimensional solution to the bifurcation problem is found numerically by assuming a Fourier decomposition of the mode that satisfies (5), the flat surface kinematic boundary conditions at $x_3 = \pm L/2$

$$u_\alpha(x_i) = \sum_{n=1}^{\infty} \left\{ \overset{n}{u}_\alpha(x_\beta) \sin\left(\frac{(2n-1)\pi x_3}{L}\right) + \overset{n}{u}{}^*_\alpha(x_\beta) \cos\left(\frac{2n\pi x_3}{L}\right) \right\},$$

$$u_3(x_i) = \sum_{n=1}^{\infty} \left\{ \overset{n}{u}_3(x_\beta) \cos\left(\frac{(2n-1)\pi x_3}{L}\right) + \overset{n}{u}{}^*_3(x_\beta) \sin\left(\frac{2n\pi x_3}{L}\right) \right\}. \tag{70}$$

Substitution of (70) into the stability functional of Hill (1957), given in (1), reduces the three-dimensional stability problem to a two-dimensional one defined on the cross-section of the beam. The reduced problem is then solved by using a finite element discretization the cross-section. For the results shown here the discretization is based on four node quadrilaterals with bilinear shape functions.

For the stability of a beam with a circular cross-section another simplification can be made by taking advantage of axisymmetry. Making the coordinate transformation from Cartesian, x_1 and x_2, to polar, r and θ (where $x_1 = r\cos\theta$ and $x_2 = r\sin\theta$), an additional Fourier decomposition of the mode can be made in the θ direction. For this case the mode is assumed to be of the form

$$u_1(r,\theta,x_3) = \sum_{n=1}^{\infty}\sum_{k=0}^{\infty} \left\{ \overset{nk}{u}_1(r) \sin(k\theta) \sin\left(\frac{(2n-1)\pi x_3}{L}\right) + \overset{nk}{u}{}^*_1(r) \sin(k\theta) \cos\left(\frac{2n\pi x_3}{L}\right) \right\},$$

$$u_2(r,\theta,x_3) = \sum_{n=1}^{\infty}\sum_{k=0}^{\infty} \left\{ \overset{nk}{u}_2(r) \cos(k\theta) \sin\left(\frac{(2n-1)\pi x_3}{L}\right) + \overset{nk}{u}{}^*_2(r) \cos(k\theta) \cos\left(\frac{2n\pi x_3}{L}\right) \right\}$$

$$u_3(r,\theta,x_3) = \sum_{n=1}^{\infty}\sum_{k=0}^{\infty} \left\{ \overset{nk}{u}_3(r) \sin(k\theta) \cos\left(\frac{(2n-1)\pi x_3}{L}\right) + \overset{nk}{u}{}^*_3(r) \sin(k\theta) \sin\left(\frac{2n\pi x_3}{L}\right) \right\}. \tag{71}$$

With the substitution of (71) into (1) the three-dimensional problem is reduced to its one-dimensional counterpart.

An LDU Cholesky decomposition of the resulting stiffness matrix for the discretized problem is performed at each load level, λ, and the minimum entry, D_m, of the diagonal matrix, $\mathbf{D}$, is found. The first bifurcation is signaled by the change in sign of D_m from positive to negative as the stretch ratio increases monotonically away from one. A bisection method is combined with the incremental change of λ for a greater accuracy in the numerical determination of λ_c. The analysis is repeated for several values of the axial wave number, n, but the lowest critical load is invariably found to correspond to $n = 1$, in agreement with the asymptotic results of Section 2. In addition, for the axisymmetric formulation of the circular beams, the lowest critical load

corresponds to a circumferential wave number $k = 1$ for compression and $k = 0$ for tension, as expected from the asymptotic results of Section 5.

4.2. *Asymptotic solution*

For the case of compression the auxiliary functions $\theta_\alpha(x_1, x_2)$, $\eta_\alpha(x_1, x_2)$, $w(x_1, x_2)$ and $\psi(x_1, x_2)$ are required. The governing equations for these functions, (A54)–(A56) and (A60), are given in variational form which leads naturally to a numerical solution scheme based on the finite element method.

For the case of tension it is necessary to find the auxiliary function $\overset{4}{g}_\alpha(x_1, x_2)$. The variational formulation of this problem is given in (A114). Since the moduli are isotropic in the x_1x_2 plane, finding a solution to (A114) is equivalent to solving a two-dimensional elasticity problem on the domain of the cross-section. Once again these functions are found using the finite element method.

To solve for the auxiliary functions used in compression and tension, the same discretization of the cross-section was used as in the calculation of the three-dimensional solution. The cross-sectional constants necessary for the evaluation of λ_4 for both compression (42) and tension (53) are calculated by numerical integration of the auxiliary functions.

5. RESULTS AND DISCUSSION

Since analytical solutions for the asymptotic problem can be found for the case of a circular cross section, this is the first case examined. The asymptotic analytical solution for the stability problem of a cylinder in compression and tension is compared with the numerical solution of its three-dimensional counterpart. The connection of our results to existing slenderness corrections of the Euler buckling load is also discussed.

More complex sections are subsequently examined in compression and tension using finite element solutions for the asymptotic and three-dimensional problems. A square section, a symmetric cruciform section and an asymmetric L-section are investigated. As an aid to the reader the $O(\varepsilon^2)$, $O(\varepsilon^4)$ and exact critical strains are depicted in all subsequent figures by dashed, dotted and solid curves, respectively.

5.1. *Compression*

The hyperelastic material model used in compression is a compressible version of the Mooney–Rivlin solid whose strain energy density is given by (55). The $O(\varepsilon^2)$ and $O(\varepsilon^4)$ asymptotic results for the critical load and mode as well as the corresponding classical engineering approximations are compared with the finite element solution to the three-dimensional stability problem. For all calculations reported here the material constants in (55) are nondimensionalized such that $A = 1$, $B = 0.8$, and $\nu = 0.3$. This nondimensionalization gives an initial Young's modulus $E = 4(A+B)(1+\nu) = 9.36$.

5.1.1. *Compression: circular section.* The first section examined is a circular cylinder with initial radius R and length L. For this case $\varepsilon = \sqrt{\pi R/L}$. The circular

cylinder in compression has the advantage of having an analytical asymptotic solution. In addition, the numerical solution of the three-dimensional problem is considerably simplified by making use of the axisymmetry of the cross-section thus reducing the three-dimensional stability problem to a one-dimensional problem according to (71). In order to study the mesh effects for the four node quadrilaterals, which are used in all subsequent calculations, the results of the numerical solution, which follows the general formulation of the problem in (70), have been compared with the axisymmetric numerical solution.

For a circular section with a normalized area, $A = 1$, the radius is $R = 1/\sqrt{\pi}$. The following area constants, defined in (A45), (A66) and (A80), are found to be

$$I_{11} = I_{22} = \frac{1}{4\pi}, \quad H_1 = H_2 = 0, \quad K = \frac{1}{12\pi^2}. \tag{72}$$

For the constants involving the Saint-Venant torsion function, defined in (A60) and found in this case to be $\psi = (1/\pi - x_1^2 - x_2^2)/2$, the following results are obtained from (A61)

$$J = \frac{1}{2\pi}, \quad I_1^{\psi} = I_2^{\psi} = 0. \tag{73}$$

As expected for a circular section, no warping occurs, i.e. $w = 0$, and the related constants, defined by (A61) and (A80), vanish

$$I_{\alpha}^{w} = K_{\alpha}^{w} = 0. \tag{74}$$

The auxiliary functions, θ_α and η_α, defined in (A54) and (A55), take the following form:

$$\theta_\alpha = -\frac{1}{4}\left(x_1^2 + x_2^2 - \frac{1}{\pi}\right)x_\alpha, \tag{75}$$

$$\eta_\alpha = \frac{1}{4}\left(x_1^2 + x_2^2 - \frac{3}{\pi}\right)x_\alpha. \tag{76}$$

The area constants which depend on θ_α and η_α are subsequently calculated from (A78) and (A79)

$$K_{\alpha\beta}^{\theta} = -\frac{1}{24\pi^2}\delta_{\alpha\beta}, \quad L_{\alpha\beta}^{\theta} = \frac{1}{48\pi^2}\delta_{\alpha\beta}, \tag{77}$$

$$K_{\alpha\beta}^{\eta} = \frac{1}{24\pi^2}\delta_{\alpha\beta}, \quad L_{\alpha\beta}^{\eta} = -\frac{7}{48\pi^2}\delta_{\alpha\beta}. \tag{78}$$

Substituting the above results into (20), the asymptotic expression for λ_c, the following expression is found for the critical stretch ratio

$$\lambda_c = 1 - \varepsilon^2\frac{\pi}{4} + \varepsilon^4\frac{\pi^2}{48}\left(\frac{3}{2E}\frac{\mathrm{d}E}{\mathrm{d}\lambda}\bigg|_{\lambda=1} + 4 - \frac{\nu(1+2\nu)}{1+\nu}\right) + O(\varepsilon^6). \tag{79}$$

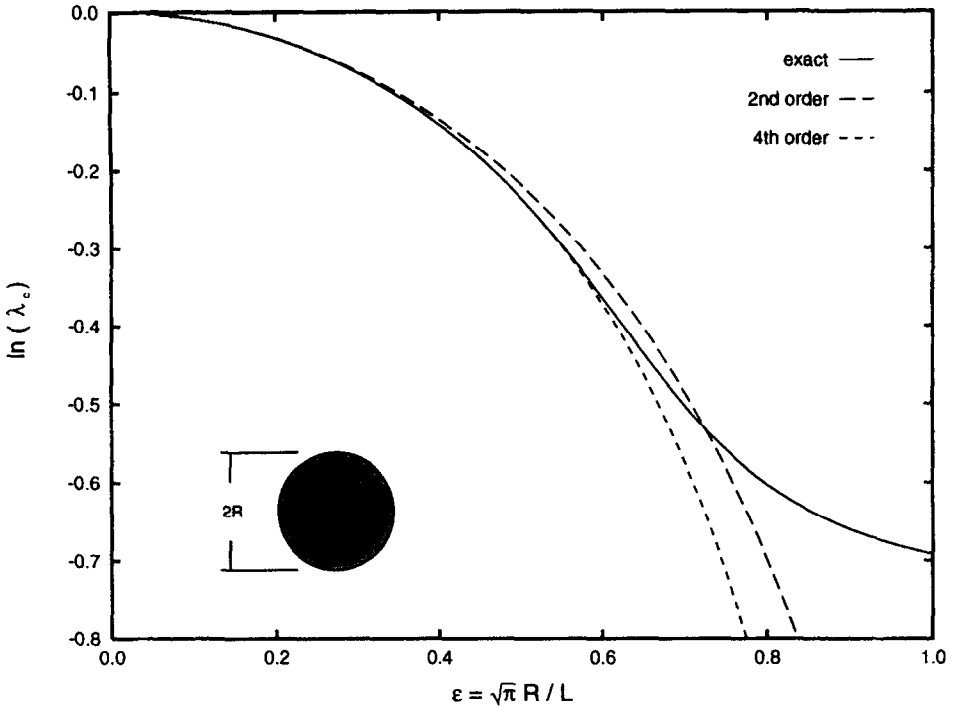

Fig. 2. Critical buckling strain, $\ln(\lambda_c)$, as a function of the slenderness parameter, ε, for the axial compression of an elastic beam with a circular cross section. Exact results are denoted by the solid curve (—), while the $O(\varepsilon^2)$ (engineering theory) and $O(\varepsilon^4)$ asymptotic results are depicted by dashed (- - -) and dotted (· · ·) curves, respectively.

The results for a circular cylinder, comparing the exact solution of the three-dimensional problem, found numerically, and the asymptotic solutions up to second order (Euler beam buckling theory) and fourth order, are shown in Fig. 2. The second order (Euler) solution gives good results up to $\varepsilon = 0.40$ where the percent error is still under 5%. The fourth order solution gives comparable results (percent error less than 5%) for values of ε up to 0.65. This shows a considerable improvement over the Euler solution. For stubbier beams ($\varepsilon > 0.65$) the fourth order asymptotic solution and the exact solution begin to diverge. Notice also that the exact solution is bounded between the second and fourth order solutions.

The $O(\varepsilon^4)$ term in (79), which provides the first slenderness correction to Euler's critical strain, merits a more detailed discussion due to the interesting history of the subject. Efforts to correct Euler's critical load to account for the beam's slenderness can be dated back to Engesser, according to Timoshenko (1936) who gives an approximate correction for Euler's formula due to shearing effects in columns with arbitrary sections. Recently, Kardomateas (1995), revisited the same question and used a three-dimensional calculation to find the critical load of an orthotropic elastic cylinder under finite compressive strain. The approximate method of Timoshenko and the exact results of Kardomateas produce critical loads for an isotropic elastic cylinder,

which are lower than the Euler load. This result is in contrast to our result in Fig. 2, where the $O(\varepsilon^4)$ correction to the critical strain is always larger in magnitude than its Euler, $O(\varepsilon^2)$, counterpart. This difference is attributed to the presence of the initial curvature of the stress–strain $(\mathrm{d}E/\mathrm{d}\lambda)_{\lambda=1}$ term in the $O(\varepsilon^4)$ term appearing in the expression for λ_c in (79). It must be pointed out that the initial curvature of the stress–strain curve, which is absent from both Timoshenko's (1936) and Kardomateas' (1995) results, depends strongly on the finite strain formulation adopted for the material, even for the linear elastic range of its response. To be more specific, consider three elastic materials with the following uniaxial responses:

(i) $\pi = E(\lambda - 1)$ (engineering stress, π,† is proportional to engineering strain, $\lambda - 1$)
(ii) $\sigma = E \ln \lambda$ (true stress, σ, is proportional to true strain, $\ln \lambda$)
(iii) $\tau = E \ln \lambda$ (Kirchhoff stress, τ, is proportional to true strain, $\ln \lambda$).

All three solids share the same linearized uniaxial behavior for infinitesimal strains. Noting the definition of the stretch-dependent Young's modulus $(E(\lambda) = \mathrm{d}\pi(\lambda)/\mathrm{d}\lambda)$ and recalling the relations between the different stress measures $(\tau = \lambda\pi = J\sigma)$ as well as the kinematic relations for the volume change in uniaxial stretching $(J = \lambda\lambda_1^2)$, where the lateral strain, $\lambda_1(\lambda)$, is related to Poisson's ratio by (66), we obtain the following results for the corresponding initial curvature of the stress–strain curve $(\mathrm{d}E/\mathrm{d}\lambda)_{\lambda=1}$

(i) $(\mathrm{d}E/\mathrm{d}\lambda)_{\lambda=1} = 0$
(ii) $(\mathrm{d}E/\mathrm{d}\lambda)_{\lambda=1} = -E(1+4\nu)$
(iii) $(\mathrm{d}E/\mathrm{d}\lambda)_{\lambda=1} = -3E.$

The first choice (i) gives an $O(\varepsilon^4)$ critical strain for the cylinder lower in absolute value than the Euler $[O(\varepsilon^2)]$ strain, while the last choice (iii) gives an $O(\varepsilon^4)$ result larger in absolute value than the Euler strain. For the constitutive choice adopted in (55), $(\mathrm{d}E/\mathrm{d}\lambda)_{\lambda=1} = -4.66$, which, in view of (79), explains why the $O(\varepsilon^4)$ correction gives a critical strain higher in absolute value than its Euler counterpart.

The influence of the initial curvature of the uniaxial stress–strain response to the first order slenderness correction for the Euler load, and the importance of the choice for the stress and strain measures, even for a linear elastic behavior, has not been discussed in the literature, to the best of our knowledge. In our asymptotic approach, we adopt a constitutive equation in its finite strain version *ab initio* and follow a full Lagrangian description of the stability problem, thus obtaining a consistent approximation of the critical load which is accurate to any order desired.

The circular cylinder is also used to determine the accuracy of the finite element discretization employed for arbitrary sections. The three-dimensional stability analysis is carried out by using the Fourier decomposition in x_3 and θ [see (71)], thus reducing the three-dimensional problem to a one-dimensional problem. The results of this calculation are compared with the general Fourier decomposition in x_3 [see (70)], used for arbitrary sections, where the circular section being meshed with four node quadrilaterals. For quadrilaterals with a maximum mesh size of $0.10R$, and for

† The engineering (1st Piola–Kirchhoff) stress, π, is not to be confused with its more standard definition as the constant 3.14159, which is used in the rest of this paper.

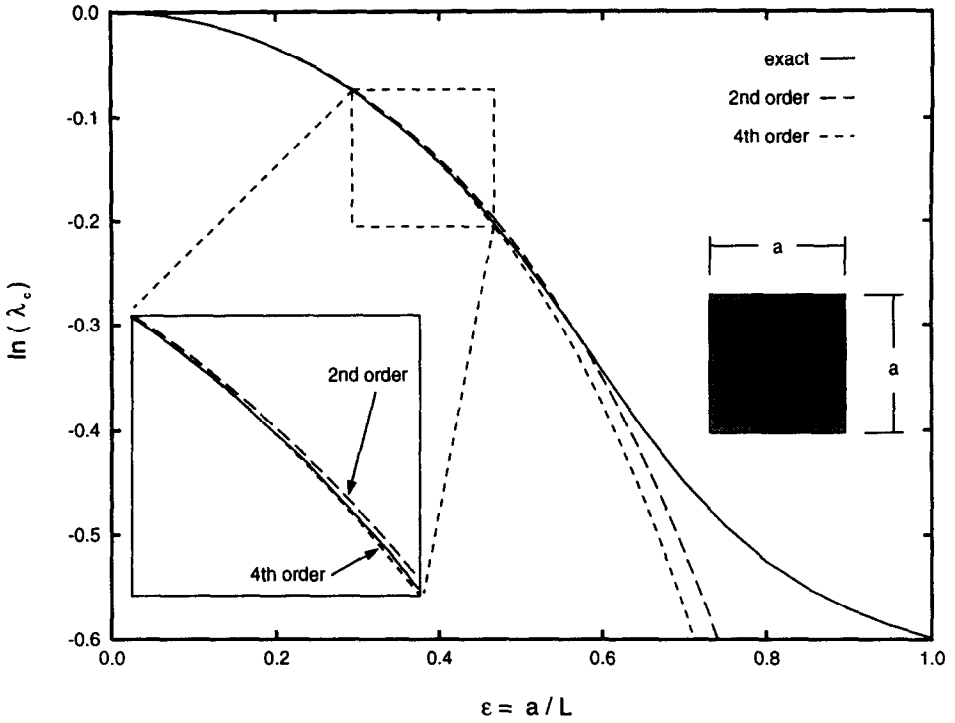

Fig. 3. Critical buckling strain, $\ln(\lambda_c)$, as a function of the slenderness parameter, ε, for the axial compression of an elastic beam with a square cross section. Exact results are denoted by the solid curve (—), while the $O(\varepsilon^2)$ (engineering theory) and $O(\varepsilon^4)$ asymptotic results are depicted by dashed (- - -) and dotted (· · ·) curves, respectively.

axisymmetric radial elements of the same size, the difference in the predicted loads is approximately 0.05% for $\varepsilon = 0.5$.

5.1.2. *Compression*: *square section.* The next shape examined is the square cross-section. The corresponding critical strain dependence on $\varepsilon = a/L$ is shown in Fig. 3. Similar to the circular case, the exact solution lies between the second (Euler buckling) and fourth order asymptotic curves, with the latter overestimating and the former underestimating the size of the critical strain. The band between the second and fourth order asymptotic curves is narrower than in the case for the circular section, but the corresponding ε region of validity of the asymptotic solution is smaller (up to about $\varepsilon = 0.5$). Hence, for $\varepsilon = 0.4$ the percent error between the fourth order solution and the exact solution is 1% while for the Euler solution the percent error is only 2%. As ε increases to 0.50 the percent error between the fourth order and exact solutions increases to 3% and for $\varepsilon = 0.60$ the error is up to 8.5%. A temporary improvement in the Euler solution occurs here only because the exact solution is crossing over the second order curve as the solutions diverge.

The calculations for the square section show that the asymptotic results up to fourth order improve the estimation of the critical strain, but only up to a lower value

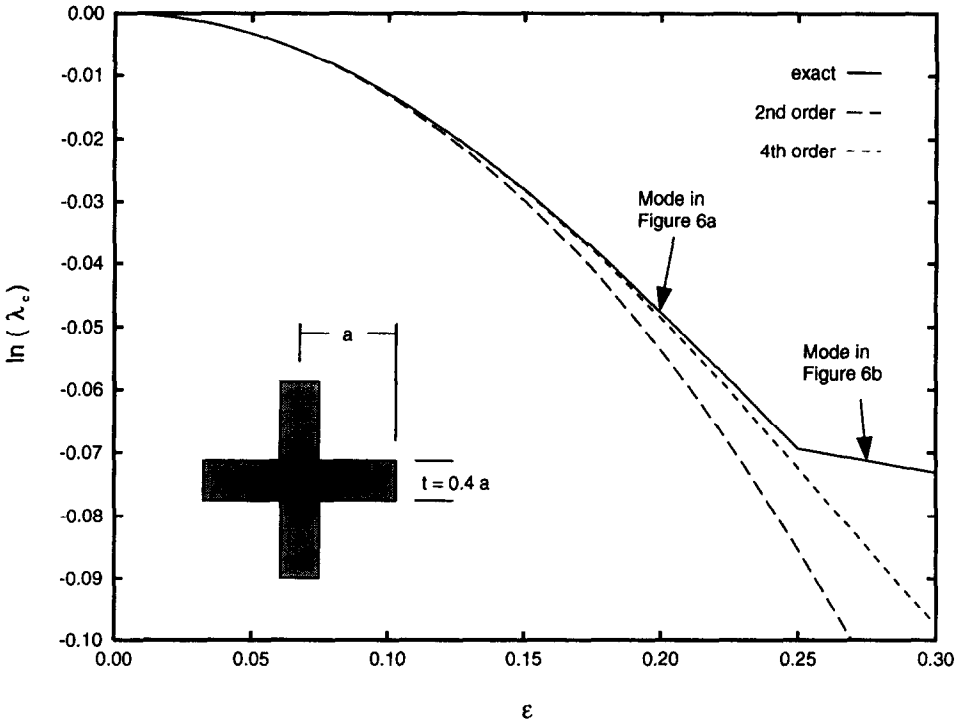

Fig. 4. Critical buckling strain, $\ln(\lambda_c)$, as a function of the slenderness parameter, ε, for the axial compression of an elastic beam with a thick cruciform cross section. Exact results are denoted by the solid curve (—), while the $O(\varepsilon^2)$ (engineering theory) and $O(\varepsilon^4)$ asymptotic results are depicted by dashed (- - -) and dotted (· · ·) curves, respectively. The discontinuity in the exact solution is due to the change of the critical mode from bending to torsion.

of ε than the improvement for the circular section. Moreover, the improvement is not as close to the exact critical load when compared to the case of the circular cylinder.

5.1.3. *Compression: cruciform section.* The investigation continues with the symmetric cruciform section which has two orthogonal axes of symmetry with four arms of length a and thickness t. From stability theory for linear elastic thin-walled beams (hereafter referred to as the engineering theory) it is known that as the ratio t/a becomes smaller shear effects become more important. Consequently the engineering theory coincides with the second order asymptotic result only for the case when the bending mode is dominant (i.e. for adequately low values of ε). The engineering theory also gives uncoupled bending and torsion modes, since the shear center coincides with the centroid of the section (see Brush and Almroth, 1975).

The critical strain's dependence on ε for the thick cruciform section, which has a t/a ratio of 0.40, is shown in Fig. 4. As expected, the critical mode for a slender beam is a bending mode as evidenced by the coincidence between the asymptotic results and exact results as $\varepsilon \to 0$. For this thick walled section the second order asymptotic results always coincide with the engineering theory, which cannot predict any torsional critical mode. Notice that unlike the circular and square sections, the magnitude of

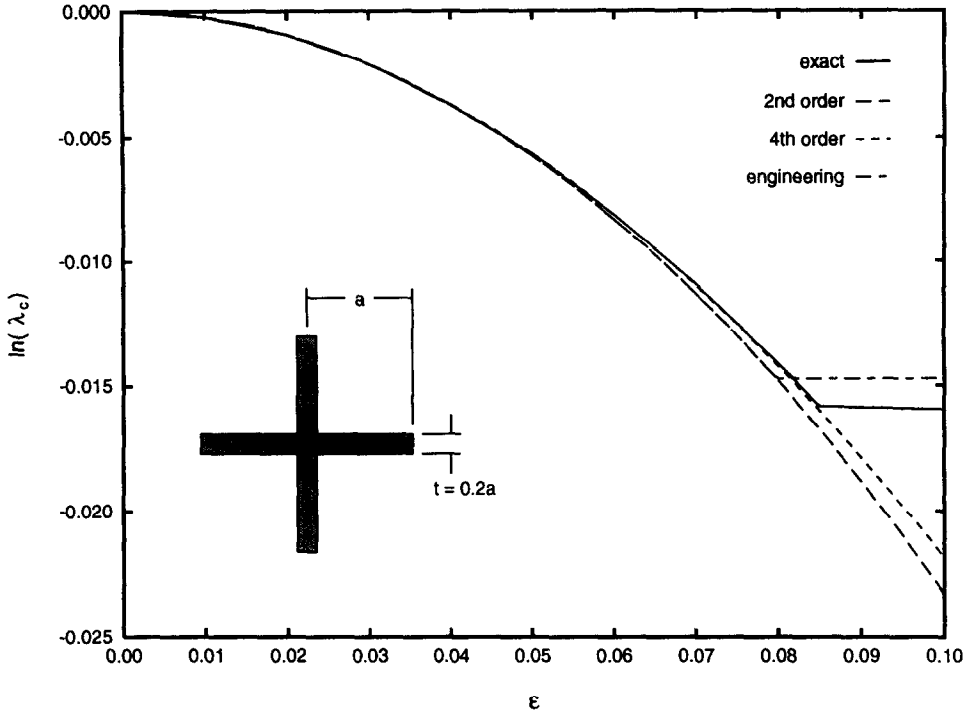

Fig. 5. Critical buckling strain, $\ln(\lambda_c)$, as a function of the slenderness parameter, ε, for the axial compression of an elastic beam with a thin cruciform cross section. Exact results are denoted by the solid curve (—), while the $O(\varepsilon^2)$ (engineering theory for bending) and $O(\varepsilon^4)$ asymptotic results are depicted by dashed (- - -) and dotted (· · ·) curves, respectively. The results of the complete engineering theory for bending and torsion, plotted in dashed–dotted curve (- · - · -), under-predict the critical strain of the torsional mode.

the exact critical strain is consistently overestimated by both the second and fourth order theories, although the latter gives a much improved estimate of the exact results than the former. Even for beams as stubby as $\varepsilon = 0.25$ the discrepancy between the fourth order and the exact solution is only 4.5% as compared to the corresponding discrepancy for the second order (engineering theory) result which is 23%. For beams stubbier than the characteristic value of $\varepsilon = 0.25$, the accuracy of the two asymptotic approximations is a moot point since the torsional mode becomes the critical buckling mode, as evidenced by the abrupt change in slope of the exact critical strain curve at $\varepsilon = 0.25$.

The critical strain's dependence on ε for the thin cruciform section, with a t/a ratio of 0.20, is depicted in Fig. 5. For relatively slender beams, $\varepsilon < 0.08$, where the critical mode is the bending one, the trends are similar to the results for the thick cruciform section case, with the exact critical strain overestimated by the two asymptotic curves and with the fourth order curve giving a better approximation than the second order curve. Notice that for this thin-walled beam, and in contrast to the thick beam, the engineering theory, depicted by the dashed–dotted curve, predicts that a torsional mode is the critical mode for $\varepsilon > 0.08$ which explains the horizontal line emerging from

the second order curve. (In the engineering theory the critical strain corresponding to the torsional mode is independent of the length of the beam.) Although the ε range of validity of the asymptotic approximations is limited by the presence of the torsional mode, the fourth order asymptotic results provide a better approximation of the exact critical strain. It is also interesting to note that the engineering theory slightly overestimates the critical strain of the torsional mode, but underestimates the transition value of the slenderness parameter ε.

The mode switch behavior of the cruciform columns is depicted in the axonometric plots of Fig. 6, which shows the bending and torsional modes of the thin-walled beam at its middle section, $x_3 = 0$, for $\varepsilon = 0.05$ and $\varepsilon = 0.10$, respectively. These results are based on the exact finite element calculations. A comparison of the exact mode (shown in the solid curve) in Fig. 6(a) with the corresponding $O(\varepsilon^4)$ asymptotic result (shown in the dotted curve) show an excellent agreement in all three components of the mode (maximum discrepancy in any component of the order of 1%). Unlike the bending mode in Fig. 6(a), the torsional mode in Fig. 6(b) has no bending and considerable warping. Had this mode been plotted also at the ends $x_3 = \pm L/2$ the torsional nature of the mode would have been obvious, which in this case is a rotation about the x_3 axis.

One can thus conclude for the cruciform section the $O(\varepsilon^4)$ approximation of the critical strain is a considerable improvement over the $O(\varepsilon^2)$ engineering theory approximation, assuming that the critical mode is a bending mode and not a torsional mode. The range of validity in ε of these asymptotic approximations increases, and their accuracy improves, for thicker beams ($t/a \to 1$), i.e. as all dimensions of the cross section become commensurate. Similar conclusions are expected for other doubly symmetric sections.

5.1.4. *Compression: L-section.* All the cross-sections investigated up to this point have at least two orthogonal axes of symmetry. This symmetry implies, from the classical engineering buckling theory (e.g. Brush and Almroth, 1975), the separation between the bending and torsional modes due to the coincidence of the shear center and the centroid of the cross-section. Moreover, for slender enough beams, the bending mode is the critical mode, in agreement with the asymptotic analysis. For asymmetric cross-sections the engineering buckling theory predicts a coupled critical mode with bending and torsional components. According to the proposed general asymptotic analysis, the torsional information is first included in the $O(\varepsilon^4)$ terms of the expansion of the critical stretch ratio. Hence a considerable improvement in the approximation of the critical strain is expected for the asymmetric cross-section case by using the $O(\varepsilon^4)$ asymptotic results.

An L-section with two legs of unequal lengths, a and $b = 0.6a$, but of equal thickness, t, is the asymmetric section used to verify the hypothesis made above. Similar to the cruciform section, the leg thickness parameter, t/a, is taken to be 0.4 for the thick L-section and 0.2 for the thin L-section.

The exact and approximate critical strains for the thick L-section are shown in Fig. 7. In contrast to the cruciform section, the exact critical strain is bounded from above and below by the $O(\varepsilon^2)$ and $O(\varepsilon^4)$ asymptotic curves. As the slenderness parameter, ε, increases there is a larger discrepancy between the second order curve and the exact

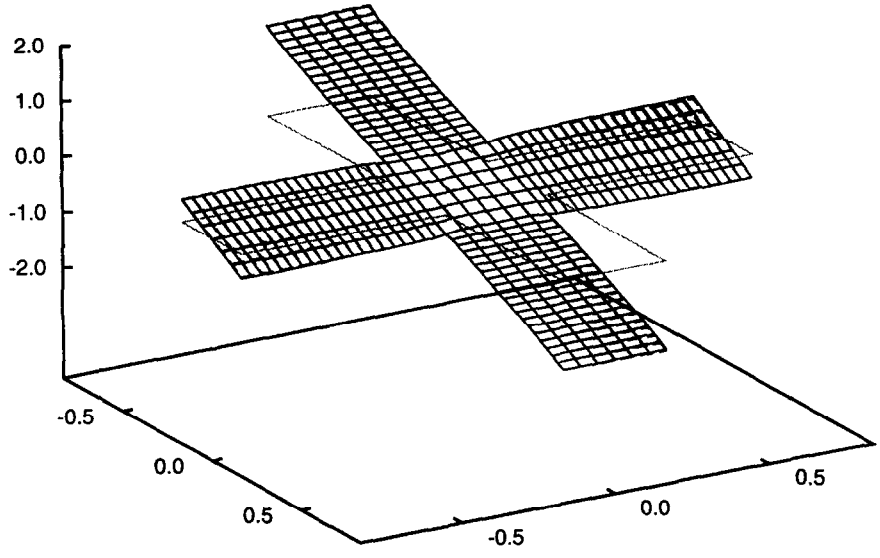

(a)

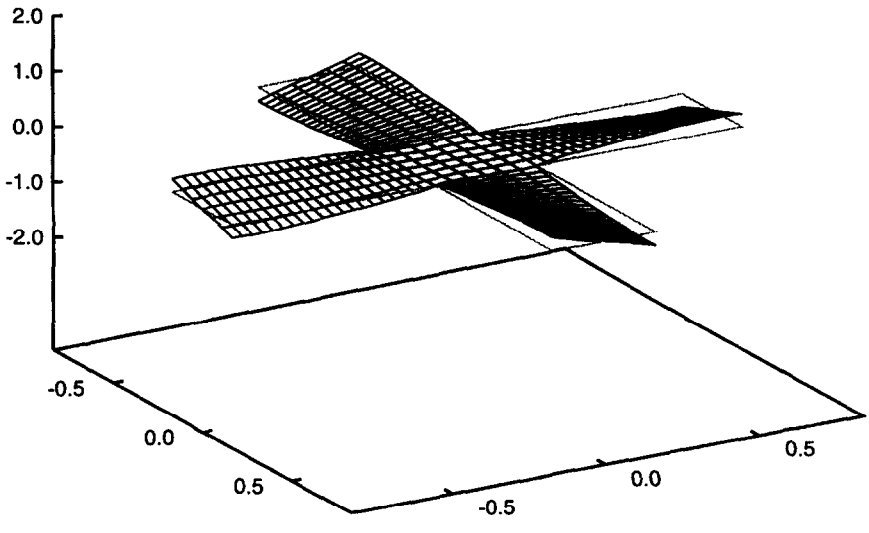

(b)

Fig. 6. Axonometric plot of critical modes at $x_3 = 0$ for a thick cruciform section. Results in (a) show the critical bending mode for an elastic beam with $\varepsilon = 0.20$ for the exact (—) and $O(\varepsilon^4)$ asymptotic (- - -) modes. The exact critical torsional/warping mode for a stubbier beam with $\varepsilon = 0.275$ is depicted in (b).

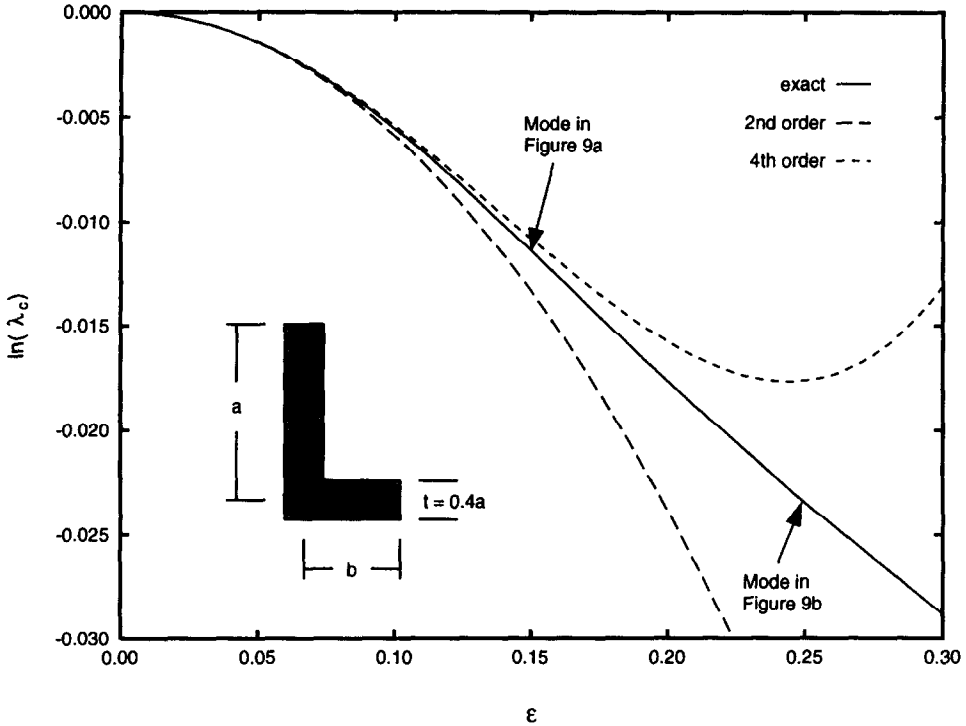

Fig. 7. Critical buckling strain, $\ln(\lambda_c)$, as a function of the slenderness parameter, ε, for the axial compression of an elastic beam with a thick L cross section. Exact results are denoted by the solid curve (—), while the $O(\varepsilon^2)$ (engineering theory) and $O(\varepsilon^4)$ asymptotic results are depicted by dashed (- - -) and dotted (· · ·) curves, respectively. Note the absence of a discontinuity in the exact critical load curve due to the mixed (combined bending and torsion) nature of the mode.

results for the L-section due to the presence of the torsional component of the eigenmode. As expected, the fourth order correction brings a considerable improvement in the prediction of the critical strain for values of ε up to 0.15. At this point the error between the fourth order asymptotic approximation and the exact solution is about 5%, while the second order asymptotic approximation differs from the exact critical load by 17%: for $\varepsilon > 0.25$ there is a severe divergence between the exact and approximate critical strains.

The exact and approximate critical strains for the thin L-section are shown in Fig. 8. Although the general trends are very similar to those of the thick L-section of Fig. 7, the ε range of validity of the approximate result is considerably smaller, about a third of the range for the thick section. As for the thin cruciform column, the classical engineering buckling prediction, plotted with a dashed–dotted curve, has been added to the results in Fig. 8. It is worth noting that the classical buckling theory for thin-walled beams gives the better overall prediction over a wider range of ε (up to $\varepsilon = 0.1$) than the asymptotic results up to fourth order.

The coupling between the bending and torsion that is always present in the eigenmodes of the L-section is depicted in Fig. 9. More specifically the results for the

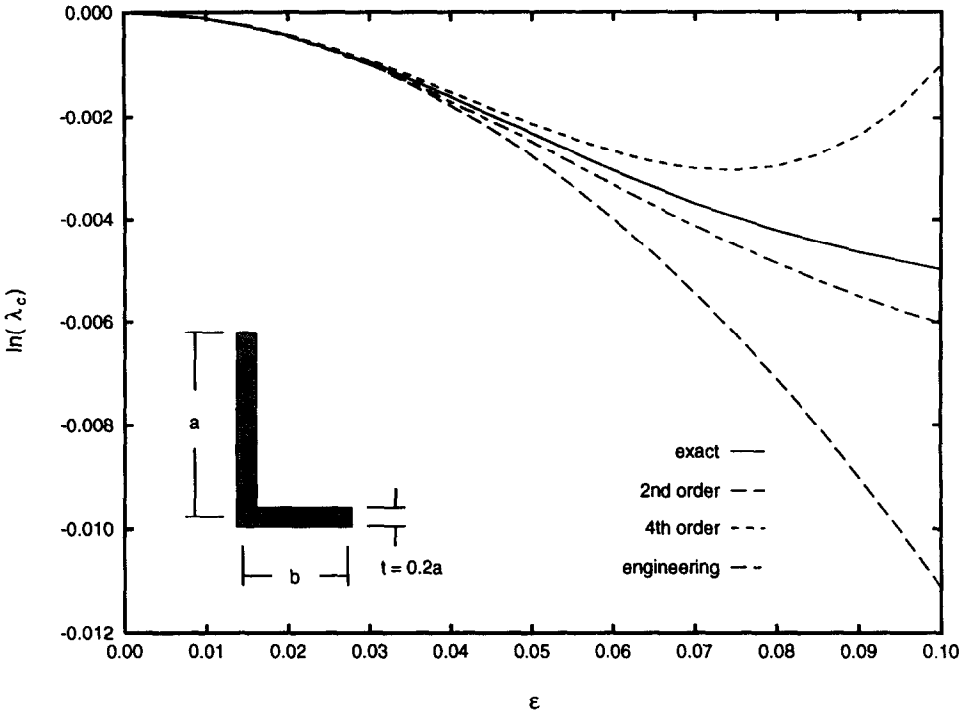

Fig. 8. Critical buckling strain, $\ln(\lambda_c)$, as a function of the slenderness parameter, ε, for the axial compression of an elastic beam with a thin L cross section. Exact results are denoted by the solid curve (—), while the $O(\varepsilon^2)$ and $O(\varepsilon^4)$ asymptotic results are depicted by dashed (- - -) and dotted (· · ·) curves, respectively. The results of the engineering theory, plotted in dashed–dotted curve (- · - ·), give in this case the best approximation of the exact critical load.

exact mode, depicted in Fig. 9(a), correspond to a thick L-section beam with $\varepsilon = 0.15$ where the bending and twisting of the cross section are evident, as is also the planarity of the deformed cross-section. The mode for a stubbier beam, $\varepsilon = 0.25$, with the same thick L-section, is depicted in Fig. 9(b). This mode shows a considerable amount of warping added to the bending and torsional components of the mode.

5.1.5. *Compression: critical mode comparison.* All the discussions thus far pertained to the accuracy of the different order asymptotic results for the critical strain. The investigation of the accuracy for the asymptotic expressions for the critical mode is also of interest and the corresponding results are plotted in Fig. 10 for two different cross-sections. In each case we calculate the relative error of the approximate eigenmode, $\mathbf{u}_a$, by taking the L_2 norm of the error, $\|\mathbf{u}_e - \mathbf{u}_a\|$ over the L_2 norm of the exact eigenmode, $\|\mathbf{u}_e\|$. The errors for the $O(\varepsilon^2)$ and $O(\varepsilon^4)$ approximations as functions of the slenderness parameter, ε, are presented with the solid and dashed curves, respectively, for the square section in Fig. 10(a) and the cruciform section in Fig. 10(b).

For both sections the error in the mode increases monotonically with the slenderness parameter ε. For $\varepsilon < 0.20$, the error in the $O(\varepsilon^4)$ approximation is almost an order of magnitude less than the error for the $O(\varepsilon^2)$ approximation. Even for much stubbier

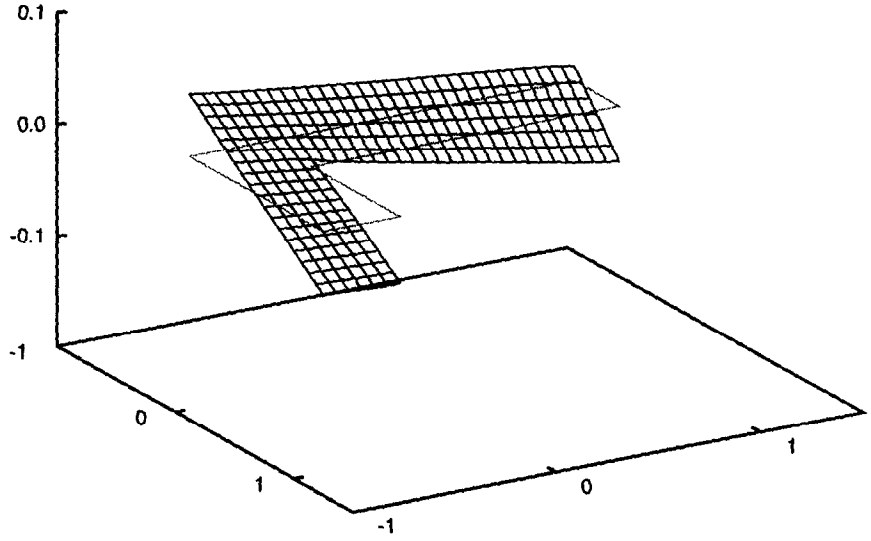

(a)

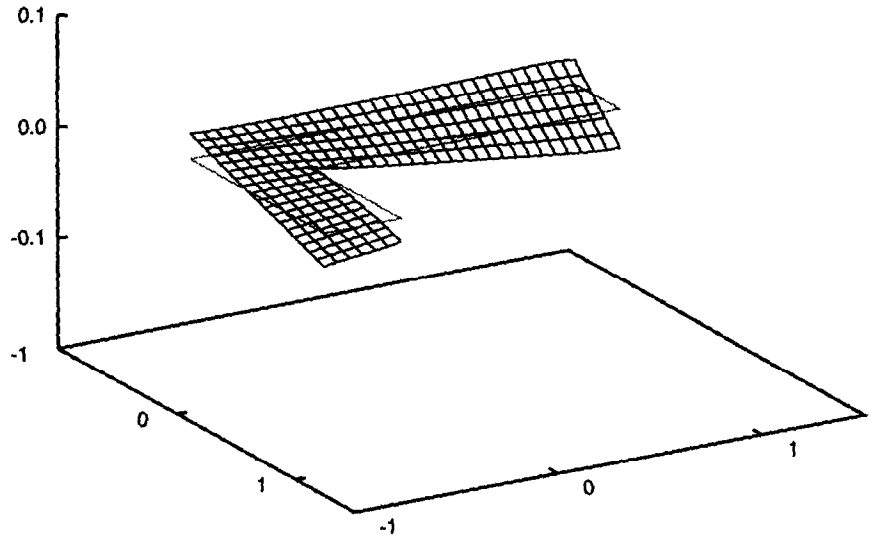

(b)

Fig. 9. Axonometric plot of critical modes at $x_3 = 0$ for a thick L-section. Results in (a) show the critical mode for a relatively slender beam with $\varepsilon = 0.15$. The mode is a combined bending/torsional mode, as expected from the engineering and asymptotic theories. The plot in (b) corresponds to a stubbier beam with $\varepsilon = 0.25$. Notice the presence of a strong warping effect in addition to the primary bending/torsional mode.

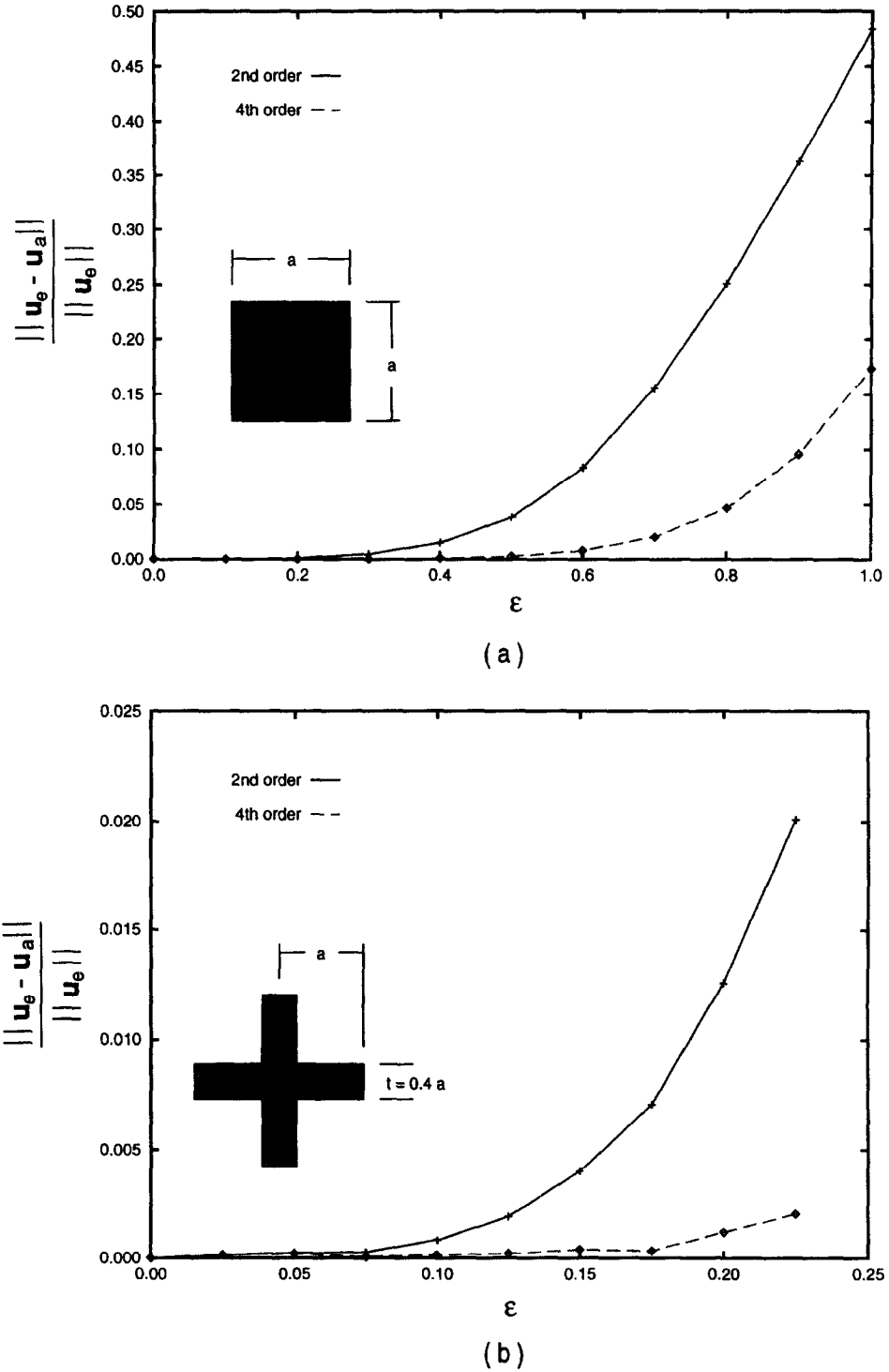

Fig. 10. Error of the asymptotic $O(\varepsilon^2)$, solid curve (—), and $O(\varepsilon^4)$, dashed curve (- - -), eigenmode as a function of the slenderness parameter, ε, for an axially compressed elastic beam with a square cross-section (a) and with a thick cruciform section (b).

beams, as in the case of the square section with $\varepsilon = 0.60$, the error in the $O(\varepsilon^4)$ approximation of the mode is still less than 1%.

5.2. *Tension*

The hypoelastic model used in tension is a finite strain version of the J_2 deformation theory of plasticity described in Section 3.2. The results from the $O(\varepsilon^2)$ and $O(\varepsilon^4)$ asymptotic analyses are compared with the finite element solution to the three-dimensional stability problem for beams with several different cross-sections. The sections investigated are the same as those for compression with the exception of the two L-shaped sections. For all calculations reported here the hardening exponent for the material's uniaxial stress strain curve is $m = 10$ and the yield strain is $\varepsilon_y = 0.001$. Consequently the strain at maximum load is $\varepsilon_0 = \ln \lambda_0 = 1/m = 0.10$.

5.2.1. *Tension: circular section.* As in the case of compression, the asymptotic solution for a circular cross-section beam with an initial radius R and length L can be found analytically. In addition to the moments of inertia [see (72)] and the material constants, which are calculated from the solid's uniaxial response [see (50) and (54)], the complete determination of the expansion of λ_c up to $O(\varepsilon^4)$ requires the constants A_g, and $A_{\rho g}$ which depend on the auxiliary functions $\overset{4}{g}_\alpha$. These functions, defined in (A114), can be solved for analytically and are found to be

$$\overset{4}{g}_\alpha = [A(x_1^2 + x_2^2) + B]x_\alpha, \tag{80}$$

where the coefficients A and B are given by

$$A = \frac{\overset{0}{\nu}}{8\overset{0}{L}_{1111}}\left(\overset{0}{S} - \overset{0}{L}_{1133}\frac{\overset{0}{L}_{3113}}{\overset{0}{L}_{3131}}\right), \quad B = -\frac{\overset{0}{\nu}}{\pi}\left(\frac{3\overset{0}{L}_{1111} + \overset{0}{L}_{1122}}{\overset{0}{L}_{1133}}A - \frac{\overset{0}{\nu}\overset{0}{L}_{3113}}{4\overset{0}{L}_{3131}}\right). \tag{81}$$

Recalling also the definition of $\rho(x_\alpha)$ given by (A97), the constants A_g, $A_{\rho g}$, and $A_{\rho\rho}$ in (54) can be evaluated as follows

$$A_g = \frac{2A + 3B\pi}{6\pi^2}, \quad A_{\rho g} = \frac{A}{6\pi^2}, \quad A_{\rho\rho} = \frac{1}{48\pi^2}. \tag{82}$$

Using (82) in (54), and recalling the constitutive relations from Section 3.2, we obtain the wanted analytical result for the $O(\varepsilon^4)$ asymptotic expansion for the critical stretch ratio of a power law type elastoplastic circular cylinder in tension. The expressions for the material constants based on the solid's uniaxial response, although straightforward, are cumbersome and will not be displayed.

The critical strain results comparing the exact solution of the three-dimensional problem, found numerically, and the analytically calculated asymptotic expansions up to second order and fourth order are shown in Fig. 11. All curves emerge at $\varepsilon_0 = 0.10$, the strain at maximum load. Note the extended range of validity of the $O(\varepsilon^4)$ asymptotic results for very stubby cylinders. Even for $\varepsilon = 1.0$ the fourth order solution shows considerable improvement over the second order solution where the percent errors are 3.6 and 17%, respectively. As expected from previous analytical and numerical investigations of the elastoplastic cylinder in tension (e.g. Hutchinson and Miles, 1974) the bifurcation in uniaxial tension occurs after the maximum load,

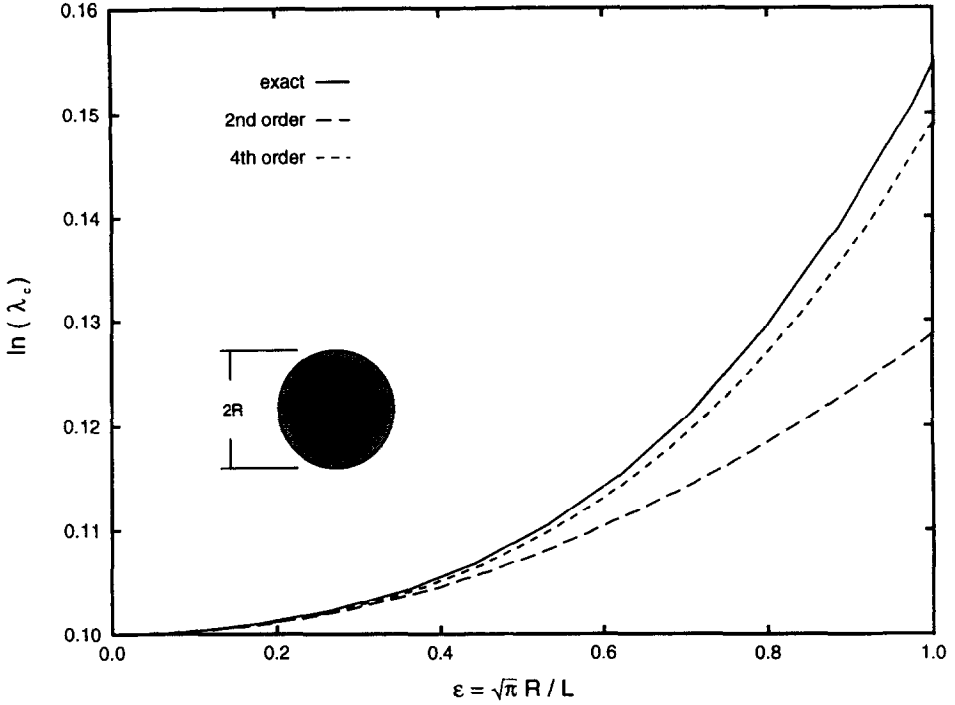

Fig. 11. Critical necking strain, $\ln(\lambda_c)$, as a function of the slenderness parameter, ε, for axial tension of a power-law type elasto-plastic beam with a circular cross-section. Exact results are denoted by the solid curve (—), while the $O(\varepsilon^2)$ and $O(\varepsilon^4)$ asymptotic results are depicted by dashed (- - -) and dotted (· · ·) curves, respectively.

and the difference between the bifurcation and maximum load strain increases monotonically away from zero with increasing ε. Our $O(\varepsilon^2)$ result coincides with Hutchinson and Miles (1974), but our $O(\varepsilon^4)$ cannot be directly compared in view of the simplifying assumptions introduced in their calculations.

As in the case of compression, the circular cross-section is used to check the accuracy of the finite element discretization used for arbitrary sections. Good agreement was found between the numerical results for the three-dimensional problem using the one-dimensional formulation and the two-dimensional formulation where the circular section was meshed with quadrilaterals. The constants in the asymptotic analysis (82) were also compared to constants found numerically, and the agreement was found to be within the same upper bounds as for the compressive case.

5.2.2. *Tension: square section.* For the case of a prismatic solid with a square cross-section loaded in tension, the exact and asymptotic strains are shown in Fig. 12. The results are similar to the case of the circular section with all the curves emerging from $\varepsilon_0 = 0.10$. As ε increases the critical strain at bifurcation increases monotonically.

The exact solution is again approximated very well by the fourth order asymptotic solution, even for large values of ε. It is interesting to note that for $\varepsilon = 1.00$, the solid

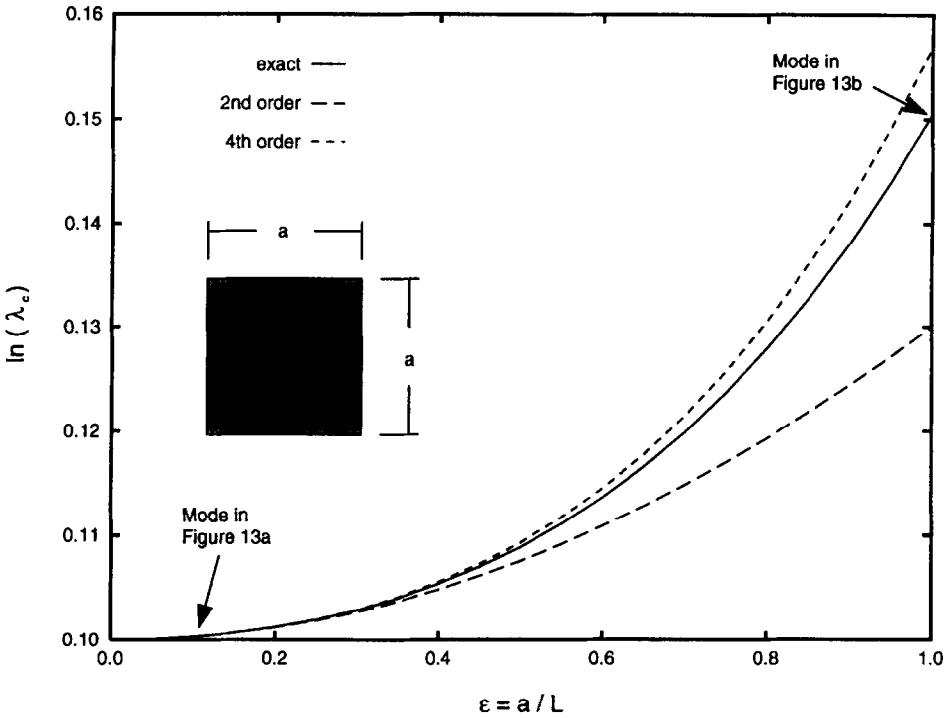

Fig. 12. Critical necking strain, $\ln(\lambda_c)$, as a function of the slenderness parameter, ε, for axial tension of a power-law type elasto-plastic beam with a square cross-section. Exact results are denoted by the solid curve (—), while the $O(\varepsilon^2)$ and $O(\varepsilon^4)$ asymptotic results are depicted by dashed (- - -) and dotted (· · ·) curves, respectively.

under consideration is a cube. For this case the percent error between the fourth order solution and the exact solution is only 3.6% while the percent error between the second order solution and the exact solution is 14%.

The shapes of the bifurcation modes for the square section can be seen in the axonometric plots in Fig. 13, with the exact results depicted in solid curves and the asymptotic results in dotted curves. As expected from the $O(\varepsilon^2)$ asymptotic result (45), for small ε the mode corresponds to a uniform flow of material across each section, exactly as seen in Fig. 13(a). For larger values of ε, Fig. 13(b) shows the mode changing to a nonuniform flow of material where the edge effects of the cross section are more pronounced. Note also the discrepancy between the exact and $O(\varepsilon^4)$ approximate mode in Fig. 13(b).

5.2.3. *Tension*: *cruciform section*. The discussion of the tension case continues with the investigation of stability for the cruciform section. As seen in Figs 14 and 15, the results are similar to those found for the square section. For the thick cruciform section in Fig. 14, the asymptotic results for the critical strain up to fourth order are in excellent agreement with the exact three-dimensional calculations. For $\varepsilon = 1.00$ the percent error between the fourth order solution and the exact solution is 3.3% while the percent error between the second order solution and the exact solution is 17%.

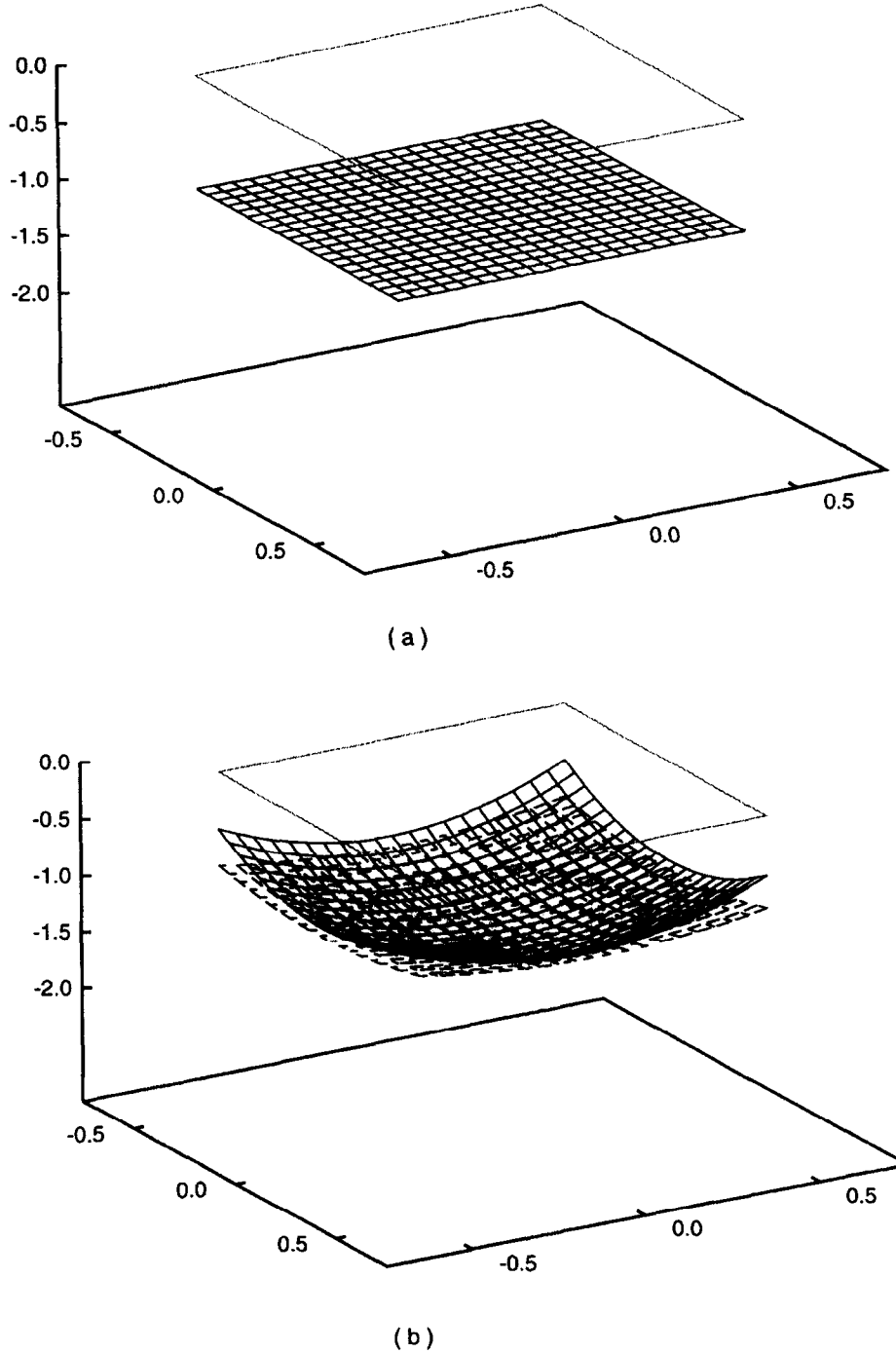

Fig. 13. Axonometric plot at $x_3 = 0$ of the exact (—) and $O(\varepsilon^4)$ asymptotic (- - -) critical necking mode (a) for a slender, $\varepsilon = 0.10$, and (b) for a stubby, $\varepsilon = 1.00$, square section power-law type elasto-plastic beam. Notice the uniform flow of material through the section for the slender beam compared to the corresponding nonuniform flow for the stubby beam.

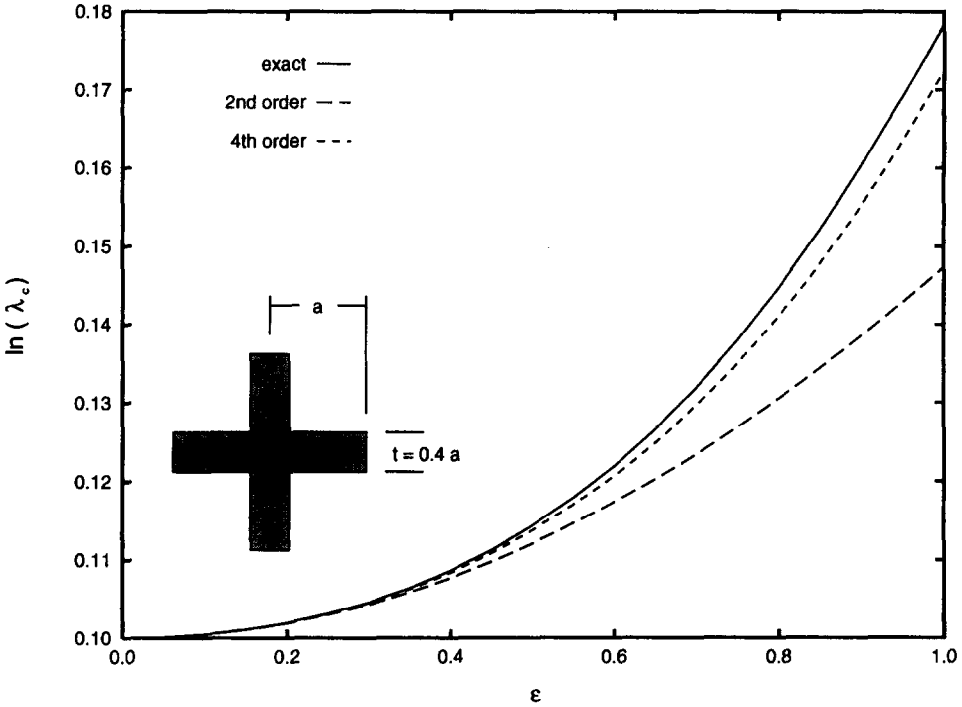

Fig. 14. Critical necking strain, $\ln(\lambda_c)$, as a function of the slenderness parameter, ε, for axial tension of a power-law type elasto-plastic beam with a thick cruciform cross-section. Exact results are denoted by the solid curve (—), while the $O(\varepsilon^2)$ and $O(\varepsilon^4)$ asymptotic results are depicted by dashed (- - -) and dotted (· · ·) curves, respectively.

For a thin cruciform section the behavior is different. Figure 15 shows that for relatively slender beams ($\varepsilon < 0.65$) the behavior is similar to that of the thick section beams with the approximate critical strains underestimating the exact one. However, for $\varepsilon > 0.84$ the behavior changes drastically due to a switch in the type of critical mode. The new mode is only available for stubby beams and cannot be predicted from our asymptotic analysis. Since no engineering theory analogous to the one used for thin-walled beam stability in compression exists for the stability of thin-walled beams in tension, the behavior after the mode switch is examined only with the help of the exact finite element solution of the stability problem. Note also that for $\varepsilon > 0.65$ the $O(\varepsilon^4)$ asymptotic results start overestimating the exact critical strain.

An axonometric representation of the two different critical modes of the thin cruciform section are depicted in Fig. 16. The mode in Fig. 16(a) is calculated for a relatively slender beam, $\varepsilon = 0.2$, and is essentially the uniform flow through the section at $x_3 = 0$, which is the primary component of the mode as $\varepsilon \to 0$. The new mode which occurs for the stubby cruciform beam is depicted in Fig. 16(b) is calculated for $\varepsilon = 1.0$. Notice that the flow is antisymmetric in one part of the cross-section while in the other part the eigenmode vanishes rapidly away from the center. This behavior, like that of torsion for the cruciform in compression, cannot be predicted by the asymptotic method presented here.

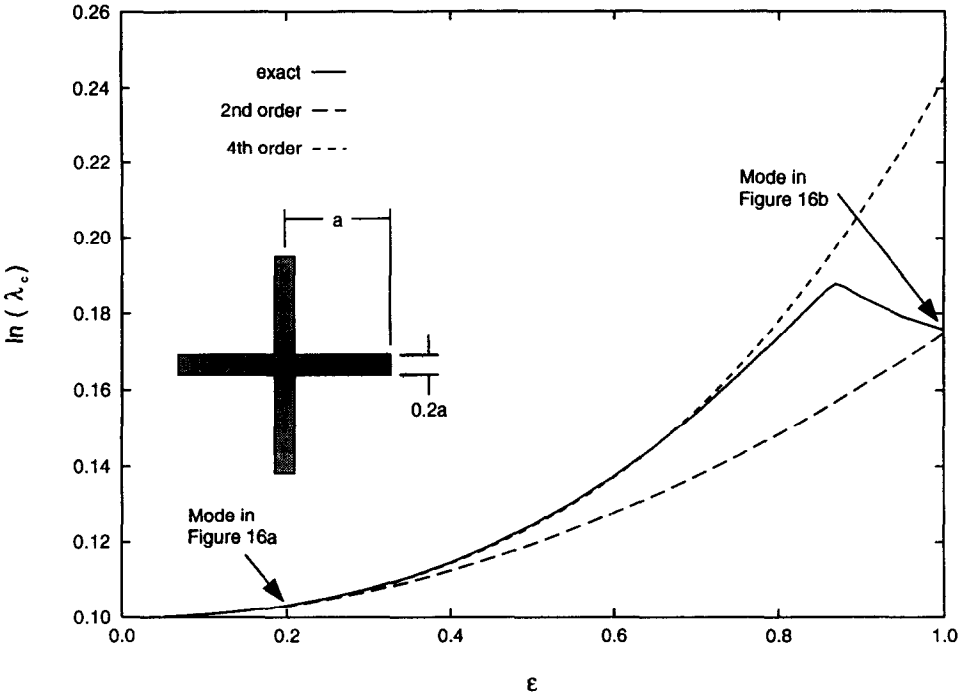

Fig. 15. Critical necking strain, $\ln(\lambda_c)$, as a function of the slenderness parameter, ε, for axial tension of a power-law type elasto-plastic beam with a thin cruciform cross-section. Exact results are denoted by the solid curve (—), while the $O(\varepsilon^2)$ and $O(\varepsilon^4)$ asymptotic results are depicted by dashed (- - -) and dotted (· · ·) curves, respectively. The discontinuity in the exact solution is due to the change of the critical mode from a symmetric flow of material through the section $x_3 = 0$ to a nonsymmetric flow of material through the section $x_3 = 0$.

5.2.4. *Tension: critical mode comparison*

Similar to the compressive case, we devote the last part of the section describing the tension results to the discussion of the error in the $O(\varepsilon^2)$ and $O(\varepsilon^4)$ asymptotic critical modes as a function of the slenderness parameter, ε. The results of these comparisons are given in Fig. 17(a) for the square section and Fig. 17(b) for the thick cruciform section. The error definitions are the same as the ones used in compression. Again the errors are monotonic functions of ε with the $O(\varepsilon^4)$ approximation being an order of magnitude better than the $O(\varepsilon^2)$ approximation. Note that even for the case of extremely stubby beams, with $\varepsilon = 1$, the $O(\varepsilon^4)$ approximation gives an error on the order of 5% for both sections.

6. CONCLUSIONS

The present work addresses the classical engineering problem of stability for axially loaded prismatic beams with arbitrary sections. Our aim is to provide a consistent

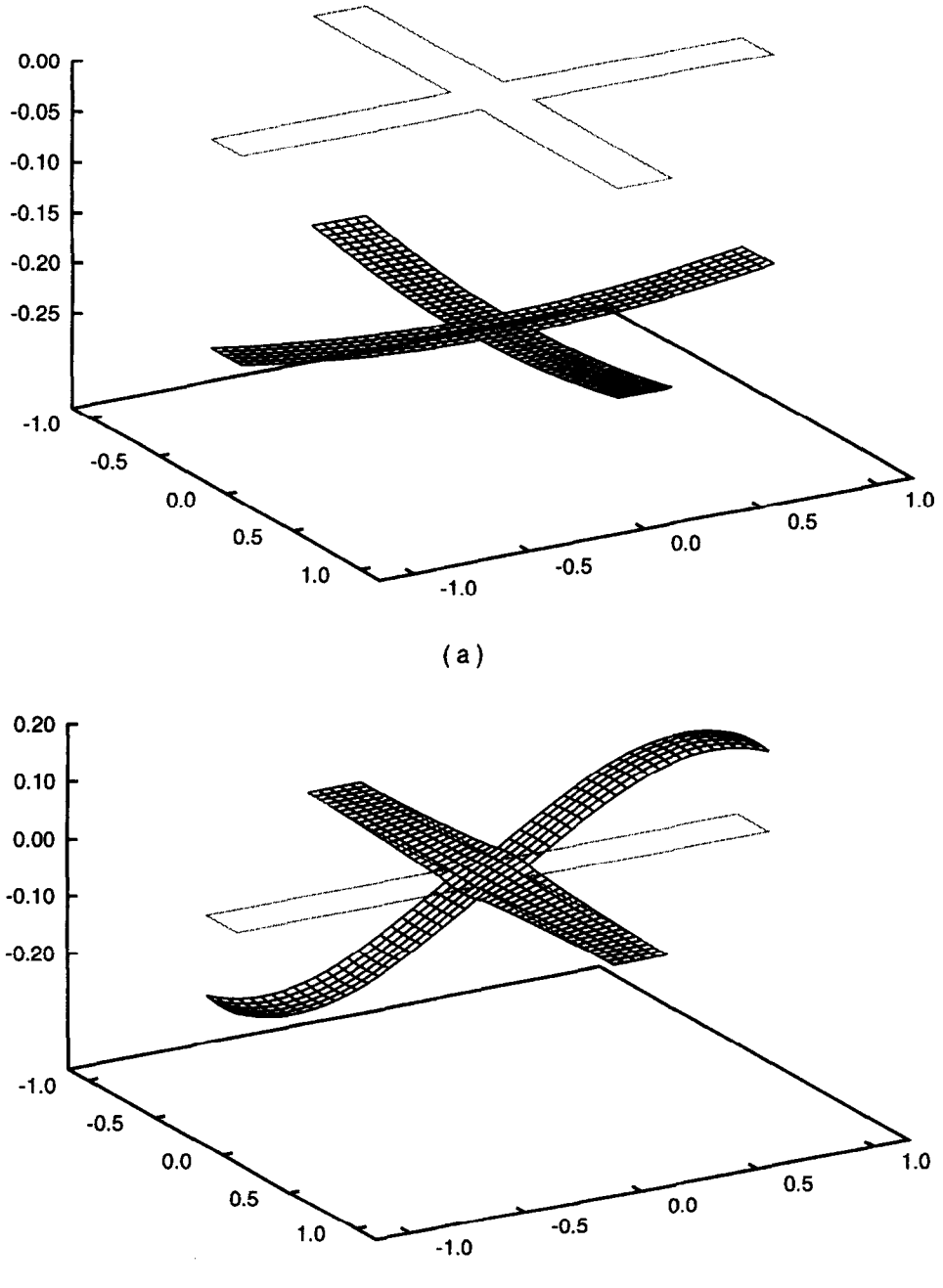

Fig. 16. Axonometric plot at $x_3 = 0$ of the exact critical necking mode (a) for a slender, $\varepsilon = 0.20$, and (b) for a stubby, $\varepsilon = 1.00$, power-law type elasto-plastic beam with a thin cruciform cross-section. Notice the nonsymmetric flow of material through the section for the stubby beam.

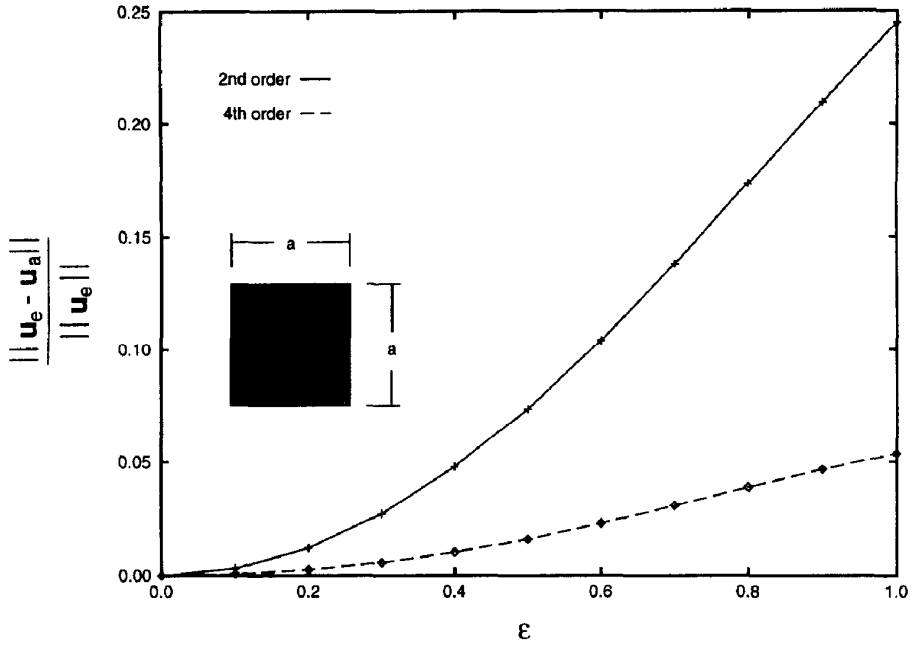

(a)

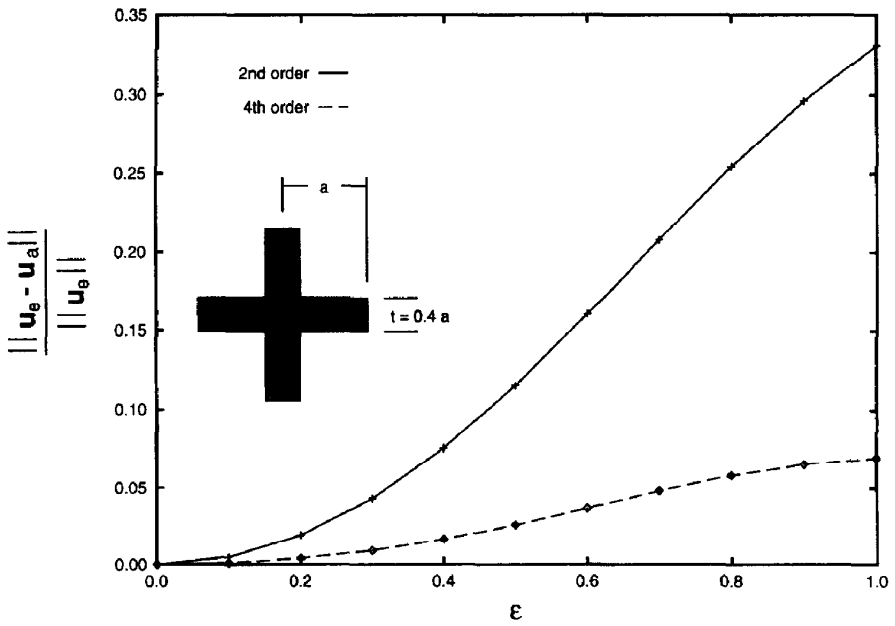

(b)

Fig. 17. Error of the asymptotic $O(\varepsilon^2)$, solid curve (—), and $O(\varepsilon^4)$, dashed curve (- - -), eigenmode as a function of the slenderness parameter, ε, (a) for a square and (b) for a thick cruciform cross-section power-law type elasto-plastic beam in uniaxial tension.

and general approach for the calculation of the critical load and mode as a function of, ε, the bar's slenderness parameter (ε^2 = area/length^2). For reasons explained in detail in the introduction, we reverse the process of the standard structural engineering approach: we first formulate the stability problem for the three-dimensional solid and then, using some recently developed multiple scale asymptotic techniques, we find the asymptotic expansions of the critical load and mode as a function of the slenderness parameters. The importance of adopting a finite strain version of the constitutive law and starting with the three-dimensional, full Lagrangian description of the stability problem is perhaps better appreciated from the example of the first slenderness correction to the Euler load of an elastic cylinder. For this case we found that even the sign of the correction is sensitive to linear constitutive law adopted, in spite of the fact that we are dealing with slender beams under small strains.

For beams with sections that have commensurate dimensions, the lowest order term in the asymptotic expansions for the critical load and mode correspond to the known classical engineering results for slender bars, while the next higher order terms provide the novel, sought after corrections for stubbier beams. To evaluate the validity of the proposed corrections, our asymptotic results are compared, for several different cross-sections, with numerically obtained solutions of the corresponding three-dimensional stability problems.

The proposed approach is valid for a homogeneous prismatic bar with any simply connected cross-section and any rate-independent material that is isotropic at zero load. As the axial loading increases, the bar becomes orthotropic about its longitudinal axis but remains isotropic in the plane of its section. The analysis can be easily generalized to orthotropic materials which are transversely isotropic with respect to the loading axis even at zero load (e.g. unidirectional reinforced materials loaded along their fiber axis).

To avoid the presence of boundary layers at the two ends, we consider the case of flat end, shear-free clamping boundary conditions. Simple support or free boundary conditions which produce no boundary layers could have been easily considered (see Trabucho and Viaño, 1989) thus covering all the boundary conditions of practical interest. For the case of more complicated boundary conditions, the method would also require the matching of asymptotic expansions at the boundary layers. By appealing to Saint-Venant's principle one can speculate that these boundary layers will have a limited effect for slender beams, unless the load induced orthotropy is important. Further investigation is necessary to address this difficult problem.

In evaluating the accuracy of the proposed asymptotic slenderness corrections of $O(\varepsilon^4)$ and also of the lowest order (engineering theory—$O(\varepsilon^2)$ for compression and $O(1)$ for tension) expressions for the critical load and mode, we consider circular sections, square and cruciform sections (all D_4 symmetric), and L-sections (asymmetric). In each case the proposed next order slenderness correction to the engineering formula gives significant gain in the accuracy of the critical load and mode. The improvements are most dramatic in the case of the circular and square sections, particularly for results in tension where the proposed $O(\varepsilon^4)$ approximation gives the critical load within 10% error even for extremely stubby beams with $\varepsilon \sim 1$. For the thick cruciform section in compression, the validity is restricted by the change of critical mode for stubby beams. Even for the completely asymmetric thick L shaped

section in compression, the proposed $O(\varepsilon^4)$ correction for the critical load significantly improves the accuracy of the engineering predictions up to $\varepsilon \sim 0.2$.

For thin-walled beams, the range of validity of our asymptotic expansions is considerably smaller due to the unaccounted presence of warping effects of $O(\varepsilon^6)$ and higher. For this particular case, where the dimensions of the cross-section are not commensurate, one needs to introduce an additional small parameter (δ^2 = thickness^2/area) and repeat the multiple scale asymptotic procedure for $\delta = \varepsilon^\alpha$. By extending the multiple scale methodology used here to the thin-walled case, one should obtain to any desired order of accuracy, the critical load and modes without the requirement of structural approximations or any hypothesis about the magnitude of the strains. This is a worthwhile future research direction to complete the present investigation for the technologically interesting case of thin-walled beams.

ACKNOWLEDGEMENTS

The partial support of ALCOA and NSF under grant G-CMS-9503956 are gratefully acknowledged. One of us (N.T.) would also like to thank L. Trabucho for bringing his work on asymptotic derivations of linear elastic beam theories to our attention. The continuing encouragement and support of Dr O. Richmond and Dr E. Chu (ALCOA) and Dr R. Stevenson (GM) during the course of this work are sincerely appreciated.

REFERENCES

Bridgman, P. W. (1952) *Studies In Large Plastic Flow and Fracture*. McGraw-Hill, New York.

Brush, D. O. and Almroth, B. O. (1975) *Buckling of Bars, Plates, and Shells*. McGraw-Hill, New York.

Green, A. E., Rivlin, R. S. and Shield, R. T. (1952) General theory of small elastic deformations superimposed on large elastic deformations. *Proceedings of the Royal Society* **A211,** 128–154.

Green, A. E. and Spencer, A. J. M. (1959) The stability of a circular cylinder under finite extension and torsion. *J. Math. Phys.* **37,** 316–338.

Hill, R. (1957) On uniqueness and stability in the theory of finite elastic strain. *Journal of the Mechanics and Physics of Solids* **5,** 229–241.

Hill, R. and Hutchinson, J. W. (1975) Bifurcation phenomena in the plane tension test. *Journal of the Mechanics and Physics of Solids* **23,** 239–264.

Hutchinson, J. W. (1974) Plastic buckling. *Advances in Applied Mechanics* **14,** 67–144.

Hutchinson, J. W. and Miles, J. P. (1974) Bifurcation analysis of the onset of necking in an elastic/plastic cylinder under uniaxial tension. *Journal of the Mechanics and Physics of Solids* **22,** 61–71.

Kardomateas, G. A. (1995) Three-dimensional elasticity solution for the buckling of transversely isotropic rods: the Euler load revisited. *Journal of Applied Mechanics* **62,** 346–355.

Levinson, M. (1968) Stability of a compressed neo-Hookean rectangular parallelopiped. *Journal of the Mechanics and Physics of Solids* **16,** 875–900.

Ogden, R. W. (1984) *Nonlinear Elastic Deformations*. Halsted Press, New York.

Rigolot, A. (1972) Sur une théorie asymptotique des poutres. *J. Mécanique* **11,** 673–703.

Stören, S. and Rice, J. R. (1975) Localized necking in thin sheets. *Journal of the Mechanics and Physics of Solids* **23,** 421–441.

Timoshenko, S. P. (1936) *Theory of Elastic Stability*. McGraw-Hill, New York.

Trabucho, L. and Viaño, J. M. (1989) Existence and characterization of higher-order terms in an asymptotic expansion method for linearized elastic beams. *Asymp. Anal.* **2,** 223–255.
Triantafyllidis, N. and Kwon, Y. J. (1987) Thickness effects on the stability of thin walled structures. *Journal of the Mechanics and Physics of Solids* **35,** 643–674.
Triantafyllidis, N. and Peek, R. (1992) On stability of the worst imperfection, shape in solids with nearly simultaneous eigenmodes. *International Journal of Solids and Structures* **29,** 2281–2299.
Wilkes, E. W. (1955) On the stability of a circular tube under end thrust. *Quarterly Journal of Mechanics and Applied Mathematics* **8,** 88–100.
Young, N. J. B. (1976) Bifurcation phenomena in the plane compression test. *Journal of the Mechanics and Physics of Solids* **24,** 77–91.

APPENDIX

The starting point for the asymptotic analysis is the governing equations for the beam stability problem on the normalized domain $\omega \times [-1/2, 1/2]$ which are recorded in Section 2.1.

Introducing the asymptotic expansions (20)–(23) into (11) and (12) and grouping terms of like order in ε, results in a sequence of governing equations, each corresponding to a term of order $O(\varepsilon^{2n})$, $n = -1, 0, 1, 2, \ldots$. The lowest order equations are those of $O(\varepsilon^{-2})$

$$\int_{-1/2}^{1/2} \int_{\omega} (\overset{0}{L}_{33\gamma\delta} \overset{0}{u}_{\gamma,\delta}) \delta\Pi_{33} \, d\omega \, dx_3 = 0. \tag{A1}$$

The next higher order equations are for $O(\varepsilon^0)$

$$\int_{-1/2}^{1/2} \int_{\omega} (\overset{2}{L}_{33\gamma\delta} \overset{0}{u}_{\gamma,\delta} + \overset{0}{L}_{33\gamma\delta} \overset{2}{u}_{\gamma,\delta} + \overset{0}{L}_{3333} \overset{0}{u}_{3,3} - \overset{0}{\Pi}_{33}) \delta\Pi_{33} \, d\omega \, dx_3 = 0, \tag{A2}$$

$$\int_{-1/2}^{1/2} \int_{\omega} (\overset{0}{L}_{3\beta\gamma 3} \overset{0}{u}_{\gamma,3} + \overset{0}{L}_{3\beta 3\delta} \overset{0}{u}_{3,\delta}) \delta\Pi_{\beta 3} \, d\omega \, dx_3 = 0, \tag{A3}$$

$$\int_{-1/2}^{1/2} \int_{\omega} (\overset{0}{L}_{\alpha 3\gamma 3} \overset{0}{u}_{\gamma,3} + \overset{0}{L}_{\alpha 33\delta} \overset{0}{u}_{3,\delta}) \delta\Pi_{3\alpha} \, d\omega \, dx_3 = 0, \tag{A4}$$

$$\int_{-1/2}^{1/2} \int_{\omega} (\overset{0}{L}_{\alpha\beta\gamma\delta} \overset{0}{u}_{\gamma,\delta}) \delta\Pi_{\beta\alpha} \, d\omega \, dx_3 = 0, \tag{A5}$$

$$\int_{-1/2}^{1/2} \int_{\omega} (\overset{0}{\Pi}_{\beta\alpha} \delta u_{\alpha,\beta} + \overset{0}{\Pi}_{3\alpha} \delta u_{\alpha,3}) \, d\omega \, dx_3 = 0, \tag{A6}$$

$$\int_{-1/2}^{1/2} \int_{\omega} (\overset{0}{\Pi}_{\beta 3} \delta u_{3,\beta} + \overset{0}{\Pi}_{33} \delta u_{3,3}) \, d\omega \, dx_3 = 0. \tag{A7}$$

The equations for $O(\varepsilon^2)$ are recorded next

$$\int_{-1/2}^{1/2} \int_{\omega} (\overset{4}{L}_{33\gamma\delta} \overset{0}{u}_{\gamma,\delta} + \overset{2}{L}_{33\gamma\delta} \overset{2}{u}_{\gamma,\delta} + \overset{0}{L}_{33\gamma\delta} \overset{4}{u}_{\gamma,\delta} + \overset{2}{L}_{3333} \overset{0}{u}_{3,3} + \overset{0}{L}_{3333} \overset{2}{u}_{3,3} - \overset{2}{\Pi}_{33}) \delta\Pi_{33} \, d\omega \, dx_3 = 0, \tag{A8}$$

$$\int_{-1/2}^{1/2}\int_{\omega}(\overset{2}{L}_{3\beta\gamma 3}\overset{0}{u}_{\gamma,3}+\overset{0}{L}_{3\beta\gamma 3}\overset{2}{u}_{\gamma,3}+\overset{2}{L}_{3\beta 3\delta}\overset{0}{u}_{3,\delta}+\overset{0}{L}_{3\beta 3\delta}\overset{2}{u}_{3,\delta}-\overset{0}{\Pi}_{\beta 3})\delta\Pi_{\beta 3}\,d\omega\,dx_3=0, \tag{A9}$$

$$\int_{-1/2}^{1/2}\int_{\omega}(\overset{2}{L}_{\alpha 3\gamma 3}\overset{0}{u}_{\gamma,3}+\overset{0}{L}_{\alpha 3\gamma 3}\overset{2}{u}_{\gamma,3}+\overset{2}{L}_{\alpha 33\delta}\overset{0}{u}_{3,\delta}+\overset{0}{L}_{\alpha 33\delta}\overset{2}{u}_{3,\delta}-\overset{0}{\Pi}_{3\alpha})\delta\Pi_{3\alpha}\,d\omega\,dx_3=0, \tag{A10}$$

$$\int_{-1/2}^{1/2}\int_{\omega}(\overset{2}{L}_{\alpha\beta\gamma\delta}\overset{0}{u}_{\gamma,\delta}+\overset{0}{L}_{\alpha\beta\gamma\delta}\overset{2}{u}_{\gamma,\delta}+\overset{0}{L}_{\alpha\beta 33}\overset{0}{u}_{3,3})\delta\Pi_{\beta\alpha}\,d\omega\,dx_3=0, \tag{A11}$$

$$\int_{-1/2}^{1/2}\int_{\omega}(\overset{2}{\Pi}_{\beta\alpha}\delta u_{\alpha,\beta}+\overset{2}{\Pi}_{3\alpha}\delta u_{\alpha,3})\,d\omega\,dx_3=0, \tag{A12}$$

$$\int_{-1/2}^{1/2}\int_{\omega}(\overset{2}{\Pi}_{\beta 3}\delta u_{3,\beta}+\overset{2}{\Pi}_{33}\delta u_{3,3})\,d\omega\,dx_3=0. \tag{A13}$$

Finally, the equations of $O(\varepsilon^4)$ are

$$\int_{-1/2}^{1/2}\int_{\omega}(\overset{6}{L}_{33\gamma\delta}\overset{0}{u}_{\gamma,\delta}+\overset{4}{L}_{33\gamma\delta}\overset{2}{u}_{\gamma,\delta}+\overset{2}{L}_{33\gamma\delta}\overset{4}{u}_{\gamma,\delta}+\overset{0}{L}_{33\gamma\delta}\overset{6}{u}_{\gamma,\delta}+\overset{4}{L}_{3333}\overset{0}{u}_{3,3}+\overset{2}{L}_{3333}\overset{2}{u}_{3,3}+\overset{0}{L}_{3333}\overset{4}{u}_{3,3}-\overset{4}{\Pi}_{33})\delta\Pi_{33}\,d\omega\,dx_3=0, \tag{A14}$$

$$\int_{-1/2}^{1/2}\int_{\omega}(\overset{4}{L}_{3\beta\gamma 3}\overset{0}{u}_{\gamma,3}+\overset{2}{L}_{3\beta\gamma 3}\overset{2}{u}_{\gamma,3}+\overset{0}{L}_{3\beta\gamma 3}\overset{4}{u}_{\gamma,3}+\overset{4}{L}_{3\beta 3\delta}\overset{0}{u}_{3,\delta}+\overset{2}{L}_{3\beta 3\delta}\overset{2}{u}_{3,\delta}+\overset{0}{L}_{3\beta 3\delta}\overset{4}{u}_{3,\delta}-\overset{2}{\Pi}_{\beta 3})\delta\Pi_{\beta 3}\,d\omega\,dx_3=0, \tag{A15}$$

$$\int_{-1/2}^{1/2}\int_{\omega}(\overset{4}{L}_{\alpha 3\gamma 3}\overset{0}{u}_{\gamma,3}+\overset{2}{L}_{\alpha 3\gamma 3}\overset{2}{u}_{\gamma,3}+\overset{0}{L}_{\alpha 3\gamma 3}\overset{4}{u}_{\gamma,3}+\overset{4}{L}_{\alpha 33\delta}\overset{0}{u}_{3,\delta}+\overset{2}{L}_{\alpha 33\delta}\overset{2}{u}_{3,\delta}+\overset{0}{L}_{\alpha 33\delta}\overset{4}{u}_{3,\delta}-\overset{2}{\Pi}_{3\alpha})\delta\Pi_{3\alpha}\,d\omega\,dx_3=0, \tag{A16}$$

$$\int_{-1/2}^{1/2}\int_{\omega}(\overset{4}{L}_{\alpha\beta\gamma\delta}\overset{0}{u}_{\gamma,\delta}+\overset{2}{L}_{\alpha\beta\gamma\delta}\overset{2}{u}_{\gamma,\delta}+\overset{0}{L}_{\alpha\beta\gamma\delta}\overset{4}{u}_{\gamma,\delta}+\overset{2}{L}_{\alpha\beta 33}\overset{0}{u}_{3,3}+\overset{0}{L}_{\alpha\beta 33}\overset{2}{u}_{3,3}-\overset{0}{\Pi}_{\beta\alpha})\delta\Pi_{\beta\alpha}\,d\omega\,dx_3=0, \tag{A17}$$

$$\int_{-1/2}^{1/2}\int_{\omega}(\overset{4}{\Pi}_{\beta\alpha}\delta u_{\alpha,\beta}+\overset{4}{\Pi}_{3\alpha}\delta u_{\alpha,3})\,d\omega\,dx_3=0, \tag{A18}$$

$$\int_{-1/2}^{1/2}\int_{\omega}(\overset{4}{\Pi}_{\beta 3}\delta u_{3,\beta}+\overset{4}{\Pi}_{33}\delta u_{3,3})\,d\omega\,dx_3=0. \tag{A19}$$

Substituting the asymptotic expansions for the displacement (9) into the essential (kinematic) conditions (5) and (6) one obtains

$$\overset{n}{u}_3=0,\quad (n=0,2,4\ldots)\quad \text{at } x_3=\pm\tfrac{1}{2}, \tag{A20}$$

$$\int_{\omega}\overset{n}{u}_{\alpha}\,d\omega=0,\quad (n=0,2,4\ldots)\quad \text{at } x_3=0, \tag{A21}$$

$$\int_{\omega}\varepsilon_{\alpha\beta}x_{\alpha}\overset{n}{u}_{\beta}\,d\omega=0,\quad (n=0,2,4\ldots)\quad \text{at } x_3=0, \tag{A22}$$

while the mode normalization condition (7) for the choice of $v_i=\overset{0}{u}_i$ yields

$$\int_{-1/2}^{1/2} \int_{\omega} \overset{0}{u}_i \overset{0}{u}_i \, d\omega \, dx_3 = C, \tag{A23}$$

$$\int_{-1/2}^{1/2} \int_{\omega} \overset{0}{u}_i \overset{n}{u}_i \, d\omega \, dx_3 = 0 \quad (n = 2, 4, 6 \ldots). \tag{A24}$$

From the governing equations (A1)–(A19), kinematic conditions (A20)–(A22) and mode normalization conditions (A23), (A24), asymptotic solutions to the stability problem are constructed for compression and tension.

The incremental moduli, $\mathbf{L}$, are evaluated on the principal solution, and hence they are functions of the stretch ratio, i.e. $\mathbf{L}(\lambda)$, and since λ_c is a function of ε, the following useful relations are recorded

$$\overset{0}{\mathbf{L}} = \mathbf{L}(\lambda_0), \tag{A25}$$

$$\overset{2}{\mathbf{L}} = \lambda_2 \left. \frac{d\mathbf{L}}{d\lambda} \right|_{\lambda=\lambda_0}, \tag{A26}$$

$$\overset{4}{\mathbf{L}} = \lambda_4 \left. \frac{d\mathbf{L}}{d\lambda} \right|_{\lambda=\lambda_0} + \frac{\lambda_2^2}{2} \left. \frac{d^2\mathbf{L}}{d\lambda^2} \right|_{\lambda=\lambda_0}. \tag{A27}$$

A.1. Compression

Derivation of λ_0. Recall from eqn (24) that the lowest order term in the expansion of the stretch ratio in compression is

$$\lambda_0 = 1. \tag{A28}$$

From (A25), the lowest order terms in the expansion of the incremental moduli are the moduli in the unstressed state, which, for an isotropic hyperelastic material, are the isotropic moduli for linear elasticity

$$\overset{0}{L}_{ijkl} = \frac{E}{1+\nu} \left[\frac{1}{2}(\delta_{ik}\delta_{jl} + \delta_{il}\delta_{jk}) + \frac{\nu}{1-2\nu} \delta_{ij}\delta_{kl} \right]. \tag{A29}$$

Derivation of λ_2, $\overset{0}{u}_i$. The determination of the next higher order term in the expansion of the critical stretch ratio and the lowest order terms in the expansion of the mode proceeds as follows. In view of the isotropy of $\overset{0}{L}_{ijkl}$, eqn (A5) gives

$$\overset{0}{u}_{1,1} = \overset{0}{u}_{2,2} = 0 \tag{A30}$$

when the cases $\alpha = \beta = 1$ and $\alpha = \beta = 2$ are considered. Equation (A5), with $\alpha = 1$ and $\beta = 2$ (or equivalently $\alpha = 2$ and $\beta = 1$), yields

$$\overset{0}{u}_{1,2} + \overset{0}{u}_{2,1} = 0. \tag{A31}$$

From (A30) and (A31), the following expression for $\overset{0}{u}_\alpha$ is found

$$\overset{0}{u}_\alpha = \overset{0}{z}_\alpha(x_3) + \varepsilon_{\alpha\beta} x_\beta \overset{0}{z}(x_3). \tag{A32}$$

From eqn (A4) we obtain

$$\overset{0}{u}_{\alpha,3} + \overset{0}{u}_{3,\alpha} = 0. \tag{A33}$$

Upon substitution of (A32) into (A33) we deduce

$$\overset{0}{z}_{,3} = 0. \tag{A34}$$

Removing the rigid body rotation from $\overset{0}{u}_\alpha$ in (A32) by using (A22) gives $\overset{0}{z}(0) = 0$. Consequently $\overset{0}{z}(x_3) = 0$ and the expression for $\overset{0}{u}_3$ is found from (A33) to be

$$\overset{0}{u}_3 = \overset{0}{z}_3(x_3) - x_\alpha \overset{0}{z}_{\alpha,3}(x_3). \tag{A35}$$

Governing equations for $\overset{0}{z}_3(x_3)$

The function $\overset{0}{z}_3(x_3)$ can be found in the following manner. Since $\overset{0}{u}_\alpha = \overset{0}{z}_\alpha(x_3)$ are independent of x_α, the following equations can be found from (A11)

$$\overset{0}{L}_{\alpha\alpha 11}\overset{2}{u}_{1,1} + \overset{0}{L}_{\alpha\alpha 22}\overset{2}{u}_{2,2} = -\overset{0}{L}_{\alpha\alpha 33}\overset{0}{u}_{3,3} \quad \text{(no sum)} \tag{A36}$$

which give

$$\overset{2}{u}_{1,1} = \overset{2}{u}_{2,2} = -\nu \overset{0}{u}_{3,3}. \tag{A37}$$

Using (A37) in (A2) we find Hooke's law

$$\overset{0}{\Pi}_{33} = E\overset{0}{u}_{3,3} \tag{A38}$$

which, when substituted into (A7) with $\delta u_3 = \delta v_3(x_3)$, gives [in conjunction with (A35)]

$$\int_{-1/2}^{1/2} \int_\omega E(\overset{0}{z}_{3,3} - x_\alpha \overset{0}{z}_{\alpha,33})\delta v_{3,3}\, d\omega\, dx_3 = 0. \tag{A39}$$

From (A39), and assuming the coordinate axes pass through the centroid of the section, the governing ordinary differential equation for $\overset{0}{z}_3(x_3)$ is found to be

$$\overset{0}{z}_{3,33} = 0. \tag{A40}$$

With the boundary condition from (A20) the solution to (A40) is found to be $\overset{0}{z}_3(x_3) = 0$. Substituting this result into (A32) and (A35), we find for $\overset{0}{u}_i$, the lowest order terms in the expansion of the eigenmode, the familiar equations for Bernoulli–Euler–Navier beam bending

$$\overset{0}{u}_\alpha = \overset{0}{z}_\alpha(x_3), \quad \overset{0}{u}_3 = -x_\alpha \overset{0}{z}_{\alpha,3}(x_3). \tag{A41}$$

Governing equations for $\overset{0}{z}_\alpha(x_3)$ The governing differential equation for $\overset{0}{z}_\alpha(x_3)$ can be found by considering (A6) and (A7). Taking $\delta u_\alpha = \delta v_\alpha(x_3)$ in (A6) and $\delta u_3 = x_\alpha \delta v_{\alpha,3}$ in (A7), the result is

$$\int_{-1/2}^{1/2} \int_\omega (\overset{0}{\Pi}_{3\alpha}\delta v_{\alpha,3})\, d\omega\, dx_3 = 0, \tag{A42}$$

$$\int_{-1/2}^{1/2} \int_\omega (\overset{0}{\Pi}_{\alpha 3}\delta v_{\alpha,3} + \overset{0}{\Pi}_{33} x_\alpha \delta v_{\alpha,33})\, d\omega\, dx_3 = 0. \tag{A43}$$

Subtracting (A42) from (A43), using the expression for $\overset{0}{\Pi}_{33}$ in (A38), $\overset{0}{\Pi}_{\alpha 3}$ in (A9) and $\overset{0}{\Pi}_{3\alpha}$ in (A10), and simplifying the result, we find

$$\int_{-1/2}^{1/2} \{[(\overset{2}{L}_{3\alpha\beta 3} - \overset{2}{L}_{\alpha 3\beta 3} - \overset{2}{L}_{3\alpha 3\beta} + \overset{2}{L}_{\alpha 33\beta})\overset{0}{z}_{\beta,3}]\delta v_{\alpha,3} - (EI_{\alpha\beta}\overset{0}{z}_{\beta,33})\delta v_{\alpha,33}\}\, dx_3 = 0, \tag{A44}$$

where $I_{\alpha\beta}$ are the moments of inertia of the normalized cross section, which are defined as follows

$$I_{\alpha\beta} = \int_\omega x_\alpha x_\beta\, d\omega. \tag{A45}$$

Making use of (A26), with the help of (A38), it can be shown that

$$\overset{2}{L}_{3113}-\overset{2}{L}_{1313}-\overset{2}{L}_{3131}+\overset{2}{L}_{1331}=\lambda_2\frac{\mathrm{d}S_{33}}{\mathrm{d}\lambda}\bigg|_{\lambda=1}=-\lambda_2 E, \tag{A46}$$

where $S_{33}=2\,\partial W/\partial C_{33}$ is the axial component of the second Piola–Kirchhoff stress and E is the initial Young's modulus. Using (A46) in (A44), we find the governing differential equations for $\overset{0}{z}_\alpha(x_3)$ in variational form

$$\int_{-1/2}^{1/2}\{(\lambda_2\delta_{\alpha\beta}\overset{0}{z}_{\beta,3})\delta v_{\alpha,3}+(I_{\alpha\beta}\overset{0}{z}_{\beta,33})\delta v_{\alpha,33}\}\,\mathrm{d}x_3=0. \tag{A47}$$

Integrating (A47) by parts gives the governing ordinary differential equation for $\overset{0}{z}_\alpha(x_3)$ in (27). The solution for (27), which includes the boundary conditions found by combining (A41) and (A21), gives $\overset{0}{z}_\alpha(x_3)$ and λ_2.

Derivation of λ_4, $\overset{2}{\mathbf{u}}_i$. The derivation of the next higher order terms in the critical stretch ratio, λ_4, and eigenmode, $\overset{2}{u}_i$, is presented here. Equation (A11), with $\alpha=1$ and $\beta=2$ (or equivalently with $\alpha=2$ and $\beta=1$), gives

$$\overset{2}{u}_{1,2}+\overset{2}{u}_{2,1}=0. \tag{A48}$$

Using (A37), (A41) and (A48), the following expression for $\overset{2}{u}_\alpha$ is found

$$\overset{2}{u}_\alpha=\overset{2}{z}_\alpha(x_3)+\varepsilon_{\alpha\beta}x_\beta\overset{2}{z}(x_3)+\nu\phi_{\alpha\beta}(x_1,x_2)\overset{0}{z}_{\beta,33}(x_3), \tag{A49}$$

where $\phi_{\alpha\beta}(x_1,x_2)$ are defined by

$$\phi_{\alpha\beta}=x_\alpha x_\beta-\delta_{\alpha\beta}\left(\frac{x_1^2+x_2^2}{2}\right). \tag{A50}$$

The next step in the analysis is to find a general expression for $\overset{2}{u}_3$. Beginning with (A7), and taking $\delta u_3=\delta\varphi(x_3)\delta v_3(x_1,x_2)$, where $\delta\varphi=0$ at $x_3=\pm 1/2$, we find

$$\int_{-1/2}^{1/2}\int_\omega(\overset{0}{\Pi}_{\alpha3}\delta\varphi\delta v_{3,\alpha}+\overset{0}{\Pi}_{33}\delta\varphi_{,3}\delta v_3)\,\mathrm{d}\omega\,\mathrm{d}x_3=0. \tag{A51}$$

Integrating (A51) by parts, and making use of the expressions for $\overset{0}{\Pi}_{\alpha3}$ from (A9) and $\overset{0}{\Pi}_{33}$ from (A2), gives

$$\int_\omega\{[(\overset{2}{L}_{3\alpha\beta3}-\overset{2}{L}_{3\alpha3\beta})\overset{0}{z}_{\beta,3}+\overset{0}{L}_{3\alpha\beta3}(\overset{2}{z}_{\beta,3}+\varepsilon_{\beta\gamma}x_\gamma\overset{2}{z}_{,3}+\nu\phi_{\beta\gamma}\overset{0}{z}_{\gamma,333})$$
$$+\overset{0}{L}_{3\alpha3\beta}\overset{2}{u}_{3,\beta}]\delta v_{3,\alpha}+[Ex_\alpha\overset{0}{z}_{\alpha,333}]\delta v_3\}\,\mathrm{d}\omega=0. \tag{A52}$$

Evaluating the expression $\overset{2}{L}_{3\alpha\beta3}-\overset{2}{L}_{3\alpha3\beta}$ in (A52), by making use of the definition of $\mathbf{L}$ in (2) and $\overset{2}{\mathbf{L}}$ in (A26), yields

$$\overset{2}{L}_{3131}-\overset{2}{L}_{3113}=\lambda_2\frac{E}{2}. \tag{A53}$$

At this point it is necessary to introduce the following auxiliary functions defined on the normalized cross-section

$$\theta_\alpha(x_1,x_2):\quad\int_\omega\theta_{\alpha,\beta}\delta\varphi_{,\beta}\,\mathrm{d}\omega=-\int_\omega\phi_{\alpha\beta}\delta\varphi_{,\beta}\,\mathrm{d}\omega,\quad\int_\omega\theta_\alpha\,\mathrm{d}\omega=0, \tag{A54}$$

$$\eta_\alpha(x_1,x_2):\quad\int_\omega\eta_{\alpha,\beta}\delta\varphi_{,\beta}\,\mathrm{d}\omega=-2\int_\omega x_\alpha\delta\varphi\,\mathrm{d}\omega,\quad\int_\omega\eta_\alpha\,\mathrm{d}\omega=0, \tag{A55}$$

$$w(x_1, x_2): \quad \int_\omega w_{,\alpha}\delta\varphi_{,\alpha}\,\mathrm{d}\omega = \int_\omega \varepsilon_{\alpha\beta}x_\beta\delta\varphi_{,\alpha}, \quad \int_\omega w\,\mathrm{d}\omega = 0. \tag{A56}$$

Substituting (A53)–(A56) into (A52), and making use of the arbitrariness of δv_3, we find the expression for $\overset{2}{u}_3$

$$\overset{2}{u}_3 = \overset{2}{z}_3(x_3) - x_\alpha \overset{2}{z}_{\alpha,3}(x_3) - w(x_1, x_2)\overset{2}{z}_{,3}(x_3) + \lambda_2(1+\nu)x_\alpha \overset{0}{z}_{\alpha,3}(x_3) + [\nu\theta_\alpha(x_1, x_2) + (1+\nu)\eta_\alpha(x_1, x_2)]\overset{0}{z}_{\alpha,333}(x_3). \tag{A57}$$

With the general expressions for $\overset{2}{u}_\alpha$ and $\overset{2}{u}_3$ in (A49) and (A57), we need to find the governing differential equations for $\overset{2}{z}(x_3)$, $\overset{2}{z}_\alpha(x_3)$ and $\overset{2}{z}_3(x_3)$.

Governing equation $\overset{2}{z}(x_3)$. To find the expression for $\overset{2}{z}(x_3)$, we use (A6) and choose $\delta u_\alpha = \varepsilon_{\alpha\beta}x_\beta\delta v(x_3)$. Simplifying the result gives

$$\int_{-1/2}^{1/2}\int_\omega [(\overset{0}{\Pi}_{3\alpha}\varepsilon_{\alpha\beta}x_\beta)\delta v_{,3}]\,\mathrm{d}\omega\mathrm{d}_3 = 0. \tag{A58}$$

Substituting the expression for $\overset{0}{\Pi}_{3\alpha}$ from (A10), and simplifying the result with the help of (A35), (A49) and (A57), we find

$$\int_{-1/2}^{1/2}\int_\omega \{[(\varepsilon_{\alpha\beta}x_\beta - w_{,\alpha})\varepsilon_{\alpha\gamma}x_\gamma]\overset{2}{z}_{,3} + [(\nu(\phi_{\alpha\beta} + \theta_{\beta,\alpha}) + (1+\nu)\eta_{\beta,\alpha})\varepsilon_{\alpha\gamma}x_\gamma]\overset{0}{z}_{\beta,333}\}\delta v_{,3}\,\mathrm{d}\omega\,\mathrm{d}x_3 = 0. \tag{A59}$$

Equation (A59) is simplified by introducing the Saint-Venant torsion function, $\psi(x_1, x_2)$. The equation for $\psi(x_1, x_2)$ can be written in variational form as follows

$$\psi(x_1, x_2): \quad \int_\omega \psi_{,\alpha}\delta\varphi_{,\alpha}\,\mathrm{d}\omega = 2\int_\omega \delta\varphi\,\mathrm{d}\omega, \quad \psi = 0 \quad \text{on } \partial\omega. \tag{A60}$$

From (A56) and (A60), the following constants can be defined

$$J = 2\int_\omega \psi\,\mathrm{d}\omega, \quad I_\alpha^\psi = 2\int_\omega \varepsilon_{\alpha\beta}x_\beta\psi\,\mathrm{d}\omega, \quad I_\alpha^w = 2\int_\omega x_\alpha w\,\mathrm{d}\omega. \tag{A61}$$

Using (A61) in (A59), and recalling the definitions (A54)–(A56), the governing equation for $\overset{2}{z}(x_3)$ is found in variational form

$$\int_{-1/2}^{1/2}\{J\overset{2}{z}_{,3} - [\nu I_\alpha^\psi + (1+\nu)I_\alpha^w]\overset{0}{z}_{\alpha,333}\}\delta v_{,3}\,\mathrm{d}x_3 = 0. \tag{A62}$$

Integrating the parts and consideration of the boundary conditions results in (33).

Governing equation for $\overset{2}{z}_3(x_3)$. To find $\overset{2}{z}_3(x_3)$ we begin with (A13), taking $\delta u_3 = \delta v(x_3)$, which gives

$$\int_{-1/2}^{1/2}\int_\omega \overset{2}{\Pi}_{33}\delta v_{,3}\,\mathrm{d}\omega\,\mathrm{d}x_3 = 0. \tag{A63}$$

Using the expression for $\overset{2}{\Pi}_{33}$ from (A8), and simplifying the result with the help of (A35), (A49) and (A57), we find

$$\int_{-1/2}^{1/2}\int_\omega \{\overset{0}{L}_{33\alpha\beta}\overset{4}{u}_{\alpha,\beta} + \overset{0}{L}_{3333}\overset{2}{z}_{3,3}\}\delta v_{,3}\,\mathrm{d}\omega\,\mathrm{d}x_3 = 0. \tag{A64}$$

At this point an expression for $\int_\omega \overset{4}{u}_{\alpha,\alpha}\,d\omega$ is needed (recall $\overset{0}{L}_{3312} = \overset{0}{L}_{3321} = 0$). To find this expression we begin with (A6), taking $\delta u_\alpha = x_\alpha \delta v(x_3)$. Substituting the expressions for $\overset{0}{\Pi}_{\beta\alpha}$ and $\overset{0}{\Pi}_{3\alpha}$ from (A17) and (A10), and simplifying the result, we find, after considerable manipulation,

$$\int_\omega \overset{4}{u}_{\alpha,\alpha}\,d\omega = \int_\omega \left\{ x_\alpha \frac{1-2\nu}{2}(\overset{2}{u}_{\alpha,33} + \overset{2}{u}_{3,\alpha 3}) - 2\nu \overset{2}{z}_{3,3} \right\} d\omega. \tag{A65}$$

Substituting (A65) into (A64), introducing the following area constants

$$H_\alpha = \int_\omega x_\alpha \left(\frac{x_1^2 + x_2^2}{2} \right) d\omega, \tag{A66}$$

and simplifying the result, we obtain, after considerable manipulation in which (A49), (A57), and the definitions (A54)–(A56) are used, the equation for $\overset{2}{z}_3(x_3)$ in variational form

$$\int_{-1/2}^{1/2} (\overset{2}{z}_{3,3} - \nu H_\alpha \overset{0}{z}_{\alpha,3333}) \delta v_{,3}\,d\omega = 0. \tag{A67}$$

The corresponding Euler equation and boundary conditions given in (36) and (37).

Governing equations for $\overset{2}{z}_\alpha(x_3)$. The last function missing for the complete determination of $\overset{2}{u}_i$ in (A49) and (A57) is $\overset{2}{z}_\alpha(x_3)$. Starting with (A12) and (A13) and successively taking $(\delta u_1, \delta u_2, \delta u_3) = (\delta v(x_3), 0, x_1 \delta v_{,3}(x_3))$ and $(\delta u_1, \delta u_2, \delta u_3) = (0, \delta v(x_3), x_2 \delta v_{,3}(x_3))$ and combining the results we find

$$\int_{-1/2}^{1/2} \int_\omega \{ (\overset{2}{\Pi}_{\alpha 3} - \overset{2}{\Pi}_{3\alpha}) \delta v_{,3} + \overset{2}{\Pi}_{33} x_\alpha \delta v_{,33} \}\,d\omega\,dx_3 = 0. \tag{A68}$$

Using (A8), (A15) and (A16) in (A68), the following result is obtained

$$\begin{aligned} \int_{-1/2}^{1/2} \int_\omega \{ & [(\overset{4}{L}_{3\alpha\beta 3} - \overset{4}{L}_{\alpha 3\beta 3}) \overset{0}{u}_{\beta,3} + (\overset{4}{L}_{3\alpha 3\beta} - \overset{4}{L}_{\alpha 33\beta}) \overset{0}{u}_{3,\beta} + (\overset{2}{L}_{3\alpha\beta 3} - \overset{2}{L}_{\alpha 3\beta 3}) \overset{2}{u}_{\beta,3} \\ & + (\overset{2}{L}_{3\alpha 3\beta} - \overset{2}{L}_{\alpha 33\beta}) \overset{2}{u}_{3,\beta}] \delta v_{,3} + [(\overset{2}{L}_{33\beta\gamma} \overset{2}{u}_{\beta,\gamma} + \overset{0}{L}_{33\beta\gamma} \overset{4}{u}_{\beta,\gamma} + \overset{2}{L}_{3333} \overset{0}{u}_{3,3} + \overset{0}{L}_{3333} \overset{2}{u}_{3,3}) x_\alpha] \delta v_{,33} \}\,d\omega\,dx_3 = 0. \end{aligned} \tag{A69}$$

In (A69) it is necessary to find an expression for $\int_\omega (\overset{0}{L}_{33\gamma\delta} \overset{4}{u}_{\gamma,\delta}) x_\alpha\,d\omega$. This can be done by considering (A6) and taking $\delta u_\alpha = \delta\varphi(x_3)\delta v_\alpha(x_1, x_2)$:

$$\int_{-1/2}^{1/2} \int_\omega \{ \overset{0}{\Pi}_{\beta\alpha} \delta\varphi \delta v_{\alpha,\beta} + \overset{0}{\Pi}_{3\alpha} \delta\varphi_{,3} \delta v_\alpha \}\,d\omega\,dx_3 = 0. \tag{A70}$$

Integrating by parts [from kinetic admissibility in (A20) $\delta\varphi(-1/2) = \delta\varphi(1/2) = 0$], and substituting the expressions for $\overset{0}{\Pi}_{3\alpha}$ and $\overset{0}{\Pi}_{\beta\alpha}$ from (A9) and (A17), we find

$$\begin{aligned} \int_\omega \{ & (\overset{2}{L}_{\alpha\beta\gamma\delta} \overset{2}{u}_{\gamma,\delta} + \overset{0}{L}_{\alpha\beta\gamma\delta} \overset{4}{u}_{\gamma,\delta} + \overset{2}{L}_{\alpha\beta 33} \overset{0}{u}_{3,3} + \overset{0}{L}_{\alpha\beta 33} \overset{2}{u}_{3,3}) \delta v_{\alpha,\beta} \\ & - (\overset{2}{L}_{\alpha 3\beta 3} \overset{0}{u}_{\beta,33} + \overset{2}{L}_{\alpha 33\beta} \overset{0}{u}_{3,\beta 3} + \overset{0}{L}_{\alpha 3\beta 3} \overset{2}{u}_{\beta,33} + \overset{0}{L}_{\alpha 33\beta} \overset{2}{u}_{3,\beta 3}) \delta v_\alpha \}\,d\omega = 0. \end{aligned} \tag{71}$$

Choosing $\delta v_\alpha(x_1, x_2) = \phi_{\alpha\eta}(x_1, x_2)$, defined in (A50), and simplifying the results, we obtain

$$\begin{aligned} \int_\omega \overset{0}{L}_{3311} \overset{4}{u}_{\beta,\beta} x_\alpha\,d\omega = \nu \int_\omega & \{ [(\overset{2}{L}_{\beta 3\gamma 3} - \overset{2}{L}_{\beta 33\gamma}) \overset{0}{u}_{\gamma,33} + G(\overset{2}{u}_{\beta,33} + \overset{2}{u}_{3,\beta 3})] \phi_{\beta\alpha} \\ & - (\overset{2}{L}_{\beta\beta\gamma\delta} \overset{2}{u}_{\gamma,\delta} + \overset{2}{L}_{\beta\beta 33} \overset{0}{u}_{3,3} + \overset{0}{L}_{\beta\beta 33} \overset{2}{u}_{3,3}) x_\alpha \}\,d\omega. \end{aligned} \tag{A72}$$

Substituting (A72) into (A69), and using the results for $\overset{0}{u}_i$ in (A41) and $\overset{2}{u}_i$ in (A49) and (A57), we find

$$\int_{-1/2}^{1/2}\int_{\omega}\{[(\overset{4}{L}_{3\alpha\beta 3}-\overset{4}{L}_{\alpha 3\beta 3}-\overset{4}{L}_{3\alpha 3\beta}+\overset{4}{L}_{\alpha 33\beta})\overset{0}{z}_{\beta,3}+(\overset{2}{L}_{3\alpha\beta 3}-\overset{2}{L}_{\alpha 3\beta 3})(\overset{2}{z}_{\beta,3}+\varepsilon_{\beta\gamma}x_\gamma\overset{2}{z}_{,3}$$
$$+\nu\phi_{\beta\gamma}\overset{0}{z}_{\gamma,333})+(\overset{2}{L}_{3\alpha 3\beta}-\overset{2}{L}_{\alpha 33\beta})(\lambda_2(1+\nu)\overset{0}{z}_{\beta,3}+(\nu\theta_{\gamma,\beta}+(1+\nu)\eta_{\gamma,\beta})\overset{0}{z}_{\gamma,333}$$
$$-\overset{2}{z}_{\beta,3}-w_{,\beta}\overset{2}{z}_{,3})]\delta v_{,3}+[\nu((\overset{2}{L}_{\beta 3\gamma 3}-\overset{2}{L}_{\beta 33\gamma})\overset{0}{z}_{\gamma,33}+G((\varepsilon_{\beta\gamma}x_\gamma-w_{,\beta})\overset{2}{z}_{,33}$$
$$+\lambda_2(1+\nu)\overset{0}{z}_{\beta,33}+(\nu\phi_{\beta\gamma}+\nu\theta_{\gamma,\beta}+(1+\nu)\eta_{\gamma,\beta})\overset{0}{z}_{\gamma,3333}))\phi_{\beta\alpha}$$
$$+((-2\nu^2\overset{2}{L}_{\beta\beta 11}+4\nu\overset{2}{L}_{3311}-\overset{2}{L}_{3333})x_\gamma\overset{0}{z}_{\gamma,33}+E(\overset{2}{z}_{,3}-x_\beta\overset{2}{z}_{\beta,33}$$
$$-w\overset{2}{z}_{,33}+\lambda_2(1+\nu)x_\beta\overset{0}{z}_{\beta,33}+(\nu\theta_\beta+(1+\nu)\eta_\beta)\overset{0}{z}_{\beta,3333}))x_\alpha]\delta v_{,33}\}\,d\omega\,dx_3=0. \tag{A73}$$

To simplify the above equation we must find expressions for $\overset{4}{L}_{1313}+\overset{4}{L}_{3131}-2\overset{4}{L}_{1331}$, $\overset{2}{L}_{1313}-\overset{2}{L}_{1331}$, $\overset{2}{L}_{3131}-\overset{2}{L}_{1331}$, and $\overset{2}{L}_{3333}-4\nu\overset{2}{L}_{3311}+2\nu^2\overset{2}{L}_{11\alpha\alpha}$. To accomplish this we use (A26) and (A27) which, upon rearrangement, results in the following

$$\overset{4}{L}_{1313}+\overset{4}{L}_{3131}-2\overset{4}{L}_{1331}=\lambda_4 E+\frac{\lambda_2^2}{2}\left(\frac{dE}{d\lambda}\bigg|_{\lambda=1}+(\nu-1)E\right), \tag{A74}$$

$$\overset{2}{L}_{1313}-\overset{2}{L}_{1331}=\lambda_2\frac{E}{2}, \tag{A75}$$

$$\overset{2}{L}_{3131}-\overset{2}{L}_{1331}=\lambda_2\frac{E}{2}, \tag{A76}$$

$$\overset{2}{L}_{3333}-4\nu\overset{2}{L}_{3311}+2\nu^2\overset{2}{L}_{11\alpha\alpha}=\lambda_2\frac{dE}{d\lambda}\bigg|_{\lambda=1}. \tag{A77}$$

Introducing the following constants, which depend only on the geometry of the cross-section,

$$L^{\eta}_{\alpha\beta}=\int_\omega x_\alpha\eta_\beta\,d\omega,\quad L^{\theta}_{\alpha\beta}=\int_\omega x_\alpha\theta_\beta\,d\omega, \tag{A78}$$

$$K^{\eta}_{\alpha\beta}=\int_\omega \phi_{\alpha\gamma}\eta_{\beta,\gamma}\,d\omega,\quad K^{\theta}_{\alpha\beta}=\int_\omega \phi_{\alpha\gamma}\theta_{\beta,\gamma}\,d\omega, \tag{A79}$$

$$K^{w}_{\alpha}=\int_\omega \phi_{\alpha\beta}w_{,\beta}\,d\omega,\quad K=\int_\omega\left(\frac{x_1^2+x_2^2}{2}\right)^2 d\omega \tag{A80}$$

and making use of the previous results, (A74)–(A77), we can simplify (A73) to obtain the variational form of the equations for $\overset{2}{z}_\alpha(x_3)$:

$$\int_{-1/2}^{1/2}\left\{\left[\lambda_2\overset{2}{z}_{\alpha,3}+\left(\lambda_4+\lambda_2^2\left(\frac{1}{2E}\frac{dE}{d\lambda}\bigg|_{\lambda=1}-1\right)\right)\overset{0}{z}_{\alpha,3}+\lambda_2\left(\frac{\nu}{2}(\delta_{\alpha\delta}\delta_{\beta\gamma}+\varepsilon_{\alpha\delta}\varepsilon_{\beta\gamma})I_{\beta\delta}\right.\right.\right.$$
$$\left.\left.+(1+\nu)I_{\alpha\gamma}\right)\overset{0}{z}_{\gamma,333}\right]\delta v_{,3}+\left[I_{\alpha\gamma}\overset{2}{z}_{\gamma,33}-\lambda_2\left(\frac{\nu}{2}(\delta_{\alpha\delta}\delta_{\beta\gamma}+\varepsilon_{\alpha\delta}\varepsilon_{\beta\gamma})I_{\beta\delta}\right.\right.$$
$$\left.\left.+(1+\nu)I_{\alpha\gamma}-\frac{1}{E}\frac{dE}{d\lambda}\bigg|_{\lambda=1}I_{\alpha\gamma}\right)\overset{0}{z}_{\gamma,33}+\frac{1}{2}\left(\frac{\nu}{1+\nu}(\varepsilon_{\alpha\beta}H_\beta+K^{w}_{\alpha})+I^{w}_{\alpha}\right)\overset{2}{z}_{,33}\right.$$

$$-\left(\frac{\nu^2}{2(1+\nu)}(K\delta_{\alpha\beta}+K^{\theta}_{\alpha\beta})+\frac{\nu}{2}K^{\eta}_{\alpha\beta}+\nu L^{\theta}_{\alpha\beta}+(1+\nu)L^{\eta}_{\alpha\beta}\right)\overset{0}{z}_{\beta,3333}\Bigg]\delta v_{,33}\Bigg\}\mathrm{d}x_3=0. \tag{A81}$$

From (A81) we deduce (39), the governing equations for $\overset{2}{z}_{\alpha}(x_3)$ and λ_4. This concludes the derivation of the equations governing the asymptotic stability problem for compression.

A.2. Tension

Derivation of λ_0. The begin the analysis for tension it is noted that the incremental moduli are isotropic in the x_1x_2 plane for all values of the axial stretch ratio λ

$$L_{\alpha\beta\gamma\delta}(\lambda)=2\hat{\mu}(\delta_{\alpha\gamma}\delta_{\beta\delta}+\delta_{\alpha\delta}\delta_{\beta\gamma})+\hat{\lambda}\delta_{\alpha\beta}\delta_{\gamma\delta}, \tag{A82}$$

where $\hat{\mu}$ and $\hat{\lambda}$ are dependent on the material and the axial stretch ratio. To show that λ_0 is the axial stretch ratio corresponding to the maximum load in tension, we proceed as follows. We begin with (A7). Taking $\delta u_3=\delta v(x_3)$, we obtain

$$\int_{-1/2}^{1/2}\int_{\omega}\overset{0}{\Pi}_{33}\delta v_{,3}\,\mathrm{d}\omega\,\mathrm{d}x_3=0. \tag{A83}$$

The expression for $\overset{0}{\Pi}_{33}$ in (A2) requires expressions for $\overset{0}{u}_i$ and $\overset{2}{u}_{\alpha}$. Starting with (A5), and in view of the in-plane isotropy of $\mathbf{L}$, and choosing the cases $\alpha=\beta=1$ and $\alpha=\beta=2$, we have

$$\overset{0}{u}_{1,1}=\overset{0}{u}_{2,2}=0 \tag{A84}$$

while choosing $\alpha=1$ and $\beta=2$ (or equivalently $\alpha=2$ and $\beta=1$), gives

$$\overset{0}{u}_{1,2}+\overset{0}{u}_{2,1}=0. \tag{A85}$$

In view of the orthotropic material behavior (since $\lambda_0\neq 1$), we find from (A3) and (A4)

$$\overset{0}{u}_{1,3}=\overset{0}{u}_{3,1}=\overset{0}{u}_{2,3}=\overset{0}{u}_{3,2}=0. \tag{A86}$$

The results of (A84)–(A86), combined with the removal of any rigid body rotation using (A22), give for $\overset{0}{u}_i$

$$\overset{0}{u}_{\alpha}=0,\quad \overset{0}{u}_3=\overset{0}{z}_3(x_3). \tag{A87}$$

To find an expression for $\overset{2}{u}_{\alpha}$ for use in (A83), we make use of (A87) and (A11), with $\alpha=\beta=1$ and $\alpha=\beta=2$, to obtain

$$\overset{0}{L}_{\alpha\alpha11}\overset{2}{u}_{1,1}+\overset{0}{L}_{\alpha\alpha22}\overset{2}{u}_{2,2}=-\overset{0}{L}_{\alpha\alpha33}\overset{0}{u}_{3,3}\quad\text{(no sum)}, \tag{A88}$$

from which we find, with the help of the in-plane isotropy of $\mathbf{L}$ in (A82),

$$\overset{2}{u}_{1,1}=\overset{2}{u}_{2,2}=\frac{-\overset{0}{L}_{1133}}{\overset{0}{L}_{1111}+\overset{0}{L}_{1122}}\overset{0}{u}_{3,3}. \tag{A89}$$

Defining the tangent Poisson's ratio, $\nu(\lambda)$, and the tangent modulus under uniaxial tension, $E(\lambda)$, as follows

$$\nu(\lambda)=\frac{\overset{0}{L}_{1133}}{\overset{0}{L}_{1111}+\overset{0}{L}_{1122}}, \tag{A90}$$

$$E(\lambda)=\overset{0}{L}_{3333}-2\nu(\lambda)\overset{0}{L}_{1133}, \tag{A91}$$

and substituting the results into (A2), we find $\overset{0}{\Pi}_{33}=E(\lambda_0)\overset{0}{z}_{3,3}$ which, from (A83), implies

$$E(\lambda_0)\overset{0}{z}_{3,33}=0\Rightarrow E(\lambda_0)=0 \tag{A92}$$

since it is assumed that $\overset{0}{z}_3(x_3) \neq 0$. The value of λ_0, found from (A92), corresponds to the maximum load in uniaxial tension.

Derivation of λ_2, $\overset{0}{u}_i$. To determine the next higher order term in the stretch ratio and the lowest order term in the eigenmode, we proceed as follows. Starting with (A13) and taking $\delta u_3 = \delta v(x_3)$

$$\int_{-1/2}^{1/2} \int_{\omega} \overset{2}{\Pi}_{33} \delta v_{,3} \, \mathrm{d}\omega \, \mathrm{d}x_3 = 0. \tag{A93}$$

According to (A8), evaluation of $\overset{2}{\Pi}_{33}$ requires (in addition to $\overset{0}{u}_i$) $\overset{2}{u}_i$ and $\overset{4}{u}_\alpha$, which are unknown at this point. An expression for $\overset{2}{u}_\alpha$ can be found by starting with (A11). Taking $\alpha = 1$ and $\beta = 2$, and making use of the in-plane isotropy of $\mathbf{L}$ in (A82), we find

$$\overset{2}{u}_{1,2} + \overset{2}{u}_{2,1} = 0. \tag{A94}$$

Combining (A94) with (A89) we obtain

$$\overset{2}{u}_\alpha = \overset{2}{z}_\alpha(x_3) + \varepsilon_{\alpha\beta} x_\beta \overset{2}{z}(x_3) - \overset{0}{v} x_\alpha \overset{0}{z}_{3,3}(x_3). \tag{A95}$$

An expression for $\overset{2}{u}_3$ can be found by considering (A7), and choosing $\delta u_3 = \delta\varphi(x_1, x_2)\delta v(x_3)$, and recalling $\overset{0}{\Pi}_{33} = 0$, which gives

$$\int_{-1/2}^{1/2} \left\{ \int_{\omega} \overset{0}{\Pi}_{\beta 3} \delta\varphi_{,\beta} \, \mathrm{d}\omega \right\} \delta v \, \mathrm{d}x_3 = 0. \tag{A96}$$

Using the definition for $\overset{0}{\Pi}_{\beta 3}$ in (A9), recalling the definition of the warping function $w(x_1, x_2)$ in (A56), and introducing the function $\rho(x_1, x_2)$

$$\rho(x_1, x_2) = \tfrac{1}{2}(x_1^2 + x_2^2 - I_{\alpha\alpha}) \tag{A97}$$

we find, with the help of (A95) and (A87), the following expression for $\overset{2}{u}_3$

$$\overset{2}{u}_3 = \overset{2}{z}_3(x_3) - \frac{\overset{0}{L}_{3113}}{\overset{0}{L}_{3131}} (x_\alpha \overset{2}{z}_{\alpha,3}(x_3) + w(x_1, x_2)\overset{2}{z}_{,3}(x_3) - \overset{0}{v}\rho(x_1, x_2)\overset{0}{z}_{,33}(x_3)). \tag{A98}$$

Governing equation for $\overset{2}{z}(x_3)$. The function $\overset{2}{z}(x_3)$ can be determined in the following manner. Considering (A6) with $\delta u_\alpha = \varepsilon_{\alpha\beta} x_\beta \delta v(x_3)$, and noticing $\overset{0}{\Pi}_{\alpha\beta} = \overset{0}{\Pi}_{\beta\alpha}$ in view of the in plane isotropy, we find

$$\int_{-1/2}^{1/2} \int_{\omega} \overset{0}{\Pi}_{3\alpha} \varepsilon_{\alpha\beta} x_\beta \delta v_{,3} \, \mathrm{d}\omega \, \mathrm{d}x_3 = 0. \tag{A99}$$

Substituting the expression for $\overset{0}{\Pi}_{3\alpha}$ from (A10) into (A99), recalling the expressions for $\overset{2}{u}_i$ in (A95) and (A98), and simplifying the result, we find the variational form of the equation for $\overset{2}{z}(x_3)$

$$\int_{-1/2}^{1/2} \left\{ \left[\overset{0}{S} I_{\alpha\alpha} + J \overset{0}{L}_{1331} \frac{\overset{0}{L}_{3113}}{\overset{0}{L}_{3131}} \right] \overset{2}{z}_{,3} \right\} \delta v_{,3} \, \mathrm{d}x_3 = 0, \tag{A100}$$

where in the derivation of (A100) we made use of the definitions of the warping function, w, in (A56), the torsion function, ψ, in (A60) and $\overset{0}{S}$ is the axial component of the second Piola–Kirchhoff stress evaluated at $\lambda = \lambda_0$. The governing differential equation for $\overset{2}{z}(x_3)$ is $\overset{2}{z}_{,33} = 0$ which, in view of the boundary conditions (A20) and (A22), gives

$$\overset{2}{z}(x_3) = 0. \tag{A101}$$

Governing equation for $\overset{0}{z}_3(x_3)$ To determine $\overset{0}{z}_3(x_3)$ we begin with (A13). Taking $\delta u_3 = \delta v(x_3)$ gives

$$\int_{-1/2}^{1/2} \int_{\omega} \overset{2}{\Pi}_{33} \delta v_{,3} \, \mathrm{d}\omega \, \mathrm{d}x_3 = 0. \tag{A102}$$

Substituting the expression for $\overset{2}{\Pi}_{33}$ in (A8), and simplifying the result with the help of (A87), (A95) and (A98), we find

$$\int_{-1/2}^{1/2} \left\{ \overset{0}{L}_{3311} \left(\int_{\omega} \overset{4}{u}_{\alpha,\alpha} \, \mathrm{d}\omega \right) + (\overset{2}{L}_{3333} - \overset{0}{\nu} \overset{2}{L}_{33\alpha\alpha}) \overset{0}{z}_{3,3} + \overset{0}{L}_{3333} \overset{2}{z}_{3,3} \right\} \delta v_{,3} \, \mathrm{d}x_3 = 0, \tag{A103}$$

where it can be seen that we need to find an expression for $\int_{\omega} \overset{4}{u}_{\alpha,\alpha} \, \mathrm{d}\omega$. To this end we use (A6) with $\delta u_\alpha = x_\alpha \delta v(x_3)$

$$\int_{-1/2}^{1/2} \int_{\omega} (\overset{0}{\Pi}_{\alpha\alpha} \delta v + \overset{0}{\Pi}_{3\alpha} x_\alpha \delta v_{,3}) \, \mathrm{d}\omega \, \mathrm{d}x_3 = 0. \tag{A104}$$

Using the expressions for $\overset{0}{\Pi}_{\alpha\beta}$ and $\overset{0}{\Pi}_{3\alpha}$ from (A17) and (A10), and simplifying the result with the help of (A87), (A95) and (A98), we find

$$\overset{0}{L}_{\beta\beta 11} \int_{\omega} \overset{4}{u}_{\alpha,\alpha} \, \mathrm{d}\omega = -2(\overset{2}{L}_{1133} - \overset{0}{\nu} \overset{2}{L}_{11\alpha\alpha}) \overset{0}{z}_{3,3} - 2 \overset{0}{L}_{1133} \overset{2}{z}_{3,3} - \overset{0}{\nu} \overset{0}{S} I_{\alpha\alpha} \overset{0}{z}_{3,333}. \tag{A105}$$

Substituting (A105) into (A103), and noticing the generalization of (A77) for $\lambda_0 \neq 1$, namely

$$\overset{2}{L}_{3333} - 4 \overset{0}{\nu} \overset{2}{L}_{3311} + 2(\nu^2)_0 \overset{2}{L}_{11\alpha\alpha} = \lambda_2 \left. \frac{\mathrm{d}E}{\mathrm{d}\lambda} \right|_{\lambda_0}, \tag{A106}$$

we find the equation for $\overset{0}{z}_3(x_3)$ in variational form

$$\int_{-1/2}^{1/2} \left\{ (\nu^2)_0 \overset{0}{S} I_{\alpha\alpha} \overset{0}{z}_{3,333} - \lambda_2 \left. \frac{\mathrm{d}E}{\mathrm{d}\lambda} \right|_{\lambda_0} \overset{0}{z}_{3,3} \right\} \delta v_{,3} \, \mathrm{d}x_3 = 0, \tag{A107}$$

to which we have to add the essential boundary condition (48). The equation for $\overset{0}{z}_3(x_3)$ is an eigenvalue equation that also gives λ_2. The solution of the eigenvalue problem for $\overset{0}{z}_3(x_3)$ and λ_2 is given in (49) and (50).

Governing equation for $\overset{2}{z}_\alpha(x_3)$. Before we derive an expression for λ_4 we need to find the governing equation for $\overset{2}{z}_\alpha(x_3)$. To this end we use (A6) and successively taking $(\delta u_1, \delta u_2) = (\delta v(x_3), 0)$ and $(\delta u_1, \delta u_2) = (0, \delta v(x_3))$

$$\int_{-1/2}^{1/2} \int_{\omega} \overset{0}{\Pi}_{3\alpha} \delta v_{,3} \, \mathrm{d}\omega \, \mathrm{d}x_3 = 0. \tag{A108}$$

Using the expression for $\overset{0}{\Pi}_{3\alpha}$ in (A10) in conjunction with (A87), (A95) and (A98) we obtain

$$\int_{-1/2}^{1/2} \int_{\omega} \overset{0}{S} \overset{2}{z}_{\alpha,3} \delta v_{,3} \, \mathrm{d}\omega \, \mathrm{d}x_3 = 0, \tag{A109}$$

which gives the governing differential equation for $\overset{2}{z}_\alpha(x_3)$, $\overset{2}{z}_{\alpha,33} = 0$, which in view of the boundary conditions (A20), $\overset{2}{z}_\alpha(\pm 1/2) = 0$, we find

$$\overset{0}{z}_\alpha(x_3) = 0. \tag{A110}$$

Derivation of λ_4, $\overset{2}{\mathrm{u}}_1$. To begin the derivation of λ_4 we use (A19) with $\delta u_3 = \delta v(x_3)$

$$\int_{-1/2}^{1/2}\int_{\omega} \overset{4}{\Pi}_{33}\delta v_{,3}\,\mathrm{d}\omega\,\mathrm{d}x_3 = 0. \tag{A111}$$

To evaluate $\overset{4}{\Pi}_{33}$ using (A14) it is necessary to find expressions for $\overset{4}{u}_i$. To find an expression for $\overset{4}{u}_\alpha$ we begin with (A6), taking $\delta u_\alpha = \delta\varphi(x_3)\delta v_\alpha(x_1, x_2)$, and simplify the result to find

$$\int_{\omega} (\overset{0}{\Pi}_{\beta\alpha}\delta v_{\alpha,\beta} - \overset{0}{\Pi}_{3\alpha,3}\delta v_\alpha)\,\mathrm{d}\omega = 0. \tag{A112}$$

Substituting the expressions for $\overset{0}{\Pi}_{\beta\alpha}$ and $\overset{0}{\Pi}_{3\alpha}$ from (A17) and (A10) into (A112), and using (A87), (A95) and (A98), we obtain

$$\int_{\omega}\Bigg\{\Bigg[\overset{0}{L}_{\alpha\beta\gamma\delta}\overset{4}{u}_{\gamma,\delta} + \overset{0}{L}_{\alpha\beta33}\overset{2}{z}_{3,3} + (\overset{2}{L}_{\alpha\beta33} - \overset{0}{\nu}\overset{2}{L}_{\alpha\beta\gamma\gamma})\overset{0}{z}_{3,3} + \overset{0}{L}_{\alpha\beta33}\frac{\overset{0}{L}_{3113}}{\overset{0}{L}_{3131}}\overset{0}{\nu}\rho(x_1, x_2)\overset{0}{z}_{3,333}\Bigg]\delta\varphi_{\alpha,\beta} + x_\alpha\overset{0}{\nu}\overset{0}{S}\overset{0}{z}_{3,333}\delta\phi_\alpha\Bigg\}\mathrm{d}\omega = 0. \tag{A113}$$

Introducing the auxiliary function $\overset{4}{g}_\alpha(x_1, x_2)$, defined on the normalized cross-section as follows

$$\overset{4}{g}_\alpha(x_1, x_2):\quad \int_{\omega}(\overset{0}{L}_{\alpha\beta\gamma\delta}\overset{4}{g}_{\gamma,\delta})\delta\varphi_{\alpha,\beta}\,\mathrm{d}\omega = -\int_{\omega}\overset{0}{\nu}\Bigg[\overset{0}{L}_{\alpha\beta33}\frac{\overset{0}{L}_{3113}}{\overset{0}{L}_{3131}}\rho\delta\varphi_{\alpha,\beta} + \overset{0}{S}x_\alpha\delta\phi_\alpha\Bigg]\mathrm{d}\omega$$

$$\int_{\omega}\overset{4}{g}_\alpha\,\mathrm{d}\omega = \int_{\omega}\varepsilon_{\alpha\beta}x_\beta\overset{4}{g}_\alpha\,\mathrm{d}\omega = 0 \tag{A114}$$

we can find the expression for $\overset{4}{u}_\alpha$ from (A113)

$$\overset{4}{u}_\alpha = \overset{4}{z}_\alpha(x_3) + \varepsilon_{\alpha\beta}x_\beta\overset{4}{z}(x_3) - \overset{0}{\nu}x_\alpha\Bigg[\overset{2}{z}_{3,3}(x_3) + \frac{\overset{2}{L}_{1133} - \overset{0}{\nu}\overset{2}{L}_{11\beta\beta}}{\overset{0}{L}_{1133}}\overset{0}{z}_{3,3}(x_3)\Bigg]$$

$$+\overset{4}{g}_\alpha(x_1, x_2)\overset{0}{z}_{3,333}(x_3). \tag{A115}$$

To obtain an expression for $\overset{4}{u}_3$ we begin with (A13), taking $\delta u_3 = \delta\varphi(x_3)\delta v(x_1, x_2)$, and simplify the result

$$\int_{\omega}\{\overset{2}{\Pi}_{\alpha3}\delta v_{,\alpha} - \overset{2}{\Pi}_{33,3}\delta v\}\,\mathrm{d}\omega = 0. \tag{A116}$$

Substituting the expressions for $\overset{2}{\Pi}_{\alpha3}$ and $\overset{2}{\Pi}_{33}$ from (A16) and (A8), we find, with the help of (A87), (A95) and (A98)

$$\int_{\omega}\Bigg\{\Bigg[\overset{0}{L}_{3131}\overset{4}{u}_{3,\alpha} + \overset{0}{L}_{3113}\Bigg(\overset{4}{z}_{\alpha,3} + \varepsilon_{\alpha\beta}x_\beta\overset{4}{z}_{,3} - \overset{0}{\nu}x_\alpha\Bigg(\overset{2}{z}_{3,33} + \frac{\overset{2}{L}_{1133} - \overset{0}{\nu}\overset{2}{L}_{11\beta\beta}}{\overset{0}{L}_{1133}}\overset{0}{z}_{3,33}\Bigg) + \overset{4}{g}_\alpha\overset{0}{z}_{3,3333}\Bigg)$$

$$-\Bigg(\overset{2}{L}_{3113} - \overset{2}{L}_{3131}\frac{\overset{0}{L}_{3113}}{\overset{0}{L}_{3131}}\Bigg)\overset{0}{\nu}x_\alpha\overset{0}{z}_{3,33}\Bigg]\delta v_{,\alpha} - \Bigg[\overset{0}{L}_{3311}\Bigg(\overset{4}{g}_{\alpha,\alpha}\overset{0}{z}_{3,3333} - 2\overset{0}{\nu}\Bigg(\overset{2}{z}_{3,33} + \frac{\overset{2}{L}_{1133} - \overset{0}{\nu}\overset{2}{L}_{11\beta\beta}}{\overset{0}{L}_{1133}}\overset{0}{z}_{3,33}\Bigg)\Bigg)$$

$$+(\overset{2}{L}_{3333} - \overset{0}{\nu}\overset{2}{L}_{33\alpha\alpha})\overset{0}{z}_{3,33} + \overset{0}{L}_{3333}\Bigg(\overset{2}{z}_{3,33} + \overset{0}{\nu}\frac{\overset{0}{L}_{3113}}{\overset{0}{L}_{3131}}\rho(x_1, x_2)\overset{0}{z}_{3,3333}\Bigg)\Bigg]\delta v\Bigg\}\mathrm{d}\omega = 0. \tag{A117}$$

Introducing the auxiliary functions $\rho^*(x_1, x_2)$, $\overset{4}{g}_3(x_1, x_2)$, $\overset{4}{f}{}^*_3(x_1, x_2)$ and $\overset{4}{g}{}^*_3(x_1, x_2)$, defined as follows

$$\rho^*(x_1, x_2):\quad \int_{\omega}\rho^*_{,\alpha}\delta v_{,\alpha}\,\mathrm{d}\omega = \int_{\omega}\rho\delta v\,\mathrm{d}\omega,\quad \int_{\omega}\rho^*\,\mathrm{d}\omega = 0, \tag{A118}$$

$$\overset{4}{g}_3(x_1,x_2): \quad \int_\omega \overset{4}{g}_{3,\alpha}\delta v_{,\alpha}\,\mathrm{d}\omega = \int_\omega \overset{4}{g}_{\alpha,\alpha}\delta v\,\mathrm{d}\omega - \int_\omega \overset{4}{g}_{\alpha,\alpha}\,\mathrm{d}\omega \int_\omega \delta v\,\mathrm{d}\omega, \quad \int_\omega \overset{4}{g}_3\,\mathrm{d}\omega = 0, \tag{A119}$$

$$\overset{4}{f}{}^*_3(x_1,x_2): \quad \int_\omega \overset{4}{f}{}^*_{3,\alpha}\delta v_{,\alpha}\,\mathrm{d}\omega = \int_\omega \overset{4}{f}_\alpha \delta v_{,\alpha}\,\mathrm{d}\omega, \quad \int_\omega \overset{4}{f}{}^*_3\,\mathrm{d}\omega = 0, \tag{A120}$$

$$\overset{4}{g}{}^*_3(x_1,x_2): \quad \int_\omega \overset{4}{g}{}^*_{3,\alpha}\delta v_{,\alpha}\,\mathrm{d}\omega = \int_\omega \overset{4}{g}_\alpha \delta v\,\mathrm{d}\omega, \quad \int_\omega \overset{4}{g}{}^*_3\,\mathrm{d}\omega = 0, \tag{A121}$$

we can find the following expression for $\overset{4}{u}_3$ from (A117)

$$\begin{aligned}
\overset{4}{u}_3 = {} & \overset{4}{z}_3(x_3) - \frac{\overset{0}{L}_{3113}}{\overset{0}{L}_{3131}}[x_\alpha \overset{4}{z}_{\alpha,3}(x_3) + w(x_1,x_2)\overset{4}{z}_{,3}(x_3) + \overset{4}{f}{}^*_3(x_1,x_2)\overset{2}{z}_{3,33}(x_3)] \\
& + \frac{1}{\overset{0}{L}_{3131}}\left[\left(\overset{2}{L}_{3113} - \overset{2}{L}_{3131}\frac{\overset{0}{L}_{3113}}{\overset{0}{L}_{3131}}\right)\overset{0}{v}\rho(x_1,x_2) - (\overset{2}{L}_{1133} - \overset{0}{v}\overset{2}{L}_{11\alpha\alpha})\frac{\overset{0}{L}_{3113}}{\overset{0}{L}_{1133}}\overset{4}{f}{}^*_3(x_1,x_2)\right]\overset{0}{z}_{3,33} \\
& + \frac{1}{\overset{0}{L}_{3131}}\left[\overset{0}{L}_{3311}\overset{4}{g}_3(x_1,x_2) - \overset{0}{L}_{3113}\overset{4}{g}{}^*_3(x_1,x_2) + \overset{0}{L}_{3333}\frac{\overset{0}{L}_{3113}}{\overset{0}{L}_{3131}}\overset{0}{v}\rho^*(x_1,x_2)\right]\overset{0}{z}_{3,333}.
\end{aligned} \tag{A122}$$

Recall that the starting point, to evaluate λ_4 and $\overset{2}{z}_3(x_3)$, is (A111). The only missing ingredient is to find an expression for $\int_\omega \overset{6}{u}_{\alpha,\alpha}\,\mathrm{d}\omega$. To do this we begin with (A12), using $\delta u_\alpha = x_\alpha \delta v(x_3)$

$$\int_\omega [\overset{2}{\Pi}_{\alpha\alpha} - x_\beta \overset{2}{\Pi}_{3\beta,3}]\,\mathrm{d}\omega = 0. \tag{A123}$$

Substituting the expressions for $\overset{2}{\Pi}_{\beta\alpha}$ and $\overset{2}{\Pi}_{3\beta}$ into (A123), we find

$$\begin{aligned}
\int_\omega \overset{0}{L}_{11\beta\beta}\overset{6}{u}_{\alpha,\alpha}\,\mathrm{d}\omega = \int_\omega \Bigg\{ & \left[2\overset{0}{v}\overset{4}{L}_{\beta\beta 11} + 2\overset{0}{v}\overset{2}{L}_{\beta\beta 11}\frac{\overset{2}{L}_{1133} - \overset{0}{v}\overset{2}{L}_{11\gamma\gamma}}{\overset{0}{L}_{1133}} - \overset{4}{L}_{\beta\beta 33}\right]\overset{0}{z}_{3,3} \\
& - \Bigg[\overset{2}{L}_{\beta\beta 11}\overset{4}{g}_{\gamma,\gamma} + \overset{0}{v}x_\beta x_\beta\left(\overset{2}{L}_{1313} - \overset{2}{L}_{1331}\frac{\overset{0}{L}_{3113}}{\overset{0}{L}_{3131}} + \overset{0}{L}_{1313}\frac{\overset{2}{L}_{1133} - \overset{0}{v}\overset{2}{L}_{11\gamma\gamma}}{\overset{0}{L}_{1133}}\right. \\
& \left. - \left(\overset{2}{L}_{3113} - \overset{2}{L}_{3131}\frac{\overset{0}{L}_{3113}}{\overset{0}{L}_{3131}}\right)\frac{\overset{0}{L}_{3113}}{\overset{0}{L}_{3131}} - (\overset{2}{L}_{1133} - \overset{0}{v}\overset{2}{L}_{11\gamma\gamma})\left(\frac{\overset{0}{L}_{3113}}{\overset{0}{L}_{3131}}\right)^2\right)\Bigg]\overset{0}{z}_{3,333} \\
& + \left[\overset{0}{L}_{1313}x_\beta\overset{4}{g}_\beta + \frac{\overset{0}{L}_{1331}}{\overset{0}{L}_{3131}}\left(\overset{0}{L}_{3311}x_\beta\overset{4}{g}_{3,\beta} - \overset{0}{L}_{3113}x_\beta\overset{4}{g}{}^*_{3,\beta} + \overset{0}{L}_{3333}\frac{\overset{0}{L}_{3113}}{\overset{0}{L}_{3131}}\overset{0}{v}x_\beta\rho^*_{,\beta}\right)\right]\overset{0}{z}_{3,33333} \\
& - [\overset{2}{L}_{\beta\beta 33} - 2\overset{0}{v}\overset{2}{L}_{\beta\beta 11}]\overset{2}{z}_{3,3} - \left[\overset{0}{v}\overset{0}{L}_{1313}x_\beta x_\beta + \frac{(\overset{0}{L}_{1331})^2}{\overset{0}{L}_{3131}}x_\beta\overset{4}{f}{}^*_{3,\beta}\right]\overset{2}{z}_{3,333} - \overset{0}{L}_{\beta\beta 33}\overset{4}{z}_{3,3}\Bigg\}\mathrm{d}\omega.
\end{aligned} \tag{A124}$$

Substituting (A115), (A122) and (A124) into (A14), the expression for $\overset{4}{\Pi}_{33}$, we can obtain the governing equation for $\overset{2}{z}_3(x_3)$ in variational form

$$\int_{-1/2}^{1/2} \left\{ (v^2)_0 \overset{0}{S} I_{\alpha\alpha} \overset{2}{z}_{3,333} - \lambda_2 \frac{\mathrm{d}E}{\mathrm{d}\lambda}\bigg|_{\lambda_0} \overset{2}{z}_{3,3} \right\} \delta v_{,3}\, \mathrm{d}x_3 = \int_{-1/2}^{1/2} \left\{ \left[\lambda_4 \frac{\mathrm{d}E}{\mathrm{d}\lambda}\bigg|_{\lambda_0} + \frac{\lambda_2^2}{2} \frac{\mathrm{d}^2 E}{\mathrm{d}\lambda^2}\bigg|_{\lambda_0} \right] \overset{0}{z}_{3,3} \right.$$

$$- \left[\lambda_2 \frac{\mathrm{d}(v^2 S)}{\mathrm{d}\lambda}\bigg|_{\lambda_0} I_{\alpha\alpha} \right] \overset{0}{z}_{3,333} + \left[\overset{0}{v} \overset{0}{S} A_g + \overset{0}{v} \overset{0}{L}_{1133} \frac{\overset{0}{L}_{1331}}{\overset{0}{L}_{3131}} A_{\rho g} \right.$$

$$\left. \left. + (v^2)_0 \overset{0}{L}_{3333} \left(\frac{\overset{0}{L}_{1331}}{\overset{0}{L}_{3131}} \right)^2 A_{\rho\rho} \right] \overset{0}{z}_{3,33333} \right\} \delta v_{,3}\, \mathrm{d}x_3, \tag{A125}$$

where the constants A_g, $A_{\rho g}$ and $A_{\rho\rho}$ are given by

$$A_g = \int_\omega x_\alpha \overset{4}{g}_\alpha \,\mathrm{d}\omega; \quad A_{\rho g} = \int_\omega \rho \overset{4}{g}_{\alpha,\alpha} \,\mathrm{d}\omega; \quad A_{\rho\rho} = \int_\omega \rho^2 \,\mathrm{d}\omega. \tag{A126}$$

From (A125) we find $\overset{2}{z}_3(x_3) = 0$ and the expression for λ_4. This concludes the derivation of the governing equations to the tensile stability problem.